GE DOCUMENT NO. 84SDS4262
SEPTEMBER 1984

NASA CR-175267

60 GHz ANTENNA SYSTEM ANALYSES FOR INTERSATELLITE LINKS PHASE B - FINAL AND SUMMARY REPORT

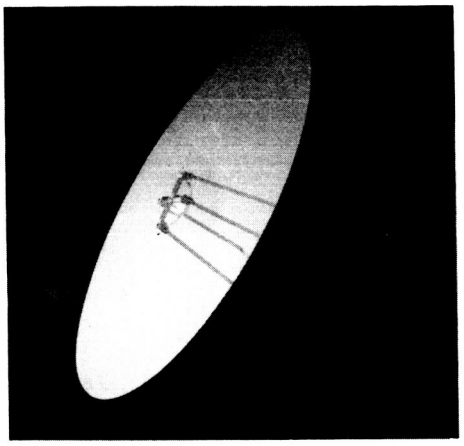

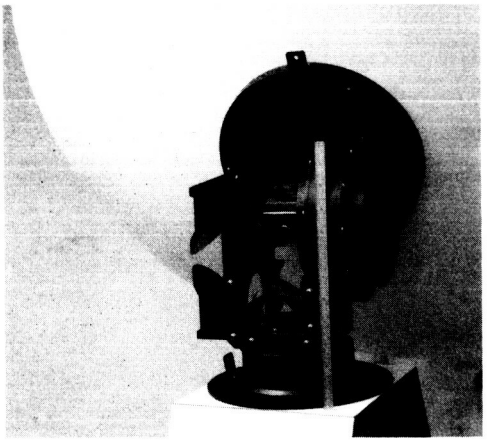

CONTRACT NAS-5-27791

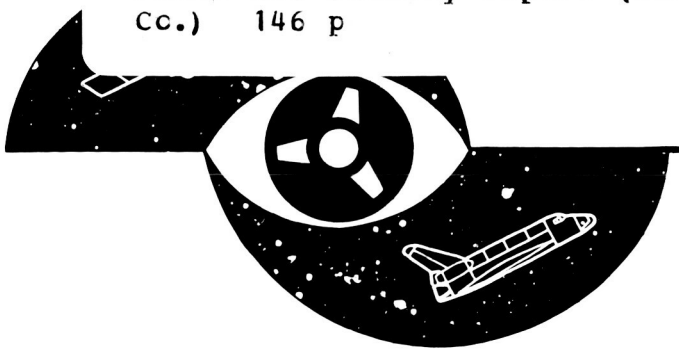

SPACE SYSTEMS DIVISION

GENERAL ELECTRIC

GE Document 84SDS4262
September 1984

60 GHz ANTENNA SYSTEM ANALYSES

FOR

INTERSATELLITE LINKS

FINAL AND SUMMARY REPORT - PHASE B

Contract NAS-5-27791

GENERAL ELECTRIC

TABLE OF CONTENTS

TABLE OF CONTENTS (Cont)

SECTION 1

INTRODUCTION AND SUMMARY

SECTION 1

INTRODUCTION AND SUMMARY

This final and summary report covers Phase A and Phase B of a 2-phase study conducted by General Electric - Space Systems Division for NASA - Goddard Space Flight Center, under Contract No. NAS-5-27791. In Phase A a tradeoff study was performed for four types of 60 GHz antenna systems applicable to both an advanced, geostationary relay satellite such as the Tracking and Data Acquisition Systems (TDAS) and to the related low-orbit user satellites. At the end of Phase A, the Phase A report (GE Document No. 84 SDS 4255, June 1984) was submitted and the preferred antenna system was selected by NASA-GSFC for a detailed conceptual design during Phase B.

Section 2 of this report presents a summary of the Phase A activity. The material is extracted from the Phase A report and covers the tradeoff results for four types of antenna systems.

Type B: Reflector/fixed feed (4 candidates)

Type M: Mechanical scan (4 candidates)

Type E: Electronic scan (3 candidates) and

Type H: Hybrid mechanical/electronic scan (1 candidate).

The 12 candidate antennas were assessed on the basis of a preliminary design and a performance analysis and then were scored against 15 weighted parameters. This process resulted in the ranking of the 12 candidates for the two applications, namely, for a geostationary satellite only, with a narrow field of view and for low orbit user satellites with a wide field of view.

For both applications the beam waveguide gimbal/Cassegrain reflector system is a clear winner scoring high in several important parameters such as volume, spacecraft impact, weight, insertion loss and power. There are only two other candidates with the capability of a wide field of view, namely, a system where the RF electronics is mounted on the back of the reflector, thereby avoiding lossy RF rotary joints and a conventional gimbal system employing multiple (for auto-track error signals) RF rotary joints where the RF loss must be compensated by a larger antenna aperture.

All the other candidates have only a narrow field of view capability. A mechanical scan system using a fixed feed and fixed paraboloid reflector and a flat plate reflector movable by a 2-axis gimbal scores almost as high as the beam waveguide system. In adition to high scores for insertion loss and power the flat plate reflector system wins out in high reliability and low development risk--it has sucessfully flown on the MIT Lincoln Lab LES 8/9 synchronous satellite.

Electronic scan systems pay an exorbitant price in complexity, development risk and cost for the feature of beam agility which is not important for the modest dynamics of the orbital scenario. The other beneficial feature, namely, inertia free beam scanning cannot outweigh the disadvantages.

Section 3 describes the conceptual design of the selected beam waveguide antenna system, shown in Figure 1-1. In this section details of the electrical and mechanical configuration are given as well as a description of the antenna pointing and control concept and the implementation of the control electronics. The host spacecraft interface and electrical and physical interactions with the host spacecraft are described. The section ends with a performance summary for the beam waveguide antenna system.

Section 4 covers the industry development status for three critical items identified during the study:

- Monopulse Front End
- Flexible Waveguide and
- RF Rotary Joints

1.1 Purpose of Study

The purpose of the study is first to investigate, classify and compare applicable antenna systems capable of establishing and maintaining intersatellite links at 60 GHz and secondly to select the most applicable system for a detailed conceptual design. The results of the study are to be applicable to the development of intersatellite links at 60 GHz for future programs.

1.2 Design Goal Specification

The design goals are listed in Table 1-1. These specifications are typical of future potential requirements for TDAS and related low-orbit user satellites. It should be noted that the original NASA-GSFC statement of work included goals for the TDAS only. The statement of work was later modified to include TDAS and user satellites, as shown in Table 1-1. The major difference between the two cases is the field of view which widens from a cone of $\pm 13^{o}$ for TDAS to $\pm 126^{o}$ for a user at the specified maximum user orbit altitude of 1500 km (see Appendix C).

The following comments are made with respect to some of the antenna systems parameters:

60 GHz BEAM WAVEGUIDE ANTENNA-FULL SCALE MOCK-UP

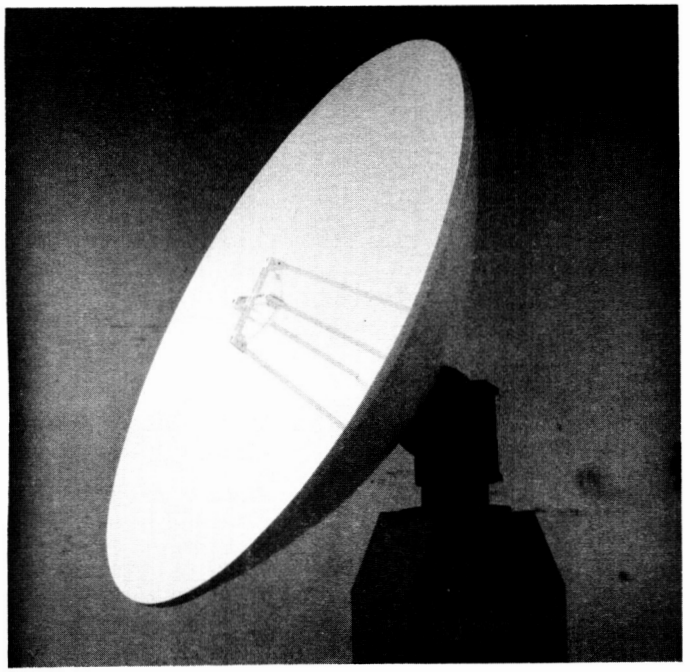

4 FT DIA. REFLECTOR
WITH SUBREFLECTOR
AND TWO-AXIS GIMBAL

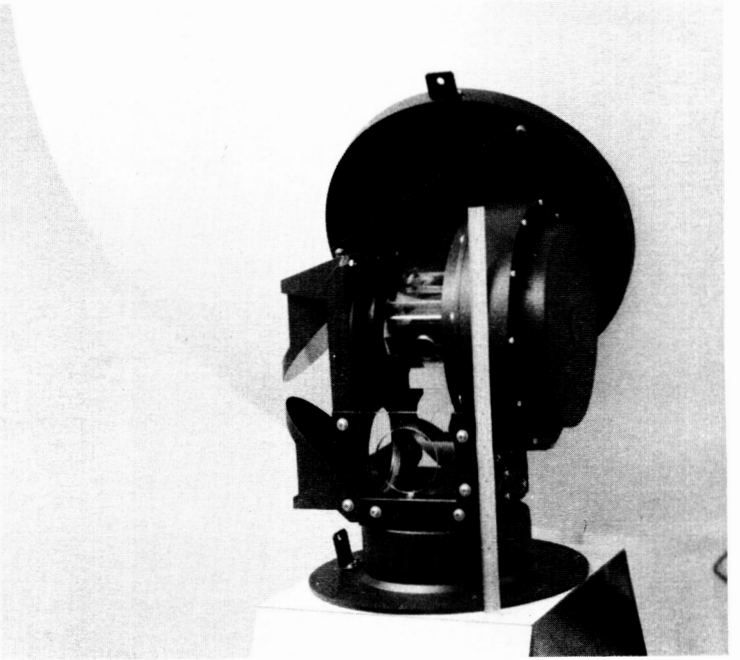

TWO-AXIS GIMBAL
WITH 60 GHz BEAM
WAVEGUIDE OPTICS

Figure 1-1. 60 GHz Beam Waveguide Antenna - Full Scale Mock-up

TABLE 1-1.

60 GHz ANTENNA SYSTEM DESIGN GOAL SPECIFICATIONS

	ORIGINAL SOW - TDAS ONLY	MODIFIED SOW - TDAS AND USERS
Frequency:	60 GHz	Same
Antenna Gain:	54 dB including losses (referenced to right hand circular polarized isotropic antenna)	Same
Polarization:	Right hand circular	Same
Link Accommodations:	5 individual pairs of forward and return links under simultaneous operation	Up to 5 individual - -
Data Rate Capability:	Up to 50 x 10^6 bits/sec per link	Same
Host Spacecraft:	Tracking and Data Acquisition System (TDAS) Satellite	--- And TDAS User Spacecraft
Field of View:	26° cone from geosynchronous orbit centered about the earth	26° cone or wider
Pointing Accuracy:	±.05 degree	Same
Linked Spacecraft:	5 earth orbiting satellites with altitudes ranging from 200 to 1500 Km, any inclination - it is assumed that each has a reciprocal antenna system with similar gain and link accommodations	TDAS (Geosynchronous) and 5 earth ---
Special Required Features:	Antenna pointing and control system (APCS) - use of dedicated on-board microprocessors to maintain pointing accuracy. Autotrack Subsystem - required feature built into the APCS. Receiver/Transmitter Mounting - allowance for local mounting of receiver front end and transmitter final output stage directly at antenna sum channel port.	Same

Frequency - The choice of 60 GHz will give considerable relief on antenna sidelobe requirements since atmospheric attenuation at 60 GHz will nearly eliminate terrestrial interference and horizon multipath effects. Related to frequency is the question of RF bandwidth. The specified five 50 megabit channels require a bandwidth in the order of 5x.05 = 0.25 GHz representing only 0.4% relative bandwidth at 60 GHz. Thus, none of the antenna candidates should be bandwidth-limited. Selection of a frequency plan to enhance resistance to RFI caused by self and/or outside interference was not considered in this study.

Antenna Gain - 54 dB of antenna gain requiring 4' antennas, 1 watt of RF power and a mixer noise figure of 5 dB at 60 GHz providing a 50 megabit link represents a balanced system for today's state-of-the-art (see Appendix D for link budget).

Data Rate Capability - With Landsat D at 85 megabits and the planned UARS at 0.5 megabits - as typical examples - a wide range of data rates is encountered which will need to be accommodated at Ku and 60 GHz.

Linked Spacecraft - It should be noted that for the TDAS forward link, i.e. TDAS to user, the TDAS EIRP requirements for command and tracking may be quite modest - as low as 1 kbit data rate which is 47 dB below the specified 50 megabits.

Alternately the G/T requirement for a user satellite may be reduced accordingly. A further observation could be made: Since it is not realistic to assume that one single antenna system will accommodate TDAS and all possible future users, it is important that the selected design concept exhibit a maximum of design modularity and flexibility, e.g. a gimbal system that can handle various antenna sizes.

Field of View - A user FOV of $\pm 126^{o}$, while theoretically possible, may not be practical due to structural self interference.

1.3 Study Flow Plan

The Study Flow Plan which was followed for this study is shown in Figure 1-2. It depicts the iterative procedure (in Phase A) leading to the selection of the preferred antenna systems and a list of weighted performance parameters which were used to assess the candidates. The end result of this iterative process is a tradeoff matrix providing a score for each candidate.

For the selected antenna system a detailed conceptual design was performed. This design activity consisted of the electrical and mechanical antenna system configuration including antenna pointing, autotrack and control electronics as well as the impact on the host spacecraft. The industry technology development status was assessed for three critical items:

- Monopulse Front End
- Flexible Waveguide and
- RF Rotary Joints

FIGURE 1-2

STUDY FLOW PLAN

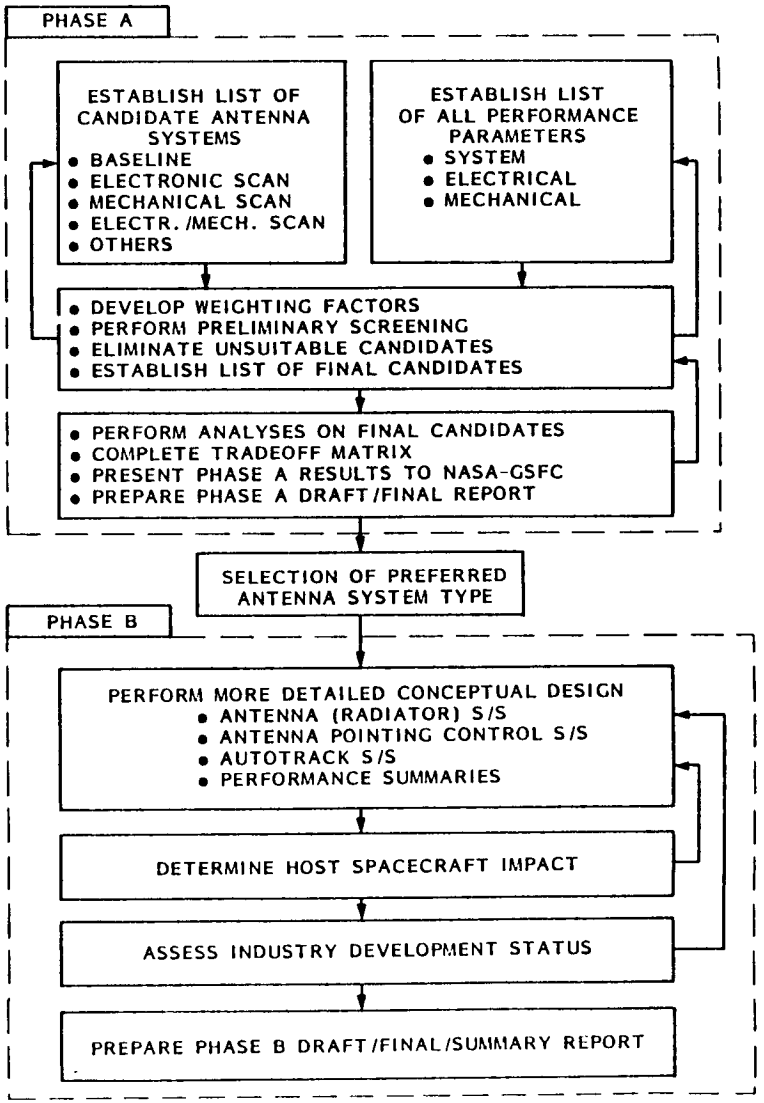

SECTION 2

PHASE A SUMMARY - TRADEOFF ANALYSIS

SECTION 2

PHASE A SUMMARY - TRADEOFF ANALYSIS

2.1 Candidate Antenna Systems

Four types of antenna systems were identified at the outset of the study and are shown schematically in Figures 2-1 to 2-4:

Figure 2-1: Type B - Reflector/Fixed Feed (4 candidates)
(Baseline)

Figure 2-2: Type M - Mechanical Scan (4 candidates)

Figure 2-3: Type E - Electronic Scan (3 candidates)

Figure 2-4: Type H - Hybrid Mechanical/Electronic Scan (1 candidate)

Type B (Baseline - Reflector/Fixed Feed (Figure 2-1)

This category is characterized by a fixed feed, i.e., a feed fixed with respect to a Cassegrain reflector system. In the case of B1 (beam waveguide) the feed is physically fixed to the spacecraft but a virtual feed moves with the reflector. B3 and B4 represent more conventional approaches using rotary joints or flexible waveguides to provide antenna articulation. In B2 all or part of the R.F. equipment is installed in a pallet on the reflector. Note that this is the only category with the potential for wide FOV (Configurations B1, B2 and B4). Since this category is inherently single-beam, 5 separate antenna systems are required to provide the 5 simultaneous links for TDAS.

Type M - Mechanical Scan (Figure 2-2)

In this second category beam scanning is accomplished by physical movement of a feed against a fixed reflector system (M1) or against a fixed lens (M2) or one reflector is moved against a fixed feed/reflector system (M3 and M4). To improve electrical performance over the scan range, dual reflector systems are used (M1 and M3) or a large F/D ratio is used (M2). M4 exhibits performance independent of scan except for physical limitations on the size of the scanned flat reflector. All four configurations are limited to a narrow FOV. M1 and M2 (with movable feeds) could accommodate multiple, independently moving feeds thereby providing multiple beams from a single reflector system. The practical implementation, however, is not feasible since feed handover and/or frequency multiplexing would be required whenever two satellite tracks cross-over. As in the first category five independent antenna systems would be required.

Type E - Electronic Scan (Figure 2-3)

In this third category beam scanning is accomplished exclusively by electronic means. No physical motion of feed or reflector(s) is involved. The configurations include pure phased arrays (E1) and phased array feeds with a fixed dual reflector system for optical magnification (E2) or a multibeam feed system with beamforming network in conjunction with a fixed, dual, folded reflector system. Electronic scanning is limited to the narrow FOV. (A spherical phased array with the potential for a wide FOV was eliminated early in the evaluation because of excessive size and weight.) This third category provides the potential for multiple independent beams from a single aperture. The complexities and attendant performance constraints involved with multiple beam formation are discussed for the various candidates. The special case of a

spherical reflector with a phased array feed was eliminated since its performance is inferior to the dual reflector approach of equal size and feed complexity.

Type H - Hybrid Electronic/Mechanical Scan (Figure 2-4)

This last category combines features of the two previous categories. Beam scanning is basically accomplished by a mechanical scan of a reflector in a dual reflector system such as M3. The resulting optical defocussing is compensated for by a fixed feed array incorporating a variable power divider and phasing network. Again only a limited FOV is available.

2.2 Weighted Performance Parameters

The selected performance parameters and their weights are shown in Table 2-2. These parameters were selected during the tradeoff process from an initially larger list as the most discriminating. Other performance parameters were eliminated as not applicable, e.g. "Commonality between GEO and LEO S/C". The antenna types clearly divide into two groups; one group with limited FOV which by definition does not have commonality and the other group with a large FOV which inherently has commonality.

Other performance parameters, such as gain, beam crossover, field of view, pointing accuracy and auto-track capability are not applicable because they are specified, i.e. they must be met. Ease or difficulty to achieve these parameters is reflected in other parameters such as cost, weight, volume, power etc.

Since the selected parameters are not all of equal importance weighting factors were assigned - at the technical discretion of General Electric. They range from a low importance of 1 to a maximum importance of 10, the highest being those

FIGURE 2-1

BASELINE TYPE

REFLECTOR/FIXED FEED

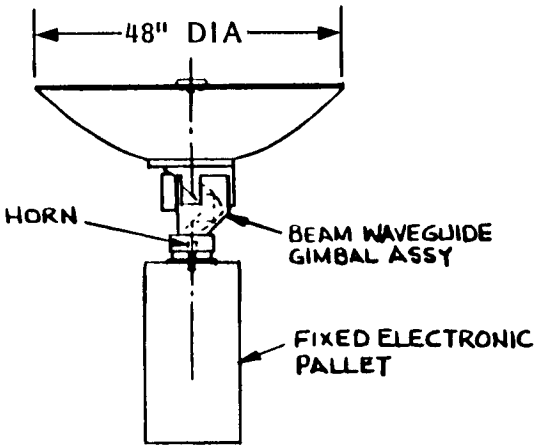

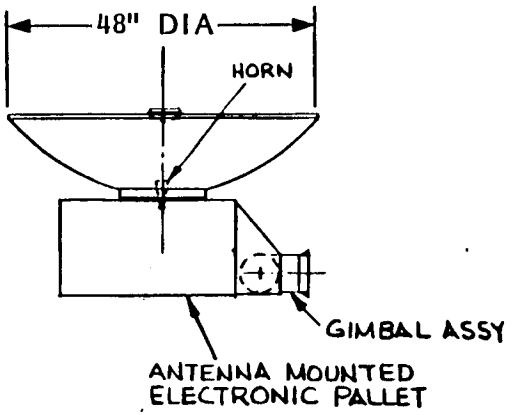

B1 BEAM WAVEGUIDE FEED, CASSEGRAIN

B2 FIXED FEED, CASSEGRAIN, ELECTRONICS PALLET

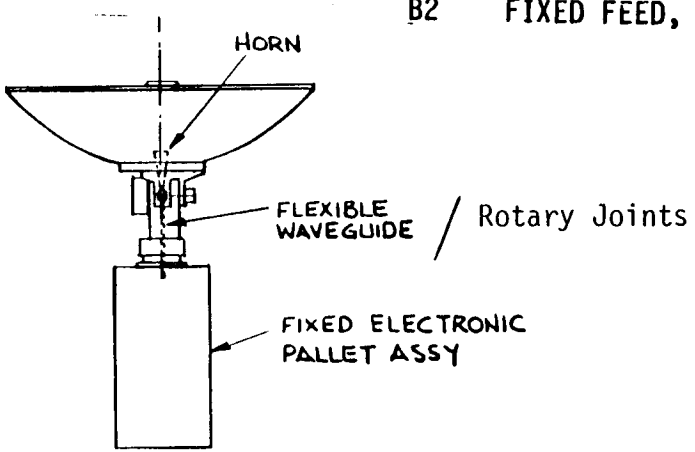

B3 FIXED FEED, CASSEGRAIN, FLEXIBLE WAVEGUIDE - 53" DIA

B4 FIXED FEED, CASSEGRAIN, ROTARY JOINTS - 69" DIA

FIGURE 2-2.

MECHANICAL SCANNING

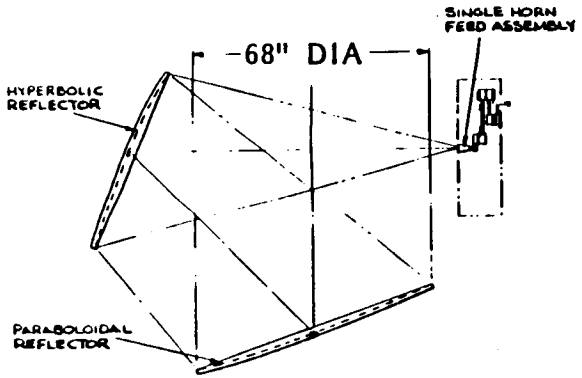

M1 MOVABLE FEED, DUAL REFLECTOR

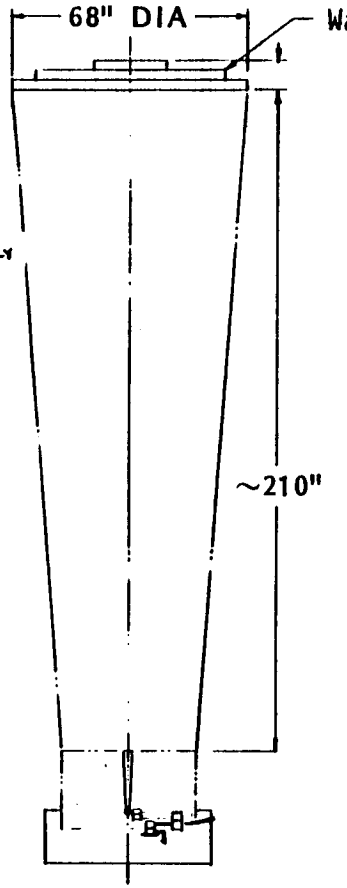

M2 MOVABLE FEED, LENS

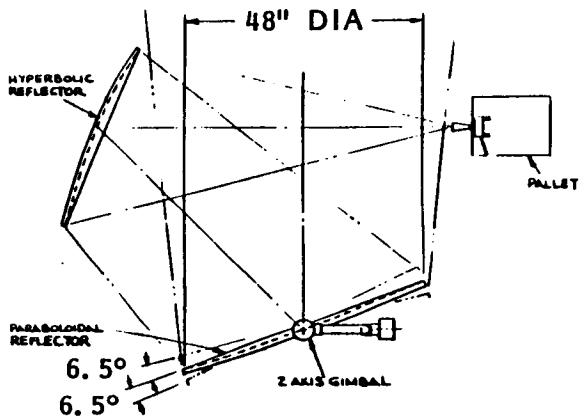

M3 FIXED FEED, DUAL REFLECTOR, MOVABLE PARABOLOID

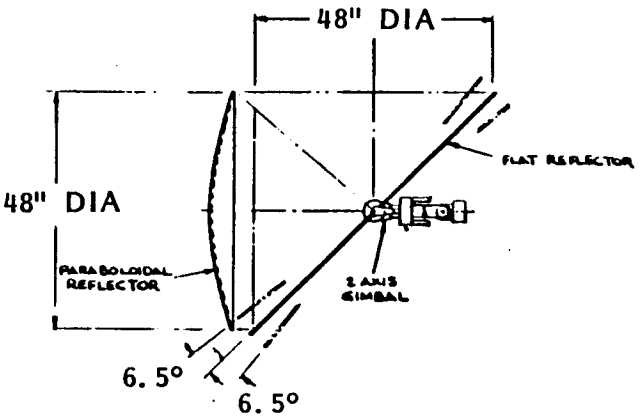

M4 FIXED FEED, DUAL REFLECTOR, MOVABLE FLAT PLATE

FIGURE 2-3

ELECTRONIC SCANNING

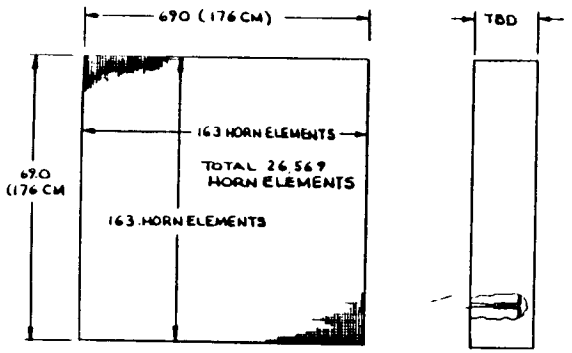

E1 PHASED ARRAY

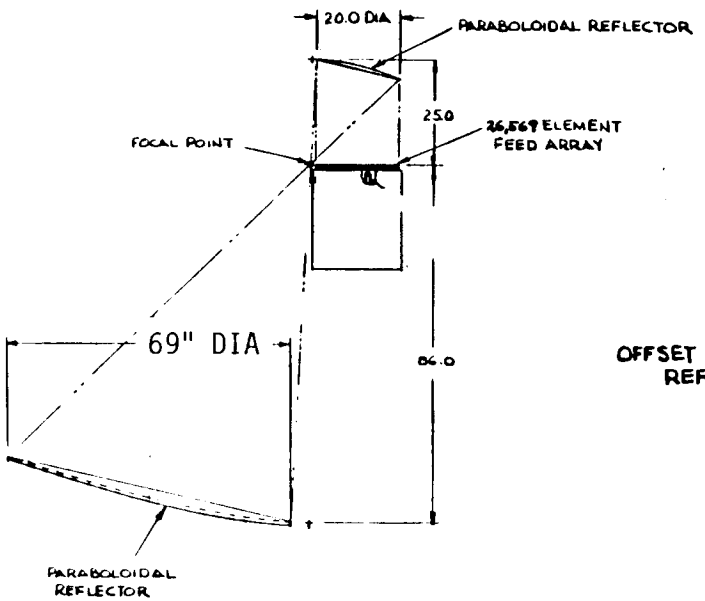

E2 MAGNIFIED PHASED ARRAY, DUAL REFLECTOR

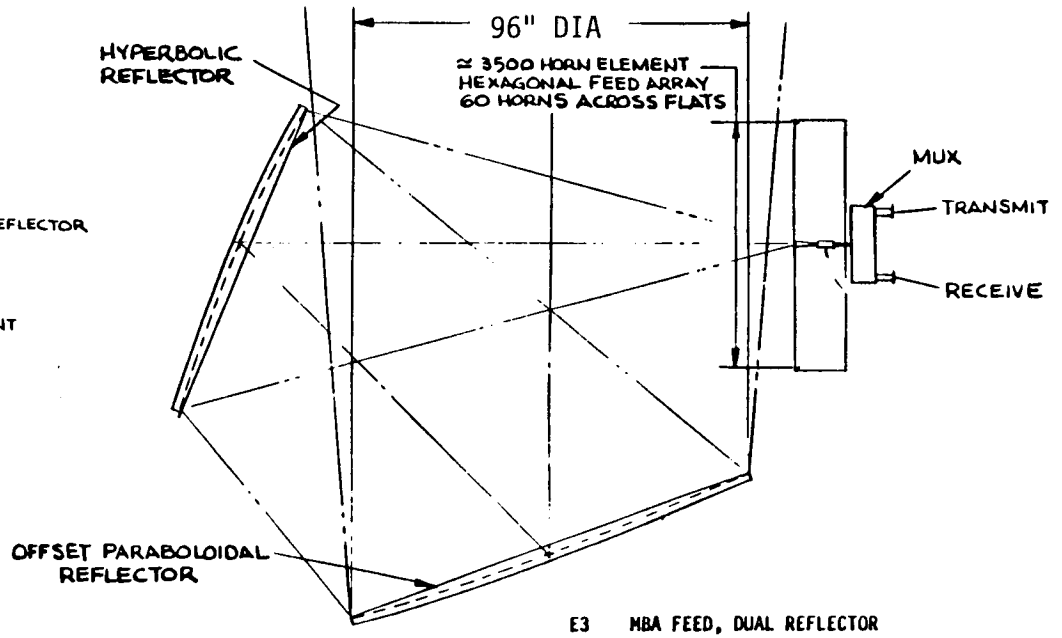

E3 MBA FEED, DUAL REFLECTOR

FIGURE 2-4

HYBRID

ELECTRONIC/MECHANICAL

SCANNING

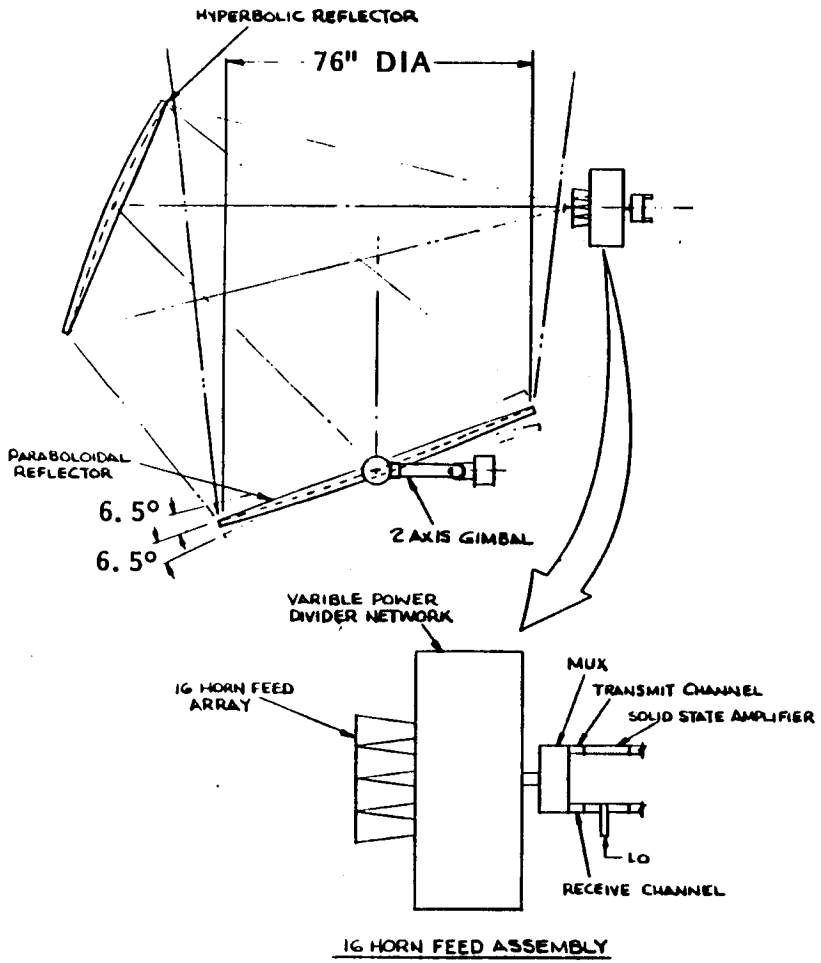

H1 ELECTRONICALLY ADJUSTABLE FEED, DUAL REFLECTOR, MOVABLE PARABOLOID

TABLE 2-2

WEIGHTING FACTORS

PERFORMANCE PARAMETER	WEIGHTING FACTOR
RELIABILITY	10
DEVELOPMENT RISK	9
STOWAGE	9
HOST S/C IMPACT	8
LOSS	8
WEIGHT	8
POWER	7
TORQUE NOISE	7
COST	5
INTEGRATION AND SYSTEM TEST IMPACT	5
ENVIRONMENT PROTECTION	5
PROCESSOR REQUIREMENTS	3
POLARIZATION PURITY	3
BEAMWIDTH	2
SIDELOBE LEVEL	1

which are most critical to achieving a successful mission with a system which includes a 60 GHz crosslink. In the following the selected parameters are defined in order.

- Reliability: Probability of cross-link providing 10 years service. Includes the internal redundancy of the sub-system. This parameter has the highest rank since all other parameters are unimportant if the sub-system does not survive.

- Development Risk: The probability that the design can be achieved during the time period of interest. Ranked high because an unobtainable system has no value.

- Stowage: The stowed volume of the antenna. Rated high since on small S/C or large ones with multiple antennas this parameter largely determines the useability of the antenna.

- Host S/C Impact: The effects on the S/C of the cross-link antenna except for those which are treated separately. Includes dynamic volume, inertial interaction, platform stability requirements, heat radiated into S/C. Ranked high because it causes penalties and cost at the system level.

- Loss: Attenuation between receiver input port, transmitter output port and antenna radiating surface. Ranked high since it is a direct measure of the efficiency of the antenna system.

- Weight/Power: Total sub-system weight and power requirement.

- Torque Noise: The effect of the acceleration of the moving portion of the antenna system on the spacecraft and payloads with excessive

pointing requirements (e.g., laser communication systems).

. Cost: Total relative sub-system cost exclusive of vehicle integration costs.

. Integration and System Test Impact: Cost of integrating antenna sub-system with S/C and cost of S/C system level testing of cross-link.

. Environment Protection: The inherent protection the design provides for the critical receiver, transmitter and antenna control electronics from the environment.

. Processor Requirements: The complexity of an antenna system dedicated processor.

. Polarization Purity: The amount of cross-polarization in the beam. Limits the isolation between two signals sharing the same RF-path. Small importance unless a system requires polarization reuse.

. Beamwidth: Low efficiency antennas must have the aperture enlarged to bring the gain up to 54 db. This results in narrower beamwidth and more difficult tracking and acquisition. Rated low because the beamwidth variation between antenna types is not large.

. Sidelobe Levels: Can effect reliability of acquisition and the isolation between multiple antennas. Importance is rated low because sidelobe and isolation effects are temporary and can be overcome by operational measures.

2.3 Phase A - Tradeoff Matrix

The complete tradeoff matrix is shown in Table 2-3. Each performance parameter was evaluated on a scale of 5 to 1, one at a time, for each of the antenna configurations. For best performance an individual score of 5 was assigned. For worst performance an individual score of 1 was assigned. Median performance was given a 3 with 2 and 4 given for in-between performance. Each configuration was then given a total weighted score by multiplying the individual score by the weighting factor and adding the columns, as shown in the example below for Configuration B1.

Weighting Factors	×	Individual Score	=	Weighted Score
10		4		40
9		3		27
5		3		15
8		5		40
5		5		25
2		5		10
1		5		5
3		5		15
8		5		40
3		4		12
9		5		45
8		5		40
7		5		35
5		5		25
7		3		21
Total Weighted Score				395

TABLE 2-3

PHASE A TRADEOFF MATRIX

PERFORMANCE PARAMETER	WEIGHTING FACTOR	BASELINE TYPE REFL.FIXED FEED				MECHANICAL SCANNING				ELECTRONIC SCANNING			HYBRID ELEC/ MECH SCANNING
CONFIGURATION NO.		B1*	B2*	B3	B4*	M1	M2	M3	M4	E1	E2	E3	H1
SYSTEM													
- RELIABILITY	10	4	3	2	3	1	1	4	5	4	3	1	2
- DEVELOPMENT RISK	9	3	3	2	1	1	1	2	5	1	1	1	1
- COST	5	3	2	3	2	1	1	3	4	1	1	1	2
- HOST SPACECRAFT IMPACT	8	5	4	3	2	2	1	2	3	1	1	1	2
- INT. & SYSTEM TEST IMPACT	5	5	2	3	3	3	3	5	5	4	4	4	5
ELECTRICAL													
- BEAMWIDTH	2	5	5	5	3	2	2	3	5	1	1	1	3
- SIDELOBE LEVEL	1	5	5	5	5	1	1	1	5	2	2	2	3
- POLARIZATION PURITY	3	5	5	5	5	2	2	2	4	1	1	1	3
- LOSS	8	5	5	2	1	2	2	3	5	1	1	1	2
- PROCESSOR REQUIREMENTS	3	4	5	5	5	4	4	4	4	2	2	1	1
MECHANICAL													
- STOWAGE	9	5	4	3	2	3	2	3	4	3	2	2	2
- WEIGHT	8	5	4	5	5	4	2	5	4	1	1	1	4
- POWER	7	5	2	4	4	4	4	5	5	1	1	1	4
- ENVIRONMENT PROTECTION	5	5	3	4	4	5	5	5	5	1	1	1	3
- TORQUE NOISE	7	3	1	3	2	4	4	3	3	5	5	5	2
WEIGHTED SCORE		395	298	289	249	234	201	311	392	185	166	143	224

* ONLY B1, B2 AND B4 HAVE THE LARGE FOV-CAPABILITY REQUIRED FOR USER SATELLITES

2.4 Ranking of Candidates

Table 2-4 shows the resulting ranking for candidates suitable for relay and user satellites. Only three of the baseline configurations qualify because of the scan requirements. Table 2-5 shows the resultant ranking for the first five candidates suitable for a relay satellite with a limited FOV requirement. Note that all 12 candidates are suitable for a relay satellite.

For both cases configuration B1, the beam waveguide antenna system scores highest and was therefore selected as the preferred system.

For the relay satellite case, configuration M4, the fixed feed/dual reflector/movable flat plate configuration is a close second.

2.5 Weight/Power/Volume Comparison

In addition to the weighted overall ranking of the candidates, it is instructive to compare their weight, power requirements and volumes. See Table 2-6. Weight is a significant factor since some of the candidates that we ranked close together on overall rankings, differ significantly in weight. For example, B2 is 37% heavier than B1 although they are ranked next to each other for TDAS use. Power input is similar for all the candidates except B2 again which requires 41% more than B1 and the phased arrays with their extreme power requirements. The volume requirements are very different for each candidate. In the case of the five candidates marked with an *, which can theoretically provide five simultaneous independent beams, it is worthwhile to compare one of them with five of the single beam designs. Two of the five (M1 and M2) have sufficiently reasonable weights and power requirements to be considered. However, in addition to all the practical problems of implementing these designs, as discussed later in the report, these antennas are more than three times as large as five B1's.

TABLE 2-4

RANKING OF CANDIDATES

DESIGNS SUITABLE FOR TDAS & USER S/C

RANK	WEIGHTED SCORE	CONFIGURATION #	CONFIGURATION
1	395	B1	BEAM WAVEGUIDE FEED, CASSEGRAIN
2	298	B2	FIXED FEED, CASSEGRAIN, ELECTRONICS PALLET
3	249	B4	FIXED FEED, CASSEGRAIN, ROTARY JOINTS

TABLE 2-5

RANKING OF CANDIDATES
DESIGNS SUITABLE FOR TDAS ONLY

RANK	WEIGHTED SCORE	CONFIGURATION #	CONFIGURATION
1	395	B1	BEAM WAVEGUIDE FEED, CASSEGRAIN
2	392	M4	FIXED FEED, DUAL REFLECTOR, MOVABLE FLAT PLATE
3	311	M3	FIXED FEED, DUAL REFLECTOR MOVABLE PARABOLOID
4	298	B2	FIXED FEED, CASSEGRAIN, ELECTRONICS PALLET
5	289	B3	FIXED FEED, CASSEGRAIN, FLEXIBLE WAVEGUIDE

TABLE 2-6.

WEIGHT/POWER/VOLUME COMPARISON

CONFIGURATION	#	WEIGHT (LBS.)	POWER (WATTS)	VOLUME (CU. FT.)
BEAM WAVEGUIDE FEED, CASSEGRAIN	B1	97	59	16
FIXED FEED, CASSEGRAIN, ELECT. PALLET	B2	133	83	30
FIXED FEED, CASSEGRAIN, FLEX WG	B3	101	64	21
FIXED FEED, CASSEGRAIN, ROTARY JOINTS	B4	122	64	56
*MOVABLE FEED, DUAL REF (SINGLE BEAM)	M1	138	64	253 (1)
*MOVABLE FEED, LENS (SINGLE BEAM)	M2	250	64	260 (1)
FIXED FEED, DUAL REF, MOVABLE PARA.	M3	115	59	99
FIXED FEED, DUAL REF, MOVABLE PLATE	M4	125	59	63
*PHASED ARRAY (SINGLE BEAM)	E1	3,660	10,117	59 (2)
*MAGNIFIED PHASED ARRAY, DUAL REF (SINGLE BEAM)	E2	3,639	10,117	169 (2)
*MBA FEED, DUAL REF	E3	325	59+	617 (1)
ELECT. ADJ FEED, DUAL REF, MOVABLE PARA.	H1	167	64	363

+ ADDITIONAL POWER OF PHASE SHIFTERS UNDETERMINED AT PRESENT
* THEORETICALLY CAPABLE OF 5 INDEPENDENT BEAMS

(1) ADD 41.7 LBS, 53.6 WATTS AND 2 CU. FT. PER ADDITIONAL BEAM
(2) ADD 421 LBS, 8000 WATTS AND 35 CU. FT. PER ADDITIONAL BEAM

2.6 Description of All Candidate Antenna Systems

In this section all 12 candidate antenna systems are described in detail. The major strengths (score of 5) and major weaknesses (score of 1) are listed for each system. Also, the loss is discussed and the related aperture size is given as well as estimated weight, power and volume.

- Weight includes the complete antenna and all fully redundant electronics. The electronics are based on a 1 watt RF transmit output level as outlined in the link budget in Appendix D.
- Power requirements include the RF electronics, gimbal (where applicable) and control electronics.
- Volume includes all electronics and the complete antenna including a 26° FOV swept volume for gimballed systems.

Configuration B1 - Beam Waveguide Feed/Cassegrain (Figure 2-5)

B1 is the classical beam waveguide configuration developed and used successfully on large ground station applications. The concept overcomes the limitations of waveguide rotary joints namely, high insertion loss and low power handling capacity. While power handling for mm wave applications is not demanding (about 1 watt), waveguide insertion loss and especially rotary joint insertion loss becomes prohibitive at 60 GHz. Theoretical attenuation in pure silver waveguide (WR 15) is 0.42 dB/ft. Attenuation in a conventional waveguide rotary joint in the same waveguide size, including required mode transitions and mode filter, is 1.2 dB or 2.4 dB for two rotary joints in a two-axis gimbal. In contrast a two-axis beam waveguide system can be designed to be nearly loss-free (0.2 dB), practically independent of the separation distance between upper and

lower axis. B1 is the clear winner for both narrow and wide FOV applications. The higher total score is due to highest individual scores in most of the heavily weighted parameters such as stowage, host S/C impact, weight, loss and power. It has no major weaknesses (score of 1). Its great advantage is also expressed by the high degree of flexibility and modularity:

- Various antenna diameters and antenna form factors (F/D, offset geometry) may be used with a given gimbal and support design.
- The gimbal tower height may be readily varied to accommodate FOV and S/C configuration requirements.
- The electronic pallet may be inside or outside the S/C envelope, in the latter case adding to the tower height.
- Interfaces between antenna/gimbal/electronics are simple and flexible.

This is the selected antenna system for which a detailed conceptual design was performed during Phase B, described in Section 3 of this report.

FIGURE 2-5

B1

BEAM WAVEGUIDE FEED, CASSEGRAIN

MAJOR STRENGTHS	WEIGHT
Usable TDAS & User	-
Stowage	9
Host S/C Impact	8
Weight	8
Loss	8
Power	7
Integration & System Test Impact	5
Environment Protection	5
Polarization Purity	3
Beamwidth	2
Sidelobe Levels	1

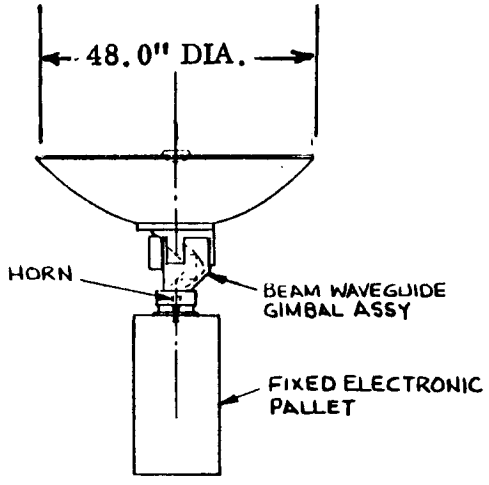

MAJOR WEAKNESSES	WEIGHT
None	-

WEIGHT (LBS)	POWER (W)	VOLUME (FT^3)
97	59	16

TOTAL SCORE

395

Configuration B2 - Fixed Feed/Cassegrain/Electronics Pallet (Figure 2-6)

In this configuration all the mm wave components are contained in the pallet that is fixed mounted to the reflector. Here the beam waveguide gimbal assembly with its small loss is eliminated, but the aperture remains practically the same. The swept volume is increased as a result of the motion of the antenna mounted pallet.

B2 scores considerably lower and ranks 4th. Its only important major strength is the low loss. Again there are no major weaknesses and weight and power compare well with B1. With the electronics unprotected by the S/C envelope and illuminated by the sun from all sides while scanning this configuration requires a complex, multi-dimensional heat pipe temperature control system to insure low noise-figure receiver performance. This has a severe negative impact on both system integration and test and hence cost. In terms of functional electrical performance B2 equals B1 and the comments made on modularity and flexibility apply equally here.

The processed signal transmission lines must go through the two gimbal axes on route to the spacecraft electronics. They must flex or be provided with rotary joints to withstand the orbital life requirements. The gimbal location on the pallet, as shown, will cause center of gravity motion of the antenna assembly during slewing, which would have an increased effect on spacecraft pointing.

FIGURE 2-6

B2

FIXED FEED, CASSEGRAIN, ELECTRONICS PALLET

MAJOR STRENGTHS	WEIGHT
Usable TDAS & User	-
Loss	8
Processor Requirements	3
Polarization Purity	3
Beamwidth	2
Sidelobe Level	1

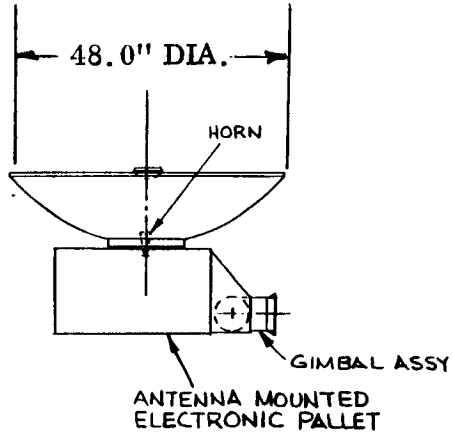

MAJOR WEAKNESSES	WEIGHT
Torque Noise	7

WEIGHT (LBS)	POWER (W)	VOLUME (FT^3)
133	83	30

TOTAL SCORE

298

Configuration B3 - Fixed Feed/Cassegrain/Felexible Waveguide (Figure 2-7)

In this configuration the beam waveguide of B1 is replaced by flexible waveguide. The flex angle/lifetime of this joint is a function of the length of the flexible waveguide. In a practical sense this configuration is limited for a relay application only ($\pm 13^{o}$ FOV). A 0.8 dB additional insertion loss was assumed for this flexible waveguide forcing a 10% increase in aperture diameter.

The flexible waveguide approach appears like a straightforward, simple solution for a narrow FOV application. However, the detailed evaluation results in low scores for many important parameters. Reliability is largely unknown and development efforts have so far been less than successful. Additional investigation during Phase B has confirmed that development risk and cost are uncertain at this time. An acceptable penalty in electrical performance is the additional flexible waveguide loss which can be recovered by an increase in antenna aperture at relatively little cost in weight and power. The implementation of a monopulse type autotrack system, however, leads to great complexity. Parallel flexible waveguides are now required or monopulse error signal processing must be accomplished in an environmentally controlled pallet mounted to the reflector. Transmit/Receive signal stability and monopulse accuracy would be critically affected by multiple flexible waveguides. It also becomes clear that design modularity and flexibility is greatly reduced by a complex interface situation.

FIGURE 2-7

B3

FIXED FEED, CASSEGRAIN, FLEXIBLE WAVEGUIDE

MAJOR STRENGTHS	WEIGHT
Polarization Purity	3
Processor Requirements	3
Beamwidth	2
Sidelobe Level	1

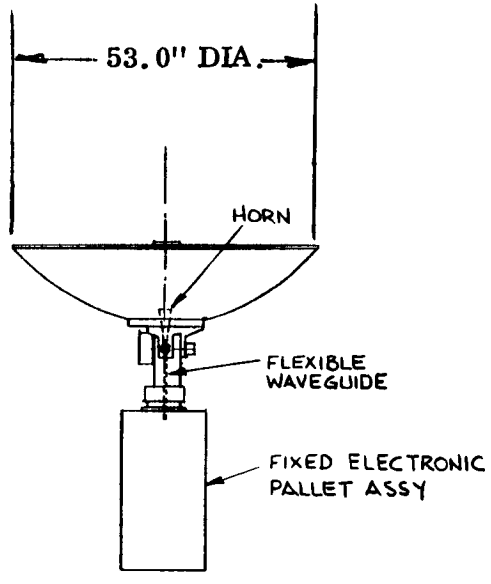

MAJOR WEAKNESSES	WEIGHT
Usable TDAS Only	-

WEIGHT (LBS)	POWER (W)	VOLUME (FT^3)
101	64	21

TOTAL SCORE

289

Configuration B4 - Fixed Feed/Cassegrain/Rotary Joints (Figure 2-6)

Configuration B4 replaces the flexible waveguide of B3 with rotary joints, one for each axis, providing the large FOV required for user application. The penalty as discussed above is insertion loss: two rotary joints (2.4 dB) and additional interconnecting waveguide (0.8 dB) result in 3.2 dB insertion loss. To recover this loss the antenna diameter has to be increased by a factor of 1.45 (69" instead of 48" for B1).

The increased aperture produces a severe ripple effect into weight, power and swept volume (especially for the full FOV). The monopulse complexity is similar to B3, but stacking of multiple rotary joints is feasible.

It is important to note, however, that for links with a more modest data rate requiring less antenna gain the lossy rotary joint solution may be very acceptable. This is especially true for the case where the antenna beamwidth has increased to a value where command pointing becomes feasible and monopulse tracking is no longer required.

To achieve the specified antenna gain of 54 dB it would be very important to improve the rotary joint loss performance. During Phase B this potential was investigated and is further discussed in Section 4.3 of this report.

FIGURE 2-8

B4

FIXED FEED, CASSEGRAIN, ROTARY JOINTS

MAJOR STRENGTHS	WEIGHT
Usable for TDAS & User	-
Polarization Purity	3
Processor Requirements	2
Sidelobe Level	1

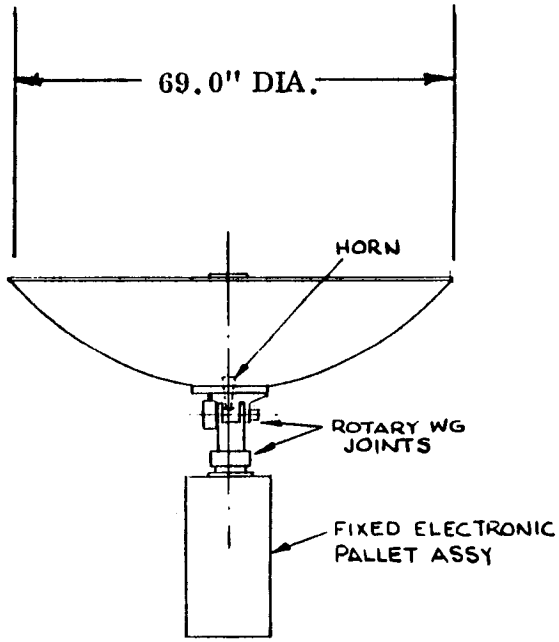

MAJOR WEAKNESSES	WEIGHT
Development Risk	9
Loss	8

WEIGHT (LBS)	POWER (W)	VOLUME (FT^3)
122	64	56

TOTAL SCORE

249

The following four configurations M1 to M4 are mechanical scan types. It must be pointed out that for all the mechanical scan systems, except for M4, there is a beam distortion that increases with scan angle. For any of these configurations further study of the effect of this distortion on the monopulse autotrack performance would be required. For example, the use of a single horn TE_{21} mode attitude sensor might be less attractive than it appears for the baseline approaches. For the hybrid configuration (H1), a multihorn sensor might be considered, but distortion effects might be serious in that case, as well.

Configuration M1 - Moveable Feed, Dual Reflector (Figure 2-9)

The combined loss of the rotary joints and of the $\pm 13^{\circ}$ beam scan is optimistically assessed at 3 dB, increasing the required aperture of the paraboloid reflector from 48" to 68".

This configuration would require a feed positioning mechanism that would border on being impractical. Not only does the feed horn have to be positioned in two orthogonal directions, it must also be tilted in angle for each particular position to minimize spillover losses. The rotary joints and waveguide losses would certainly be excessive penalties to pay for the use of this concept. In addition, two large precision reflector surfaces are required instead of one which adds to the complexity of an already complicated concept.

The dual reflector folded optics provides the equivalent of a very large F/D ratio ($F/D \sim 5$) and keeps the scan loss to less than 1/2 dB.

FIGURE 2-9

M1

MOVABLE FEED, DUAL REFLECTOR

MAJOR STRENGTHS	WEIGHT
Environment Protection	5

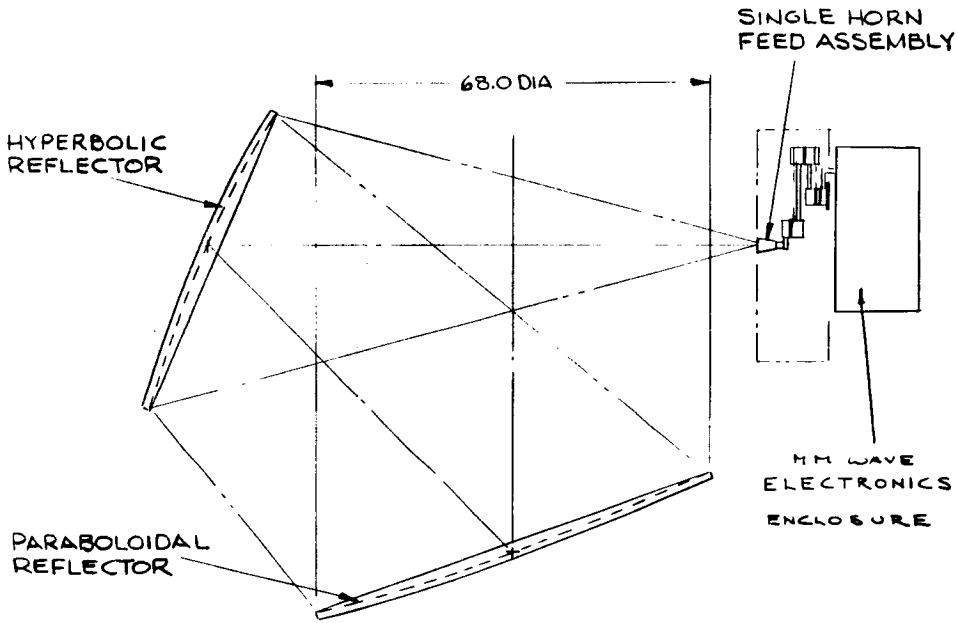

MAJOR WEAKNESSES	WEIGHT
Usable TDAS Only	-
Reliability	10
Development Risk	9
Cost	5
Sidelobe Level	1

WEIGHT (LBS)	POWER (W)	VOLUME (FT^3)
138	64	253

TOTAL SCORE

234

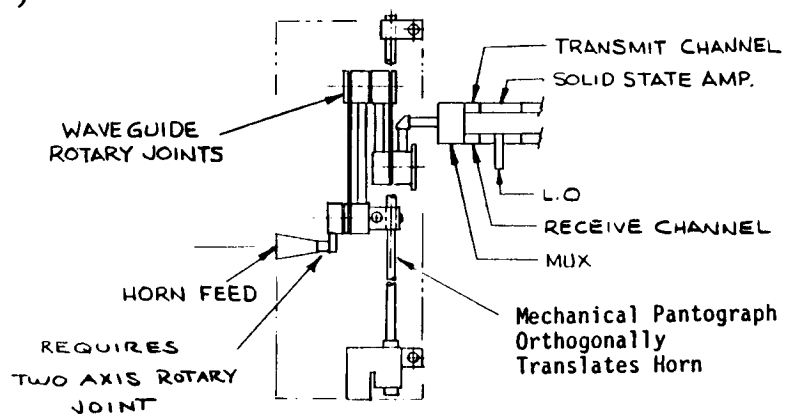

HORN FEED AND TRANSPORT MECHANISM

Configuration M2 - Movable Feed, Lens (Figure 2-10)

This waveguide lens approach is dimensioned for comparable performance to M1. Both aperture diameter and focal length are becoming excessive.

This configuration contains all the disadvantages of the M1 concept for the horn feed and transport mechanism. In addition, its total length and volume make this concept impractical for spacecraft integration.

FIGURE 2-10

M2

MOVABLE FEED, LENS

MAJOR STRENGTHS	WEIGHT
Environment Protection	5
MAJOR WEAKNESSES	**WEIGHT**
Usable TDAS Only	-
Reliability	10
Development Risk	9
Host S/C Impact	8
Cost	5
Sidelobe Level	1

WEIGHT (LBS)	POWER (W)	VOLUME (FT^3)
250	64	260

TOTAL SCORE

201

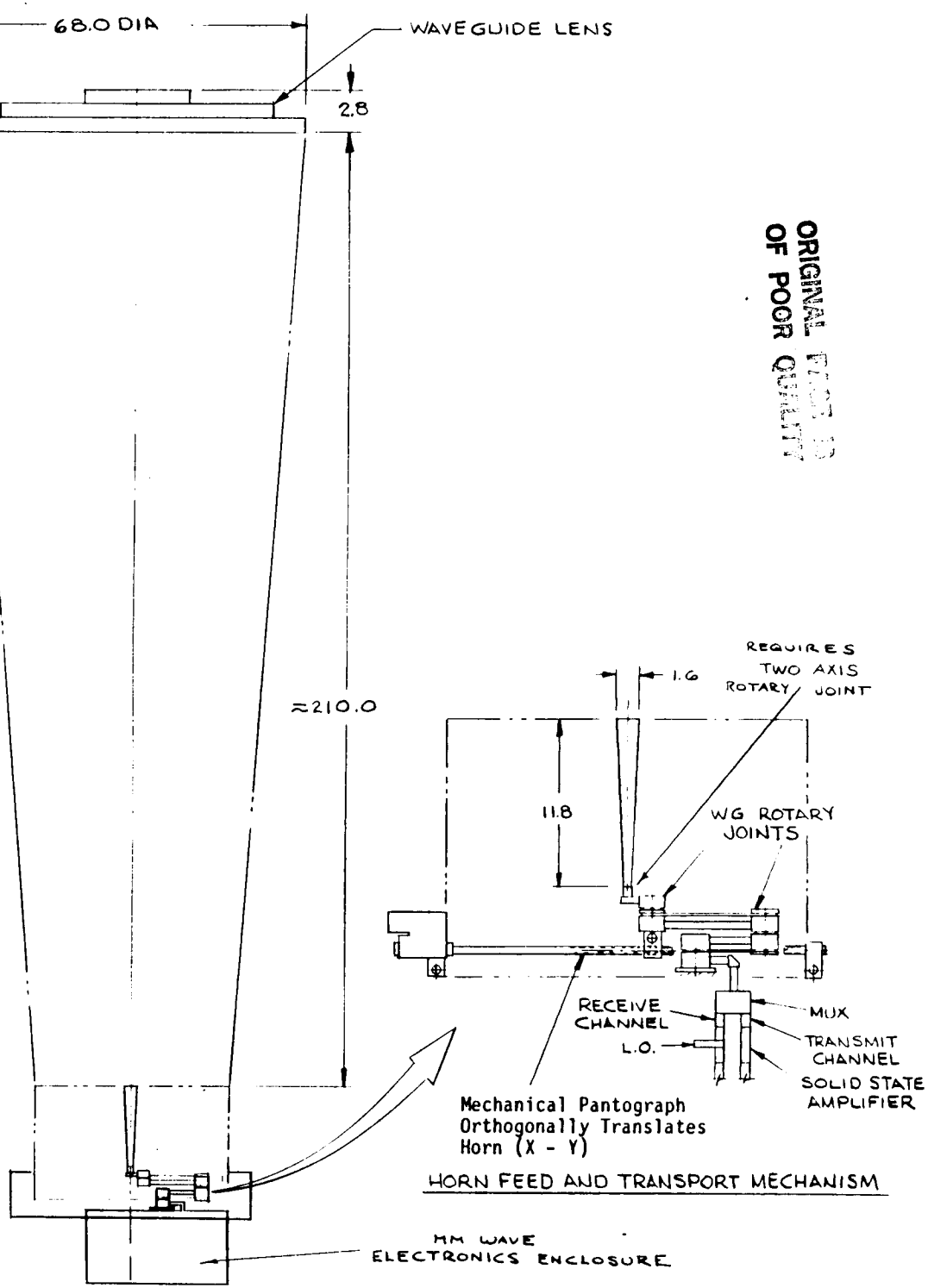

Configuration #3 - Fixed Feed, Dual Reflector, Movable Paraboloid (Figure 2-11)

This fixed feed concept without rotary joints is quite efficient. The large equivalent focal length of the folded optics keeps the scan loss small and the projected aperture remains at 48". The gimballed paraboloid reflector is elliptical in contour, approximately 61" x 53".

This configuration requires two large precision reflector surfaces and support structure to support them and maintain alignment. In addition, its geometry prohibits large FOV capability, and requires a large stowage volume for spacecraft integration.

FIGURE 2-11

M3

FIXED FEED, DUAL REFLECTOR

MOVABLE PARABOLOID

MAJOR STRENGTHS	WEIGHT
Power	7
Environment Protection	5
Integration & System Test Impact	5

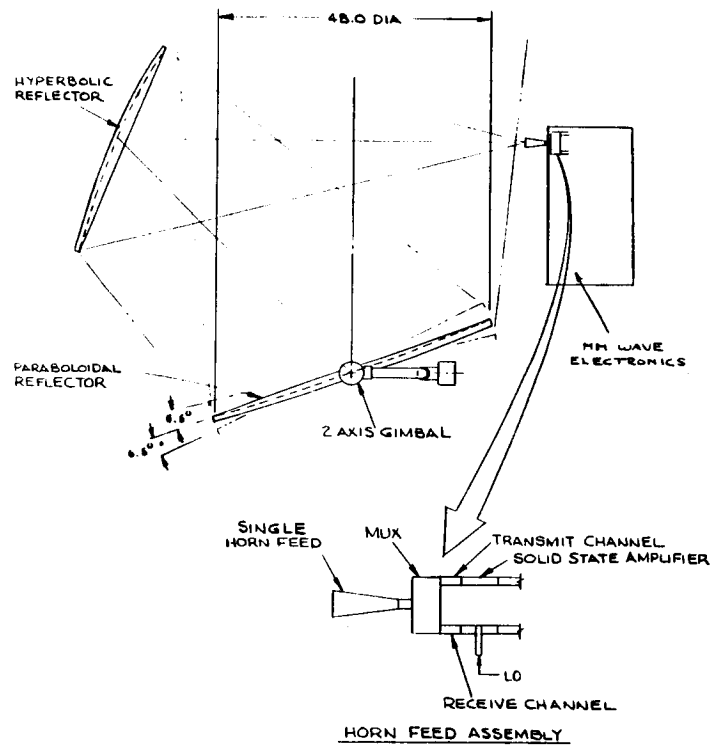

HORN FEED ASSEMBLY

MAJOR WEAKNESSES	WEIGHT
Usable TDAS Only Sidelobe Level	1

WEIGHT (LBS)	POWER (W)	VOLUME (FT^3)
115	59	99

TOTAL SCORE

311

Configuration M4 - Fixed Feed, Dual Reflector, Movable Flat Plate (Figure 2-12)

A fixed (deployed) paraboloid reflector and a fixed feed are used to form the beam which is then reflected by the flat reflector mounted on the 2-axis gimbal. Moving the flat reflector by 1^{o} deflects the beam by 2^{o} so that a gimbal angle of only $\pm 6.5^{o}$ provides the required beam scan of $\pm 13^{o}$. If the flat reflector is made large enough to simulate an infinite flat plane no beam degradation with scan is experienced.

This is an attractive candidate with proven performance on the MIT Lincoln Lab LES 8/9 satellites. However, the configuration requires two precision reflector surfaces (one of which is flat), a deployment mechanism for the reflectors and 2-axis gimbal and hence a rather large stowage volume.

As for M3 the projected aperture remains at 48", whereas the gimballed flat reflector, nominally positioned at 45^{o}, is elliptical in contour, measuring approximately 75" x 53".

FIGURE 2-12

M4

FIXED FEED, DUAL REFLECTOR MOVABLE FLAT PLATE

MAJOR STRENGTHS	WEIGHT
Reliability	10
Development Risk	9
Loss	8
Power	7
Environment Protection	5
Integration & Sys. Test Impact	5
Beamwidth	2
Sidelobe Level	1

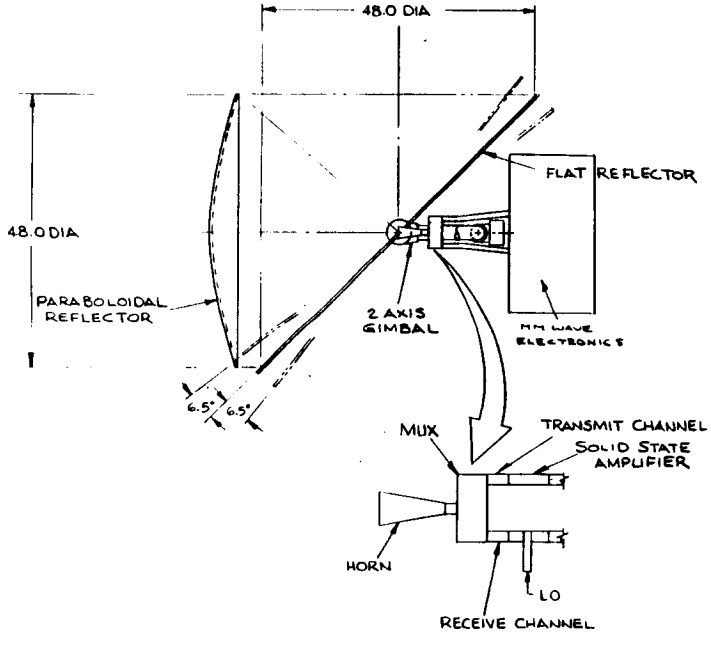

HORN FEED ASSEMBLY

MAJOR WEAKNESSES	WEIGHT
Usable TDAS Only	-
None	

WEIGHT (LBS)	POWER (W)	VOLUME (FT^3)
125	59	63

TOTAL SCORE

392

The following three configurations E1 to E3 are electronic scan types.

Configuration E1 - Phased Array (Figure 2-13)

As described in detail in the Phase A report the large size of this array is driven by the attempt to achieve 54 dB of peak gain over the coverage area with a single transmit/receive aperture with shared phase shifters. If separate transmit and receive apertures are used, the size of each aperture can be substantially reduced.

For the transmit phased array, the phase shifter (with a loss of 3 dB - see Phase A report) can be moved to the low power side of the amplifier, the filter requirements would be substantially eased resulting in about 0.2 dB loss, and no circulator (0.2 dB loss) is needed. This reduction of 4.0 dB of loss between the amplifier output and the horn element means that a transmit array of about 10,000 elements would be adequate (44" x 44"). For the receive array, the phase shifter must still be between the horn and the summing network to avoid the requirement for thousands of mixers, low noise amplifiers, and a means of generating thousands of coherent mm LO signals (i.e. generating 10 W at 40 GHz and dividing it 12,600 ways with a low loss waveguide power divider). The phase shifter can be a ferrite, non-reciprocal device, however, with only 1.0 dB of loss. The receive array could be realized with about 12,600 horns (48" x 48"). Thus by using separate transmit and receive arrays, the total number of horns required would be reduced by about 15%. The DC to RF efficiency would be increased 2.5 times, the antenna beamwidth would increase by 63%, and thermal and mechanical assembly problems would be eased. The implications of multibeam operation from a single array are discussed in Appendix A of the Phase A report.

The list of major weaknesses speaks for itself. The large number of elements to provide 54 dB of gain over a scan angle of +13Y002oZ002 is an overwhelming disadvantage which cannot be made up by the two advantages of beam agility and inertia-free beam scan.

One other factor must be considered in the use of a phased array: The power consumed by the phase shifter and its associated circuitry. At the present state-of-the-art, diode 5 bit phase shifters require about 100 mw of continuous power. Not only must provision be made to supply the required 2 to 3 kw of power per array but the thermal problem arising from the phase shifters would exceed that of the amplifiers and would require a large dedicated radiator area. Using separate arrays for transmit and receive with non-reciprocal, latching ferrite phase shifters eliminates the problem of high average power but high peak power is still required for the phase shifters.

FIGURE 2-13

E1

PHASED ARRAY

MAJOR STRENGTHS	WEIGHT
None	-

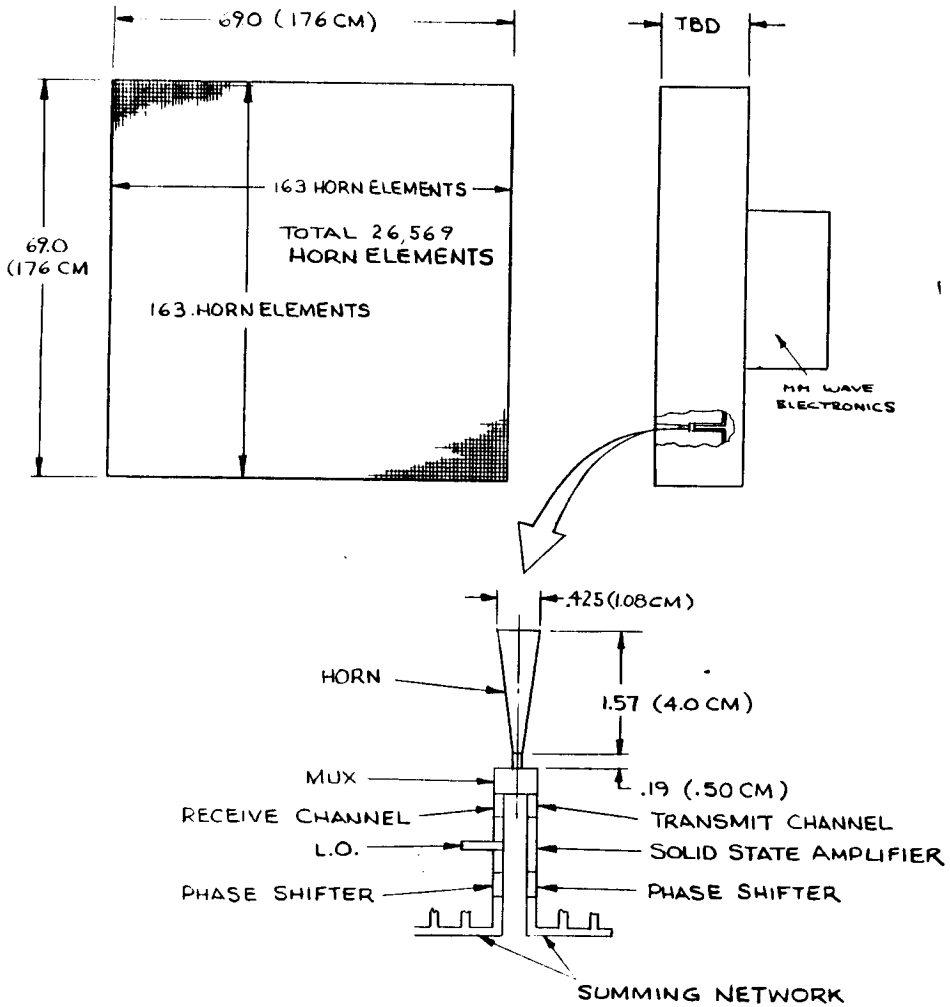

MAJOR WEAKNESSES	WEIGHT
Usable TDAS Only	-
Development Risk	10
Loss	8
Weight	8
Host S/C Impact	8
Power	7
Cost	5
Environment Protection	5
Polarization Purity	3
Beamwidth	2

WEIGHT (LBS)	POWER (W)	VOLUME (FT^3)
3660	10,117	59

TOTAL SCORE

185

Configuration E2 - Magnified Phased Array (Figure 2-14)

In a magnified phased array, the magnified image of a reduced size array appears in the aperture plane of the large paraboloid.[1] The size of this image, and thus the size of the large paraboloid, is defined by the size of an unmagnified array that can meet the performance requirements. This size was determined for configuration E1 as a 69" square. For this reason as well as those discussed in the next paragraph, the 69" diameter shown in the figure is probably too small.

The use of dual confocal paraboloids as shown (or lens arrangements) has been studied[1, 2] as a means to "magnify" a small (low gain) array so as to function as a larger (higher gain) phased array. This approach offers little for the present application.

The magnified phased array is subject to all the limitations and restrictions as the basic phased arrays previously discussed. For example, for a perfect optical system the same number of components would be required but each feed horn aperture might be reduced in size by a factor of 3, at a cost of two precision reflectors and increasing the required scanning angle by three. The smaller feeds and wider scan angles will lead to serious mutual coupling problems. In addition, the optics are not perfect[2]. Spillover and scan distortions, especially in the plane of symmetry, would require an increase in the number of elements over that of the basic phased array to overcome the gain loss. Studies have shown[2] that for the same beamwidth, only a few degrees of scan are possible without substantial scan loss (i.e., for a magnification of 3 and a scan of 2.3 degrees about 8 dB of scan loss can be expected). No practical way of achieving 13 degrees of scan with 54 dB of edge of scan gain can be seen at present with this method.

1) "Imaging Reflector Arrangements to Form a Scanning Using a Small Array", by C. Dragon and M. J. Gans, the BELL SYSTEM TECHNICAL JOURNAL, Vol. 58, No. 2, Feb. 1979, pp. 501-515.

2) "Phased-Array-Fed Antenna Configuration Study", by R. M. Sorbello, A. I. Zaghloul, B. S. Lee, S. Siddiqi, B. D. Geller, COMSAT LABORATORIES, Final Report, submitted to NASA Lewis Research Center, Oct. 1983. Contract No. NAS3-23250, Report Nos. CR 168231/2.

FIGURE 2-14

E2

MAGNIFIED PHASED ARRAY, DUAL REFLECTOR

MAJOR STRENGTHS	WEIGHT
None	-

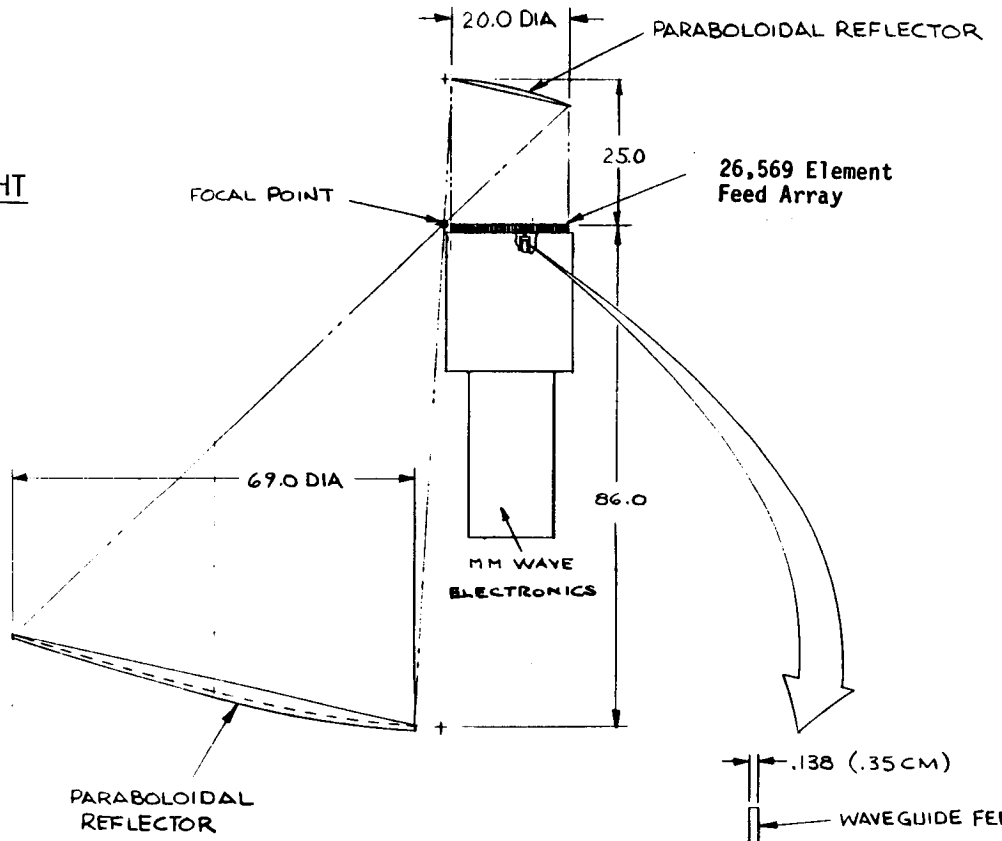

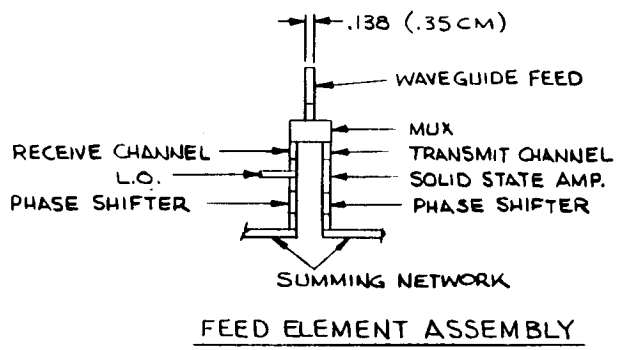

FEED ELEMENT ASSEMBLY

MAJOR WEAKNESSES	WEIGHT
Usable TDAS Only	-
Development Risk	9
Loss	8
Weight	8
Host S/C Impact	8
Power	7
Cost	5
Environment Protection	5
Polarization Purity	1
Beamwidth	1

WEIGHT (LBS)	POWER W)	VOLUME (FT^3)
3,639	10,117	169

TOTAL SCORE

166

Configuration E3 - MBA Feed, Dual Reflector (Figure 2-15)

The large aperture size of this configuration is driven by the minimum gain required in conjunction with all the loss mechanisms described in detail in the Phase A report. It can be seen that the two very large precision reflectors along with thousands of feeds and the complex beam forming network results in a system with nothing to recommend it. It also depends upon the development of a reciprocal, low loss variable power divider and phase shifter which does not yet exist at 60 GHz.

FIGURE 2-15

E3

MBA FEED, DUAL REFLECTOR

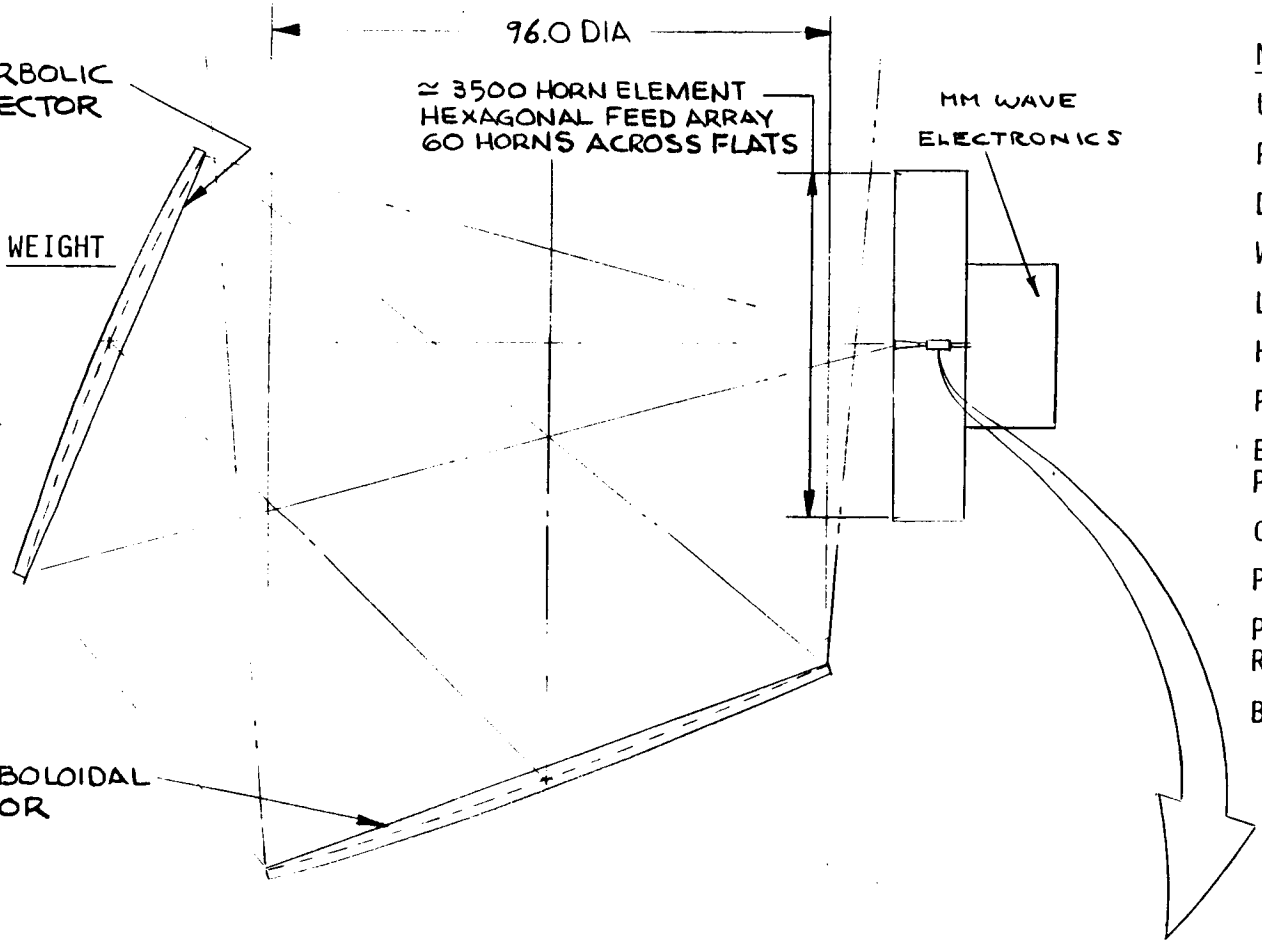

MAJOR STRENGTHS	WEIGHT
None	

MAJOR WEAKNESSES	WEIGHT
Usable TDAS Only	-
Reliability	10
Development Risk	9
Weight	8
Loss	8
Host S/C Impact	8
Power	7
Environment Protection	5
Cost	5
Polarization Purity	3
Processor Requirements	3
Beamwidth	2

WEIGHT (LBS)	POWER (W)	VOLUME (FT^3)
325	59 +	617

TOTAL SCORE
143

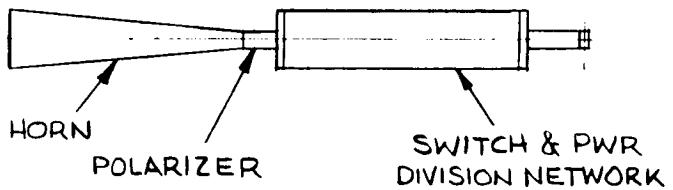

HORN ELEMENT ASSEMBLY

+ADDITIONAL POWER OF PHASE SHIFTERS IS IMPOSSIBLE TO ASSESS NOW

Configuration H1 - Electronically Adjustable Feed, Dual Reflector, Movable Paraboloid (Figure 2-16)

The large aperture size of this configuration is required to achieve the specified gain through a layer of phase shifters and two layers of variable power dividers, or more.

At least two levels of variable power dividers are required for a four feed array. This would be the minimum feed array that would allow for fine beam pointing by electronic means. An insertion loss of 2 dB for the divider tree must be provided for by an increase in aperture diameter of 26%.

If it is desired to compensate for beam distortion due to scanning, at least a seven element ring array feed should be employed. This will require three levels of variable power dividers and in addition a variable phase shifter behind each horn is needed. This adds up to 4 dB of insertion loss, or an aperture diameter increase of 58%, from 48" to 76". As in the case of the MBA antennas, 60 GHz reciprocal variable power dividers are required for this approach and they have not yet been demonstrated.

In this approach the beam deterioration and sidelobe increase with beam scan of the M3 configuration can be substantially compensated for by use of a multiple feed array in which the phase and amplitude distribution is varied with the scan angle. This requires a reciprocal phase shifter behind each feed and at least two levels (for a four feed array) of reciprocal variable power dividers which are new component developments. The losses in this beam forming network must be compensated for by an increase in aperture size over the M3 size.

FIGURE 2-16

H1

ELECTRONICALLY ADJUSTABLE FEED, DUAL REFLECTOR, MOVABLE PARABOLOID

MAJOR STRENGTHS	WEIGHT
Integration & System Test Impact	5

MAJOR WEAKNESSES	WEIGHT
Usable TDAS Only Development Risk	9
Processor Requirements	3

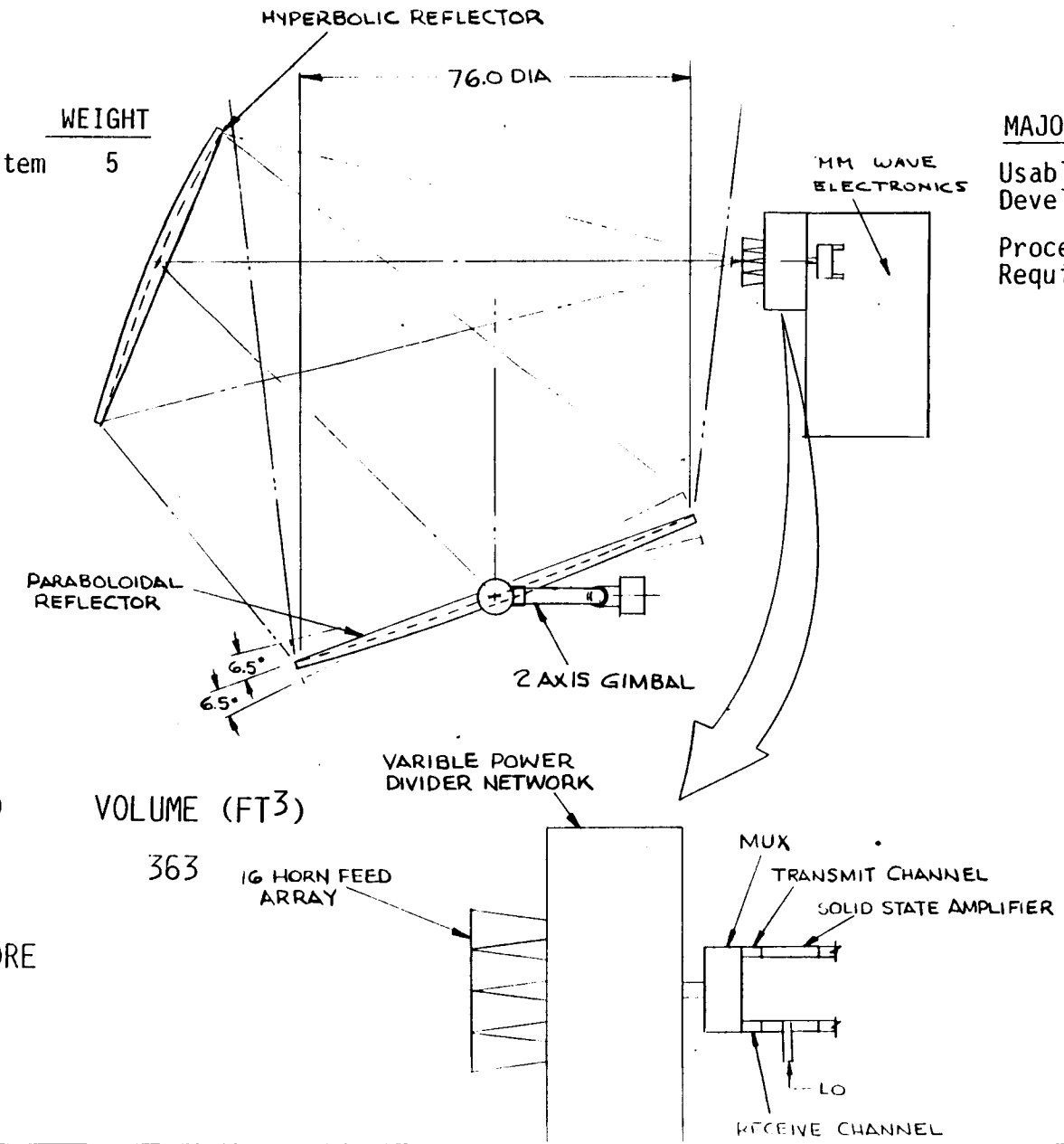

WEIGHT (LBS)	POWER (W)	VOLUME (FT^3)
167	64	363

TOTAL SCORE

224

2.7 Selection of Preferred Antenna System

On the basis of its highest score the beam waveguide antenna system (Configuration B1/Figure 2-5) was selected as the preferred system for further study during Phase B. Its main advantages are summarized below:

- It is applicable to both relay and user satellites and generally to any spacecraft requiring intersatellite links.
- Its field of view is unlimited except for physical selfinterference depending on reflector size and mounting tower height.
- It provides flexibility due to its modularity, i.e. the beam waveguide gimbal system can accommodate various relector sizes and can be adapted to other frequency ranges, including multiple frequency ranges.
- It scores highest in most electrical and mechanical performance parameters and also with respect to host spacecraft impact, integration and system test impact.
- It has no unknown development risks and is fully within the accepted state of the art. Its development cost and schedule can be reliably predicted for a given application.
- Its high RF efficiency results in minimum antenna aperture size and overall power for a given link capacity.
- It provides inherent protection against the space environment for sensitive RF and control circuitry.

APPENDIX C

FIELD OF VIEW REQUIREMENTS FOR GEOSYNCHRONOUS AND USER SATELLITES

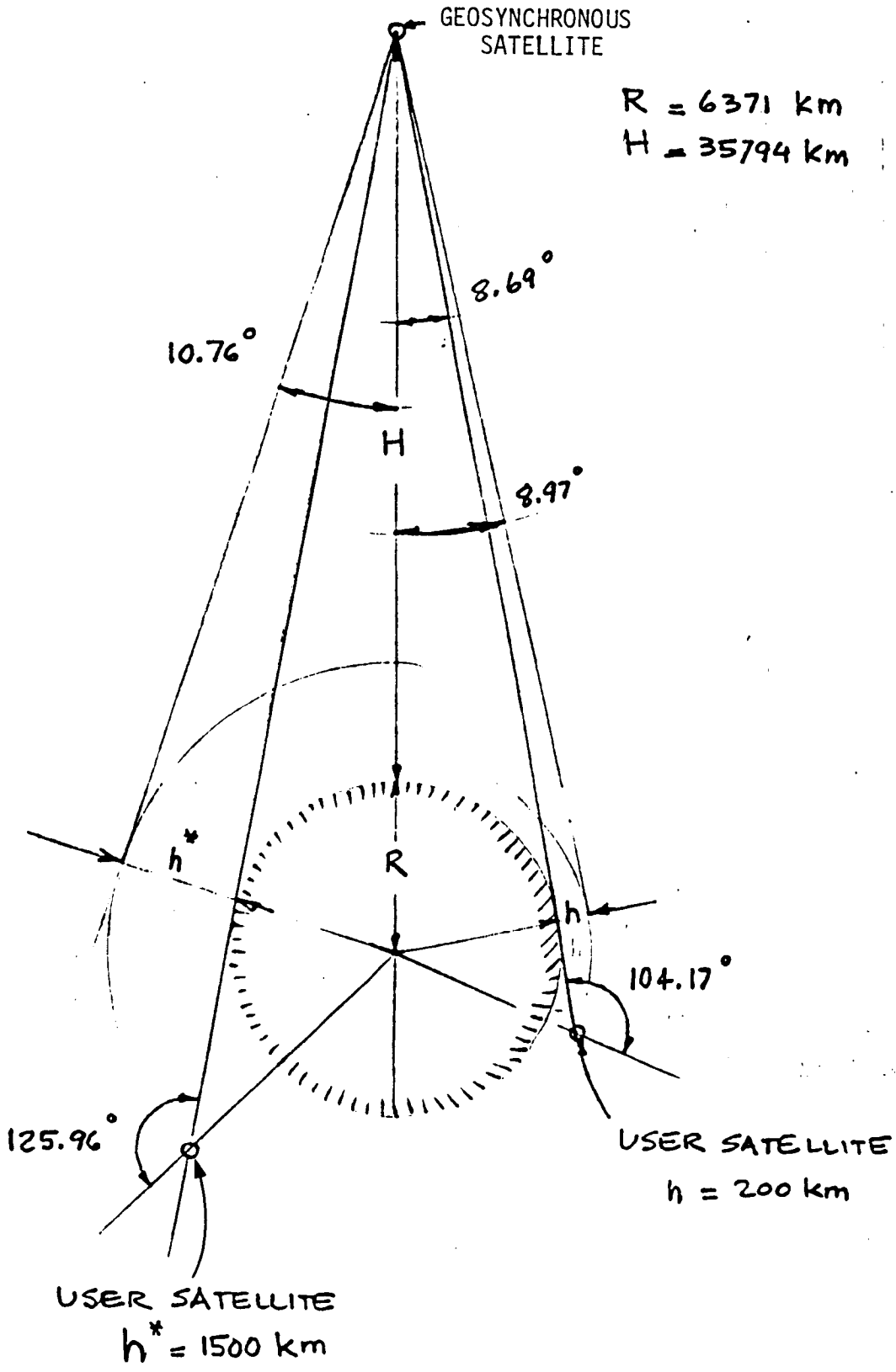

APPENDIX D

LINK BUDGET

Transmit Power	P_T (dBW)
Transmit Antenna Pk. Gain	54 dB
Pointing Loss	-0.1 dB
Free Space Loss	-221.3 dB (36.6 + 20 log f + 20 log d)
Receiver Antenna Gain	54.0 dB
Receiver Pointing Loss	-0.1 dB
Polarization Loss	-0.1 dB (2 dB Axial Ratio)
Noise Power Density	-198.1 dBW/Hz
Available P_r/N_0	(84.5 + P_T) dBW/Hz
Data Rate 50 MBps	77 dB
Eb/N_0 @ 10^{-7} BER	4.8 (R = 1/2, K = 7 Viterbi Decoder)
Required P_r/N_0	81.8 dBW/Hz
Margin	3 dB
Required P_r/N_0 with Margin	84.8 dBW/Hz
Transmit Power Required - P_T	0.3 dBW = 1.07 watts

SECTION 3

PHASE B - CONCEPTUAL DESIGN OF SELECTED BEAM WAVEGUIDE ANTENNA SYSTEM

SECTION 3

PHASE B - CONCEPTUAL DESIGN OF SELECTED BEAM WAVEGUIDE ANTENNA SYSTEM

3.1 ELECTRICAL CONFIGURATION

Figure 1-1 shows a full scale mock-up of the selected beam waveguide antenna system consisting of

Main Reflector
Sub-Reflector
Beam Waveguide 2 Axis Gimbal and
Feed System

The beam waveguide geometry is shown in Figure 3.1-1 in relation to the θ, ϕ coordinate system.

3.1.1 Main Reflector

During the Phase A trade study the baseline aperture diameter was chosen to be 48". Thus the overall aperture efficiency to achieve the required 54 dB of antenna gain was just under 43%. The best practical design for a center fed Cassegrain to meet the present requirements could exceed 70% efficiency, and thus reduce the aperture diameter to just under 1M (37.6"). To accomplish this would require shaping both the sub-reflector and the main aperture[1], maintaining tolerances of .003" RMS over the environments, pointing to $\pm$ .03 Deg., use of the most precise (expensive) alignment techniques, etc. The trade between aperture diameter and cost and schedule impact will have to be made in each instance with the specific program impact in mind. In many cases, a compromise position will be reached, such as shaping just the sub-reflector[2], holding tolerances to .005" RMS, pointing to $\pm$ .05 Deg., etc., and achieving 60% - 65% efficiency and 1 M diameter.

3.1.2 Sub-Reflector

For the baseline trade study the sub-reflector diameter was chosen to be 4.23" in diameter (21.5 wavelengths). This selection was based upon trades involving the beam waveguide parameters, aperture blockage considerations, monopulse feed requirements, and aperture distribution efficiency. Support of the sub-reflector does not pose any additional problems with respect to any other Cassegrain antenna design. Only the aperture efficiency is critical since

sidelobes are the lowest weighted parameter for this application. The chosen F/D of 0.25 of the main reflector means that the upper edge of the sub-reflector is in a line with the edge of the main reflector. This allows the quartz cloth thermal covering to lie flat across both apertures and keep thermal gradients to a minimum as the antenna aspect angle to the sun varies. It is important that tight (.003" RMS) tolerances be held on the subreflector; however, this is not a problem over its small diameter.

3.1.3 Beam Waveguide

The refocusing reflectors are identical offset paraboloids which face each other to provide a rotationally symmetric beam, as demonstrated by Mizusawa and Kitsurawa [3]. Their projected apertures are 3.44" in diameter (17.5 wavelengths at 60 GHz). The mirror sequence shown in Figure 3.1-1 assures that all rotations take place with reference to flat reflectors so that no variation with rotation will occur and that the phase center of the feed horn is always at one focal point of the paraboloid pair and the other focal point is at the focal point of the Cassegrain antenna. The reflector surfaces are easily held to the required tolerance of .001" RMS (2 electrical degrees). In fact, the optical quality reflectors that were used for a bench test model to allow for laser alignment were relatively inexpensive. The losses through the beam waveguide were shown by both analysis and measurement to be less than 0.2 dB.

3.1.4 Feed Horn

The beam waveguide tracking application requires a compact feed horn which is capable of forming both a sum and a difference beam. To this end a dual mode conical horn is used to provide a symmetrical sum beam, and a higher order mode is employed to form the monopulse beam (see Figure 3.1-2). The aperture diameter is just over 1.1" and the sum pattern half power beamwidth is about 12 degrees. The spillover level on the refocusing paraboloids is below -30 dB with respect to the beam peak on one side and below -18 dB on the other. This insures proper operation of the beam waveguide.

The difference mode coupler shown in Figure 3.1-2 picks off the TE_{21} mode which has its amplitude peak at about 15 Deg. off the sum mode peak and has a phase which varies at a rate of 2 electrical degrees for each mechanical degree of rotation about the axis of symmetry (Ø) (twice the rate of the sum mode) thus providing a differential rate of one electrical degree per mechanical degree .

After magnification by the main aperture, of course, the sum pattern beamwidth is reduced to under 0.3 Deg., and the difference beam peaks will be at about 0.35 Deg. with respect to the sum peak. The differential phase shift between the two will remain at one electrical degree per degree of mechanical rotation about the Ø axis.

The difference pattern peaks are about 6 dB below the sum peak so that the monopulse will have a sensitivity with Angle θ of about 2.2 V/V/Deg. near boresight. With adequate S/N Ratio this will provide extremely tight tracking (better than 0.01^{o}). The lock-on angle is limited by the angle at which the sum beam first null occurs because the sidelobes are phase reversed with respect to the main lobe and thus would provide an ambiguous output. For this reason it would be wise to set a threshold at an angle off the main beam peak where the gain is higher than the sidelobe peak. Thus it could be set at $\pm$ 0.2 Deg., which is within the open loop pointing capability of most modern spacecraft. Table 3.1-1 is a loss budget for the antenna.

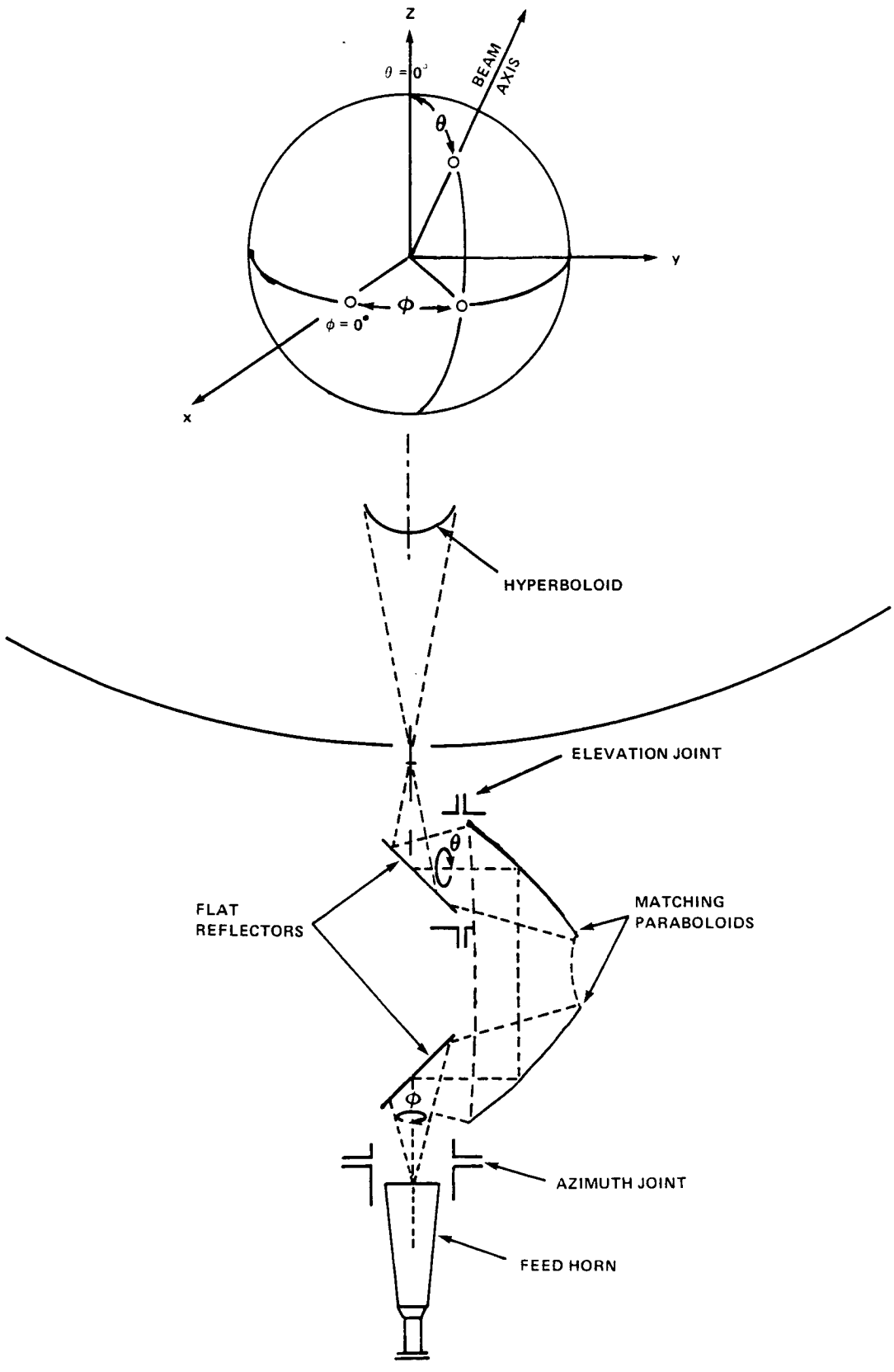

Figure 3.1-1. Beam Waveguide Antenna Geometry and Θ,ϕ Coordinate System

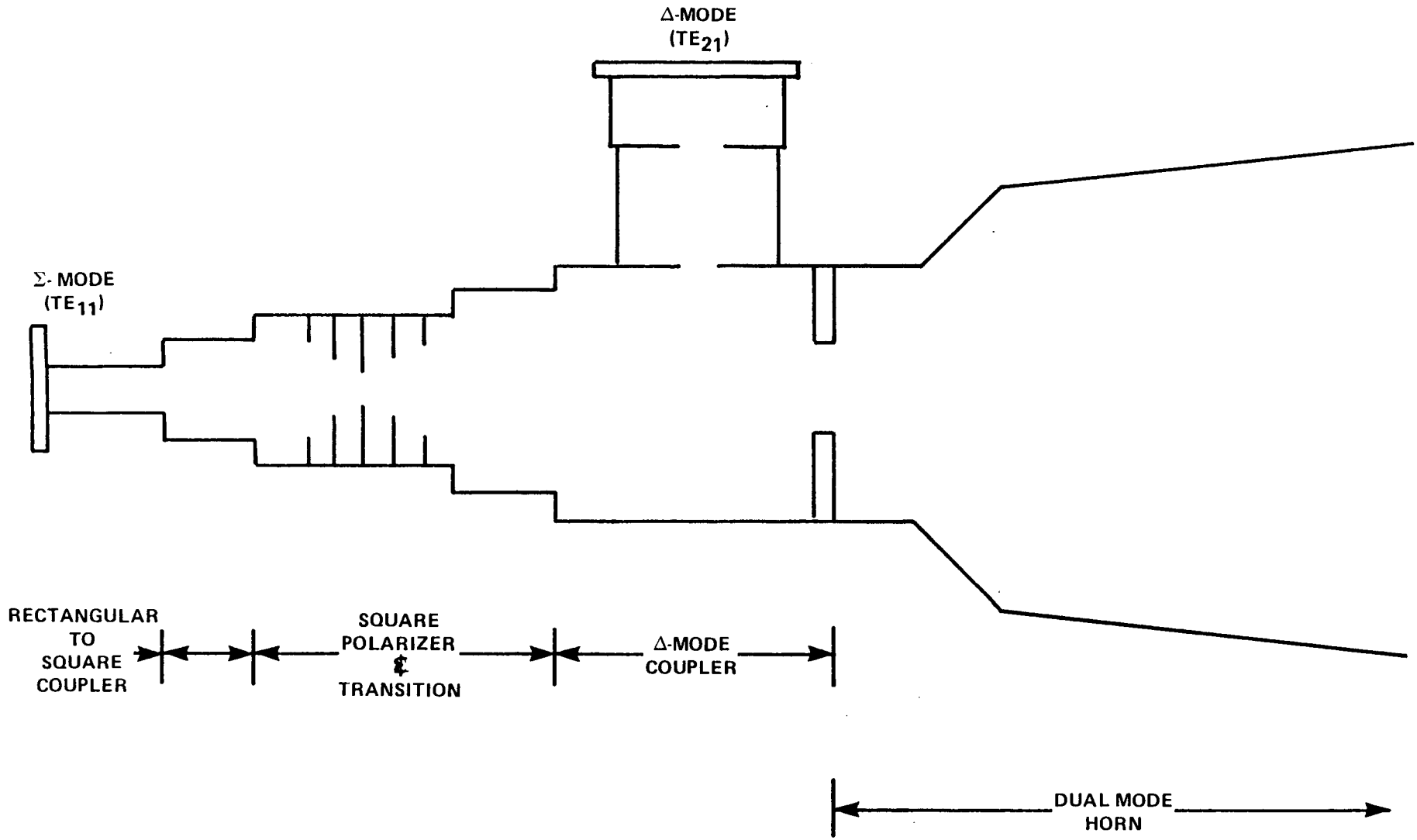

Figure 3.1-2. Schematic of Beam Waveguide Feed Using TE_{11}/TE_{21} Single Port Mode Coupler

TABLE 3.1-1

ANTENNA LOSS BUDGET

	LOSS (DB)	
Paraboloid (not shaped, .005" RMS)		
Tolerance	0.44	
Aperture Distribution	0.2	
Spillover	0.2	
Phase (sub-refl. shaping)	0.1	
Sub-Reflector (shaped, .003" RMS)		
Tolerance	0.16	
Spillover	0.2	
Beam Waveguide	0.2	
Pointing & Polarization	0.1	
Alignments	0.05	
Feedhorn (including OMT & Polarizer)		
I^2R	0.1	
VSWR	0.1	
Sum of Losses		1.85 dB
Uniform Aperture Gain (48" Dia.)		57.69 dB
Net Gain		55.84 dB
Gain Margin		1.84 dB

REFERENCES

1. "High Efficiency Antenna Reflector", by W. F. Williams, Microwave Journal, p. 79, 7/65.

2. "Shaping of Subreflectors in Cassegrain Antennas for Maximum Aperture Efficiency", by G. W. Collins, IEEE Trans. on Ant. & Prop., Vol. AP-21, # 3, 5/73. Also "Comments on" "Shaping, etc."., by Do-Boi-Hugg, IEEE Trans. on Ant. & Prop., Vol. AP-28, # 2, 3/80.

3. "A Beam Waveguide Feed Having a Symmetric Beam for Cassegrain Antennas", by Motoo Mizusawa and Takashi Kitsurawa, IEEE Trans. on Ant. and Prop., p. 884, 11/73.

3.2 Mechanical Configuration

3.2.1 Configuration Description

3.2.1.1 Parabolic Reflector Assembly

The parabolic reflector assembly (figure 3.2.-1) with its subreflector measures 48 inches in diameter by 17.5 inches deep. It is locked to the top of the base housing with its aperature vertical for the launch condition. After injection into its operational orbit, it is released and deployed for operation. The reflector travel is limited by hardstops to the angle defined in the requirements of paragraph 3.2.3.2.

3.2.1.2 Beam Waveguide Gimbal Assembly

The beam waveguide gimbal assembly consists of an azimuth drive axis and an elevation drive axis with internal clearance to permit the transmission of RF engergy through a series of optical surfaces to the antenna reflector. (see Figure 3.2-2). The two axis beam waveguide gimbal assembly is enclosed within a beryllium housing which measures 8 inches by 10 1/2 inches by 14 inches long. The antenna reflector attaches to a platform located at the top of the gimbal assembly.

3.2.1.3 Electronics Equipment Assembly

The equipment assembly is 10 inches by 16 inches by 28 inches long and is located directly below the gimbal assembly. The equipment mounted within the electronics enclosure is shown in figure 3.2.-3.

3.2.2 Parabolic Reflector/Subreflector Assembly

3.2.2.1 Configuration

The Reflector/Subreflector assembly is a modified version of the space qualified space telescope High Gain Antenna and Landstat "D" Narrow Coverage Antenna designs. It is comprised of three subassemblies, Reflector Assembly, Subreflector Assembly and Subreflector Support Assembly. The overall arrangement of these assemblies is shown in Figure 3.2-1 and the typical physical characteristics are presented in table 3.2-1.

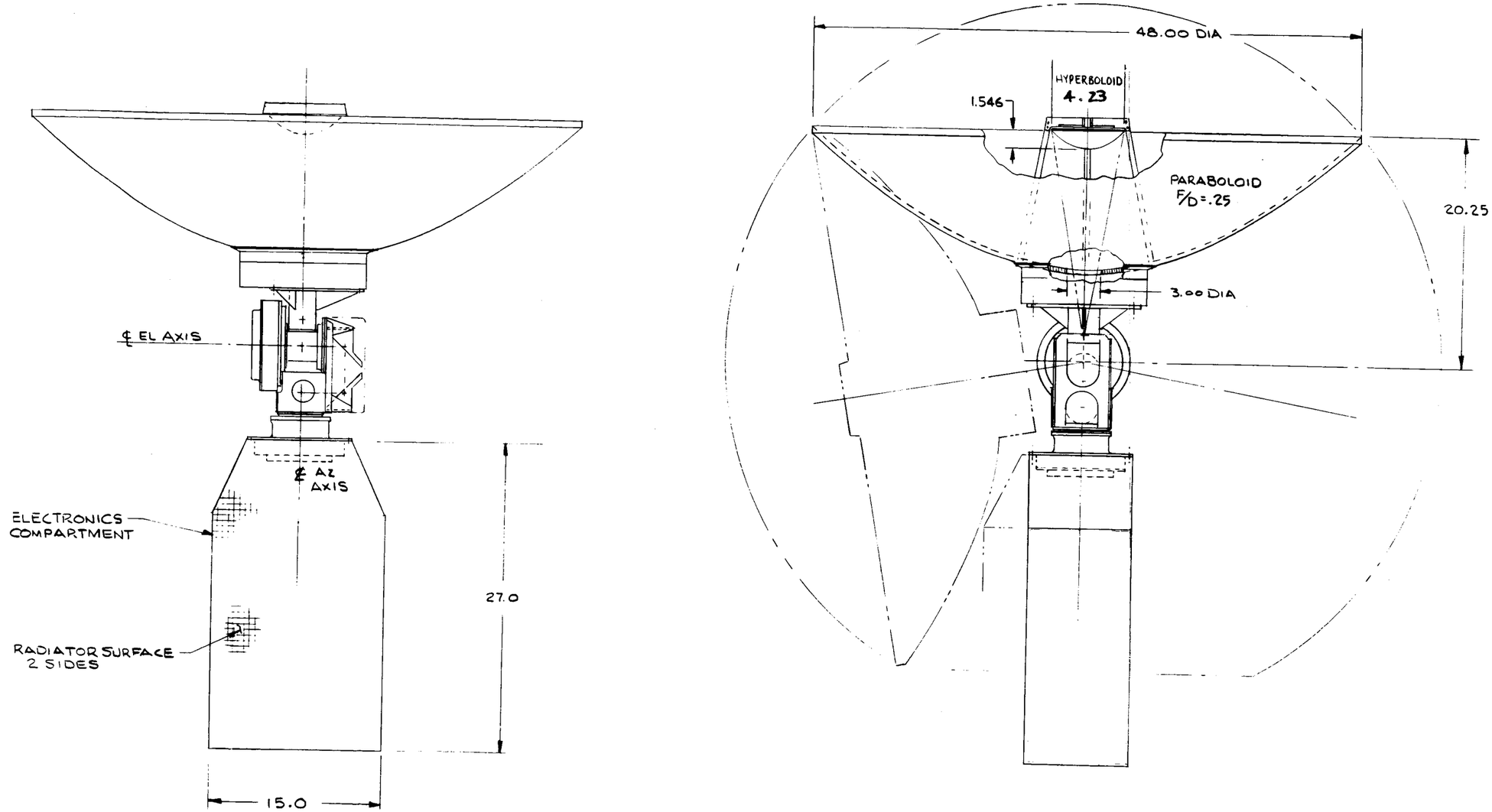

Figure 3.2-1. Two-Axis Beam Waveguide Antenna Assembly

FOLDOUT FRAME

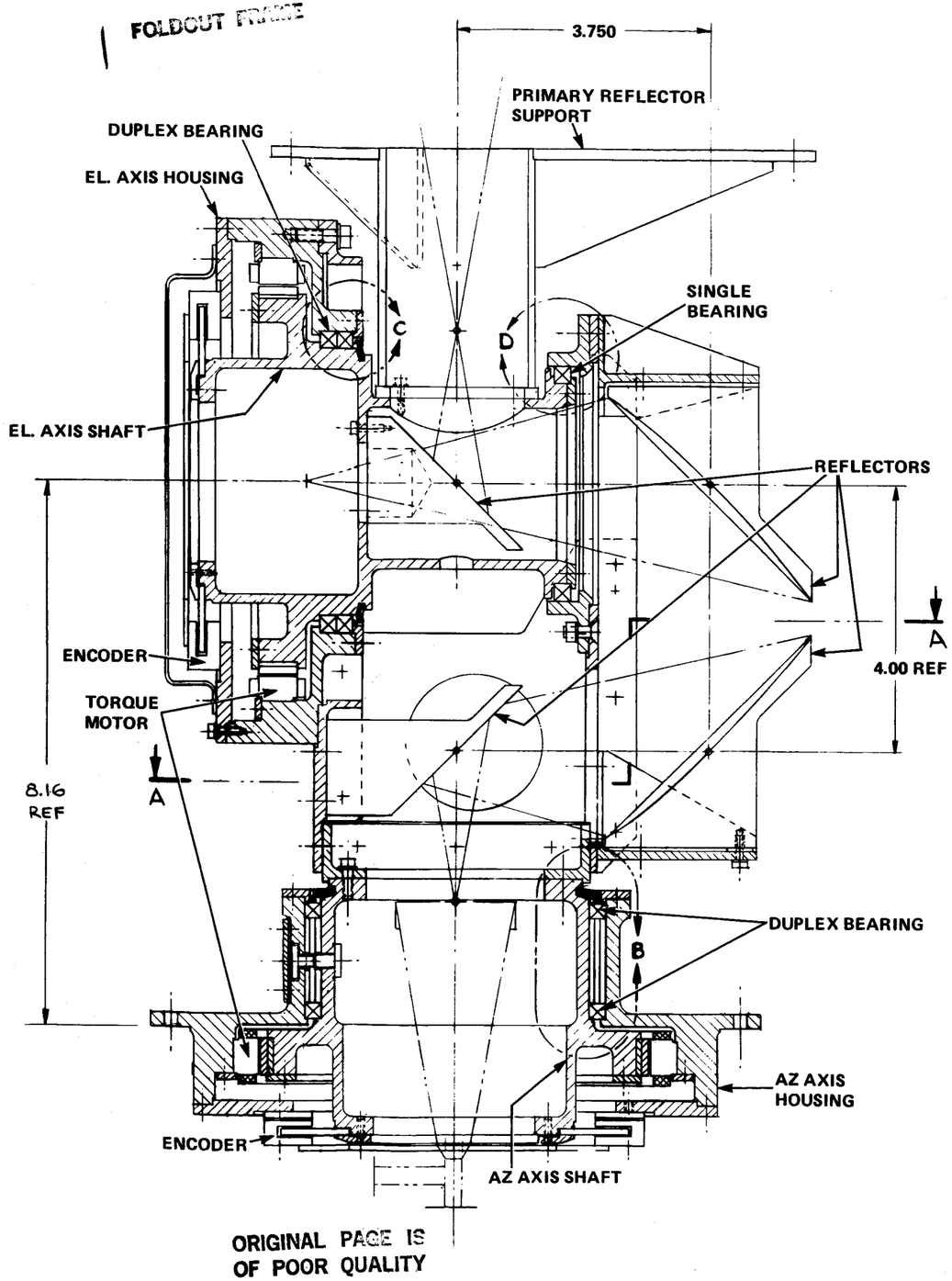

ORIGINAL PAGE IS
OF POOR QUALITY

FOLDOUT FRAME

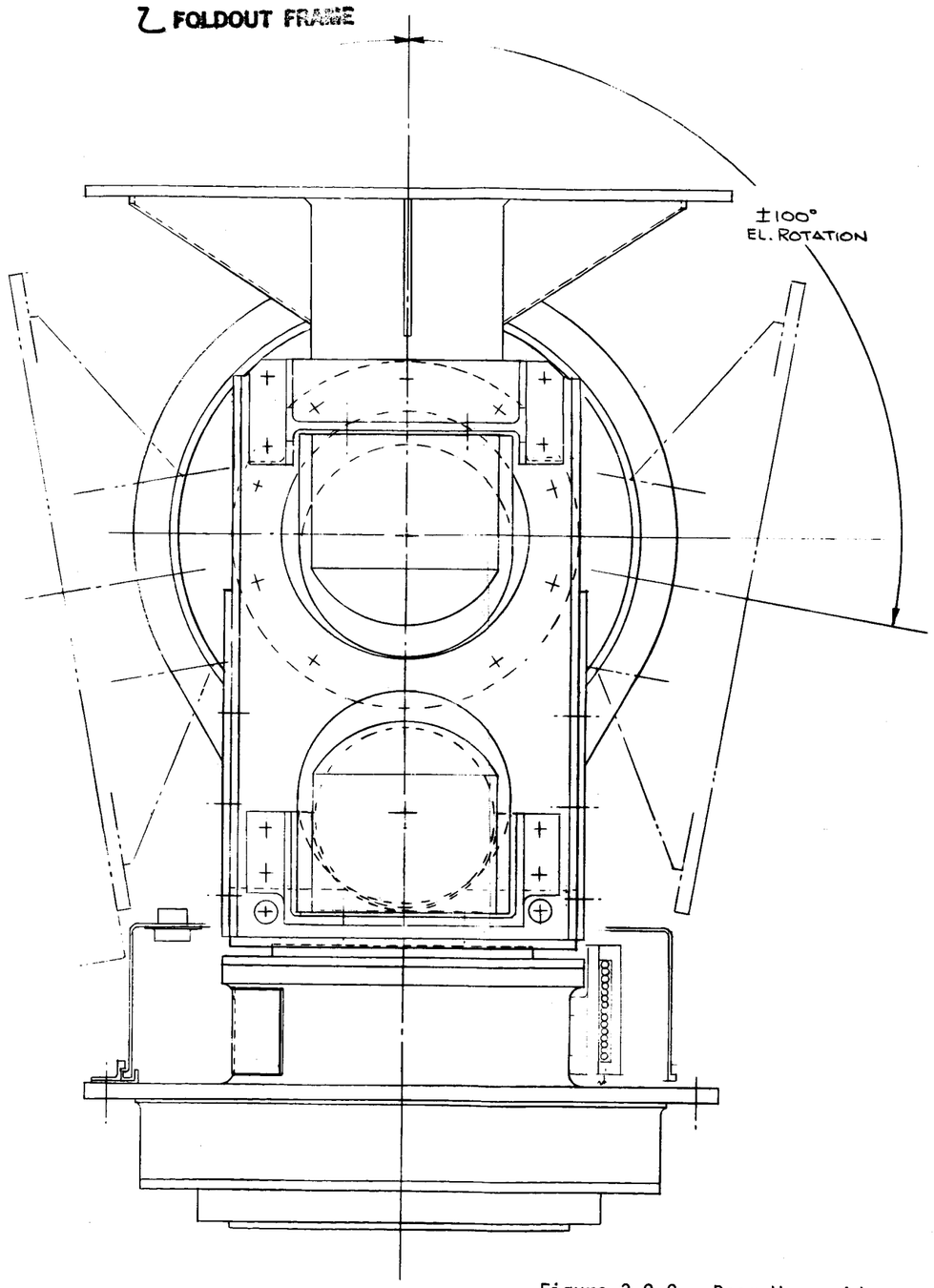

Figure 3.2-2. Beam Waveguide Gimbal Assembly

1 FOLDOUT FRAME

ORIGINAL PAGE IS
OF POOR QUALITY

2 FOLDOUT FRAME

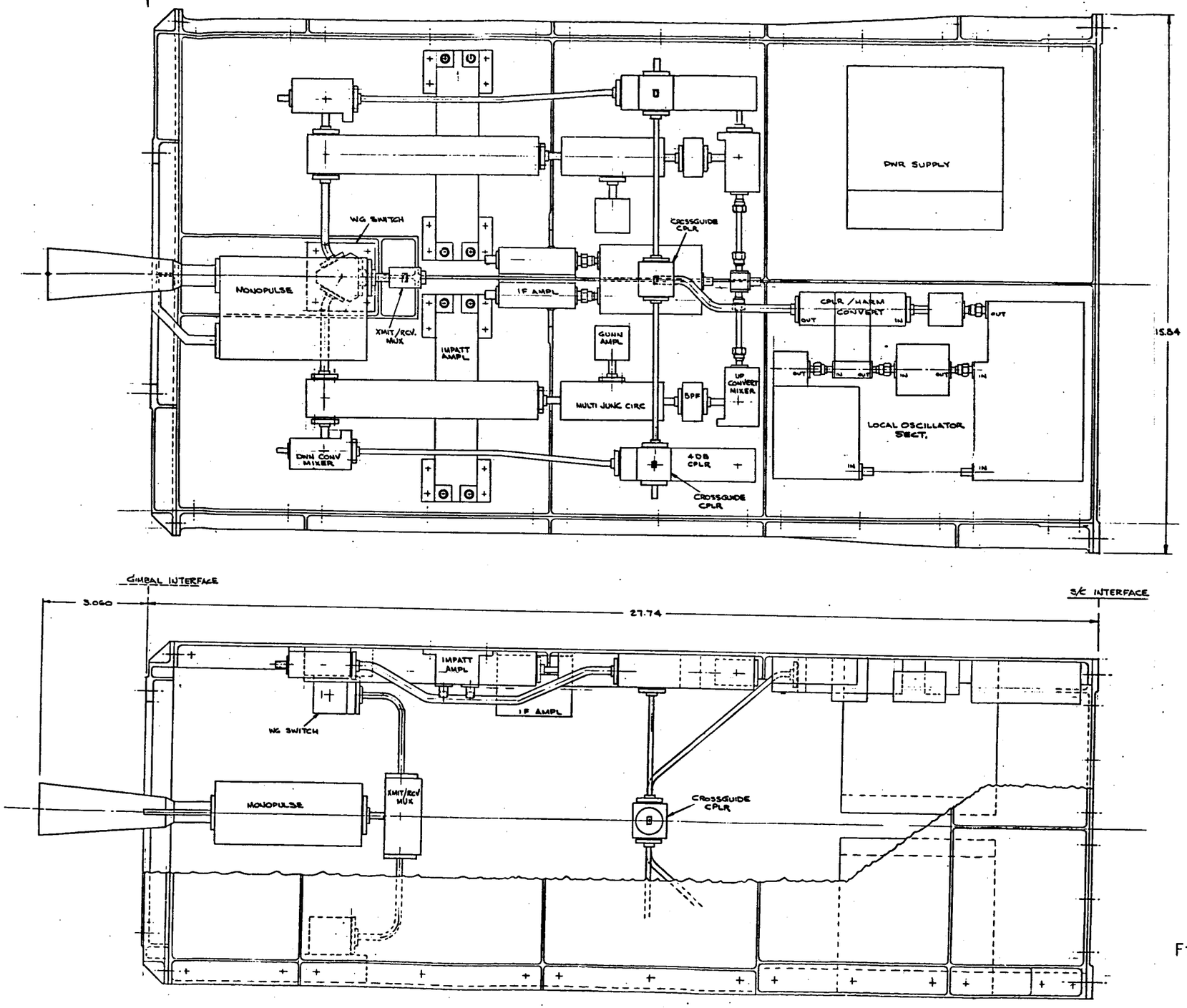

Figure 3.2-3. Electronic Equipment Enclosure

Table 3.2-1

Typical Physical Characteristics

For

Reflector/Subreflector Assembly

Diameter - Parabolic Refl.	48 inches	
Diameter - Subreflector	4.23 inches	
Focal length	12 inches	
F/D Ratio	0.25	
Overall length	17.5 inches	
Weight		
Reflector	8.5	
Sub Reflector	0.9	
S.R. Support	1.2	
Total		10.6 lbs
Surface Accuracy (RMS)	.005 inches	
Fundametal Natural Frequency	> 40 Hz	
Temperature Range	$\pm$ 120^{o}C	
Factors of Safety		
Yield	1.4	
Ultimate	1.8	

3.2.2.2 Construction

The parabolic reflector is constructed using graphite epoxy (GY 70/F 550) face sheets bonded to and separated by aluminum honeycomb flex core sections. Each face sheet consists of a minimum of two layers of graphite fabric laid up in perpendicular warp directions on both sides of the honeycomb core. The center core is 1/4 inch flexcore (2.1 lb/ft 3) with heavier core material being used at the high stress points of attachment. The depth of the core is approximately 0.4 inch. One surface of the flexcore is specially notched for venting purposes since the manufacturer does not perforate it like they do for hexagonal core material. Vent holes are provided on the backside of the reflector to prevent air entrapment.

A back structure consisting of a truncated thin wall cone is attached to the back surface of the reflector. This section provides the mounting interface to the gimbal and the supporting structure for the quadripod subreflector support. The truncated conical section is moulded of graphite epoxy and is precisely epoxy bonded to the back surface of the reflector using a pre-aligned tooling fixture while the relector itself is still on its mold. The outer edges of the reflector are rounded off to meet EVA safety requirements and enclosed with 5 mil graphite unidirectional tape and epoxy bonded to the honeycomb sandwich face sheets. Bonded to the inner face sheet is a 0.001 inch thick aluminum foil which has been formed to the mold surface during the initial layup of the reflector. This provides the reflecting surface of the reflector. A 0.001 inch thick aluminum is also bonded to the outer (back) surface to provide a balanced structure to minimize fabrication and orbital distortion. At completion of reflector fabrication, after its reflecting surface has been measured and accepted, a layer approximately 3 mils thick, of diffuse reflecting white paint is applied to the reflecting and outer exposed surfaces to diffuse incident solar heat*. An approximate 1.5 inch diameter hole through the reflector vertex permits the R.F. signal from the sub reflector to pass into the beam waveguide assembly and vice versa.

The Quadripod Subreflector Support consists of four moulded Kevlar/ epoxy tubes which attach to the paraboloid reflector back structure and to the tabs on the subreflector support ring. The diameter of each tube has been minimized to reduce antenna blockage. Kevlar epoxy material has been selected

---

* Unless the front face of the reflector is covered with an astroquartz shroud.

because it is a dielectric material with a low coeficient of thermal expansion, low density, high modulus and strength properties.

The Subreflector is a hyperboloic which is constructed of machined aluminum. It is attached to the support ring by three adjustable fasteners which permit the sub reflector to be mechanically aligned at assembly and then fine tuned during antenna range tests. A layer of diffuse reflecting white paint is applied to the reflecting surface to disperse solar energy and reduce the maximum temperature of the subreflector and beam waveguide reflectors.

The process utilized in fabricating a Parabolic Reflector/Subreflector assembly are primarily adhesive bonding, chemical conversion coating and/or anodizing of aluminum, and passivation of stainless steel.

3.2.2.3 Thermal Control

Thermal control of the Parabolic Reflector/Subreflector Assembly is designed to minimize thermal gradients across the reflector surface and minimize heat flow into and from the Gimbal Assembly. To accomplish this the reflector apperture is covered with an astroquartz shroud and the reflecting and outer surfaces are covered with a white diffuse reflecting paint to diffuse solar heat input. The back surface of the reflector and back support is covered with a multilayer insulation blanket. Thermal insulating washers placed between the reflector back support and the gimbal minimizes heat flow into and from the Gimbal Assembly.

3.2.3 Beam Waveguide Gimbal Assembly

3.2.3.1 Configuration

The beam waveguide gimbal is a two axis, elevation over azimuth precision gimbal. Each axis is positioned by a direct drive DC torquer motor with inputs from an optical shaft encoder. The beryllium housing contains the bearings, the encoders, the torquers and the RF optics as shown in figure 3.2-2.

3.2.3.2 Performance Requirements

The following requirements listed in the table 3.2-2 were used in the design of the gimbal drive.

Requirements	Value
Pointing Accuracy	
Open Loop	± .057 Degrees
Closed Loop	± .050 Degrees
Tracking Rate	0.006 to 0.6 Degrees/sec
Stiction and Hysteresis	
at zero rate	± .015 Degrees
Slew Rate	
(Azimuth and Elevation)	6 Degrees/sec.
Gimbal Angle	
. Azimuth	± 200 degrees
. Elevation	- 10 to + 125 degrees
Operating Life	10 year life
Torque Margin	100% for tracking rate
Redundancy	All elements (except bearings)

Two Axis BWG Gimbal Requirements

Table 3.2-2

3.2.3.3. Hardware Description

The structural platform at the top of the gimbal assembly is designed to support a 48 inch diameter reflector weighing up to 20 pounds. Antenna diameters up to 96 inches can be mounted on the two axis gimbal structure depending upon the spacecraft configuration constraints and the structural requirements. (see Figure 3.2.-4) The two axis gimbal structure is fabricated of beryllium for maximum stiffness to weigh ratio. The low coefficient of expansion of the beryllium also minimizes the thermal distortions of the gimbal system in order to meet the stringent pointing and operational requirements.

The bearings are Kaydon large bore precision bearings (ABEC-6). The balls and races used in the bearings are stainless steel. The bearings are lubricated by Braylcote 8152 oil. The azimuth axis rotates on a duplex bearing pair and the elevation axis rotates on a duplex pair plus a single bearing. The gimbal bearings are preloaded for maximum structural stiffness and operational pointing accuracy.

Each axis is driven by a direct drive DC torquer motor. The position of each axis is determined by an Itek Optical Encoder with two reading stations to meet pointing accuracy requirements of paragraph 3.2.3.2. Additional resolution may be achieved by the addition of more reading stations, if greater resolution is required.

The RF optics consist of four precision machined and polished aluminum surfaces mounted inside the housing. A laser beam is used in conjunction with alignment fixtures for the initial alignment of the RF optics within the close tolerance beryllium housing. Final alignment of the mirrors will be accomplished during the initial RF testing of the antenna assembly.

A cable wrap assembly will provide the power across the gimbal joints. The cable wrap harness minimizes flexing of the harness and connections during gimbal operation.

FOLDOUT FRAME

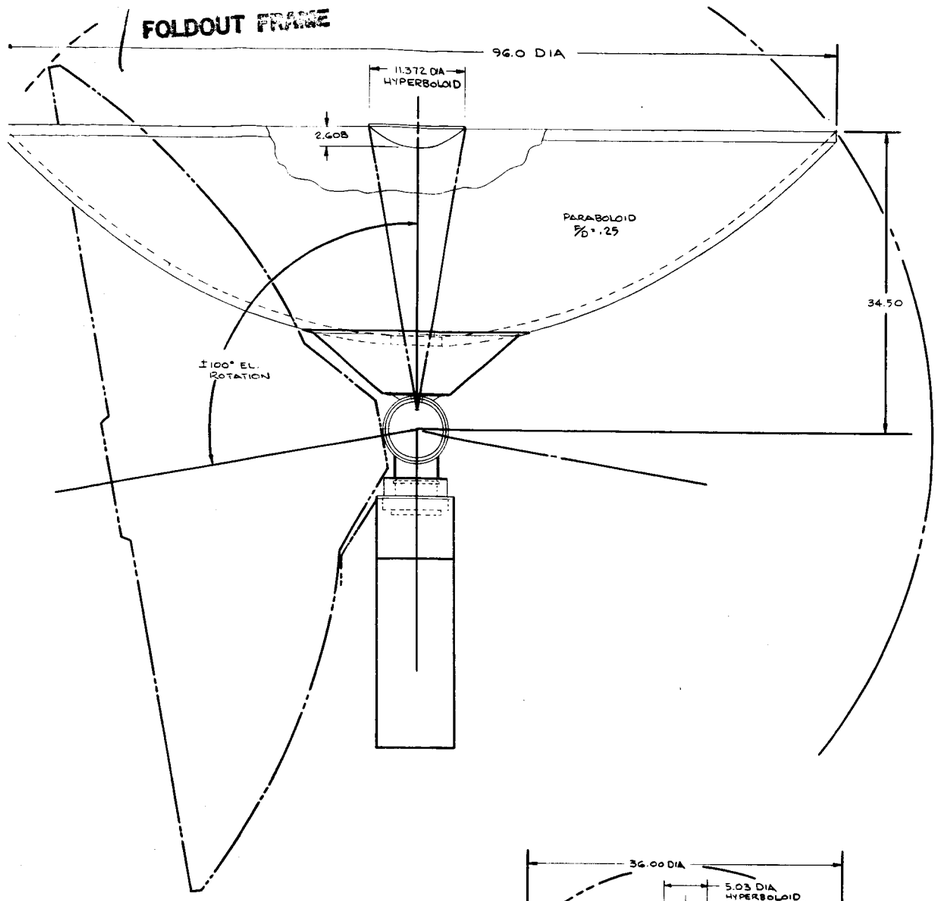

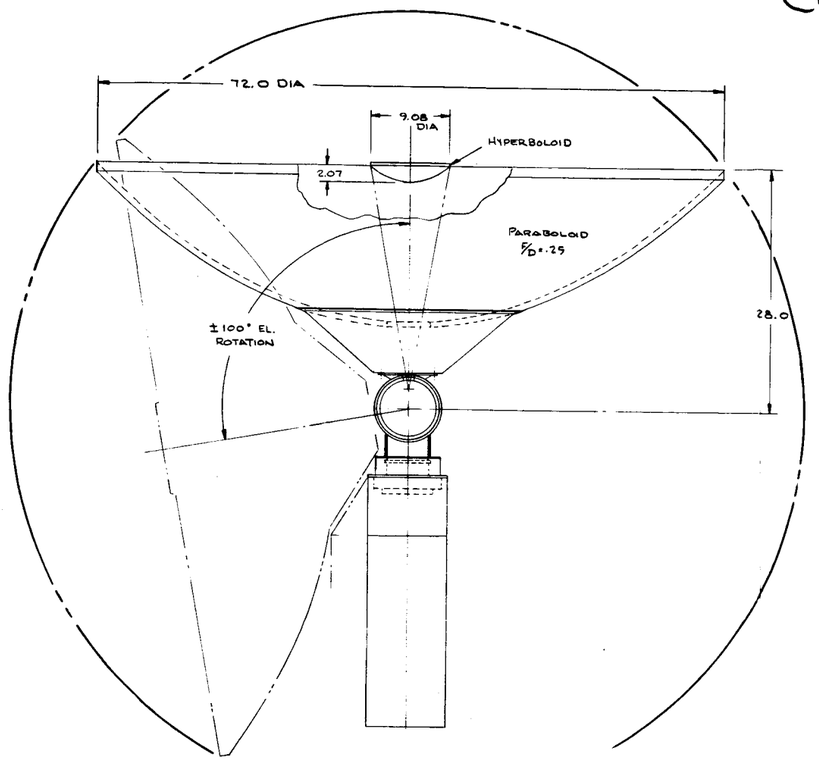

FOLDOUT FRAME

ORIGINAL PAGE IS OF POOR QUALITY

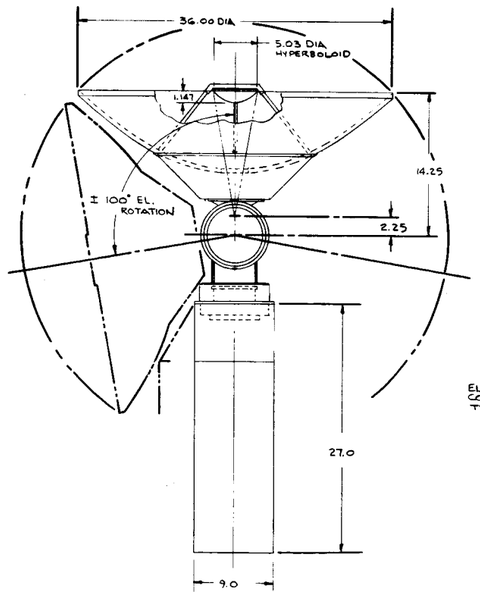

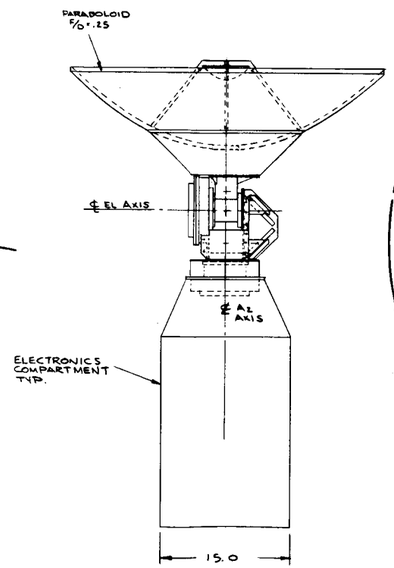

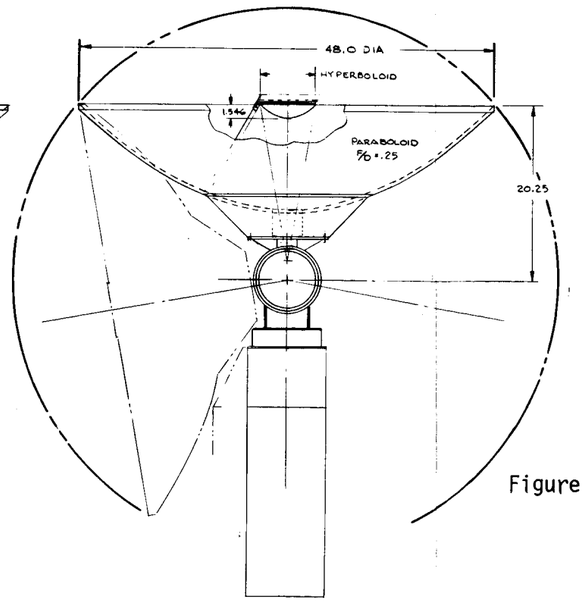

Figure 3.2-4. Family of Reflectors Mounted on Beam Waveguide Gimbal Assembly

ORIGINAL PAGE IS OF POOR QUALITY

The antenna gimbal assembly is isolated from the external orbital environment in order to minimize the temperature effects on the pointing and operational requirements of the system. The external surfaces of the gimbal housing is wrapped with multi-layer thermal blankets. The heat path across the antenna/gimbal housing interface is isolated by the use of thermal spacers. Because of the close fit of the bearings, it will be necessary to add heaters on the elevation axis bearing housing and/or shaft. The heaters will provide a constant temperature gradient across the bearings, thereby maintaining the established operating preload. Both prime and redundant heaters will be required for reliable operation and the deisgn will establish the heater size for a 50% duty cycle.

3.2.4 Electronics Enclosure

3.2.4.1 Equipment Arrangement

The equipment is mounted to the structural walls of the equipment housing. The redundant RF components are mounted on opposite walls of the housing for easy access.

3.2.4.2 Structural Assembly

The 10 inch by 16 inch rectangular equipment housing is made of beryllium. The four machined beryllium pieces are bolted together to form the assembly. Removal of one housing wall permits easy access to the equipment for assembly and test. The beryllium housings are designed to give the gimbal assembly a high natural frequency with the antenna in a stowed position.

3.2.4.3 Thermal Control

The pedestal housing is covered with multi-layer thermal blankets. Openings for thermal radiators can be made in the blankets if it is required to dissipate high local heating from some components during orbital flight.

3.2.4.4 Spacecraft Interface

The entire gimbal antenna assembly can be attached to any spacecraft via four mounting bolts located in the corners of the structural pedestal base.

3.2.5 Weight and Mass Properties

	Weight (lbs)
Antenna Assembly	
Antenna	10.6
Ant. Thermal Control	5.9
Gimbal Assembly	
Mechanism	20.2
Thermal Control	.6
Position Controller	17.9
M M Wave Electronics	
Feed	.1
Monopulse Modulator	.8
Transponder	12.8
Local Oscillator	8.8
Power Conditioner	6.1
Thermal Control	1.0
Housing & Hardware	12.5
	97.3

Inertias about Rotating Axes

Upper Gimbal	4340 lbs in^2
Lower Gimbal	3180 lbs in^2 (MAX)

3.3 Antenna Pointing and Auto-Track Control

3.3.1 Pointing and Tracking Requirement Analysis

The goal for the Antenna Pointing and Control Subsystem (APCS) of Intersatellite Antenna System is to establish and maintain forward and return links at 60 GHz between a satellite at the geosynchronous orbit and up to five (5) user satellites orbiting near earth. The user satellite orbit altitude may range from 200 to 1500 Km and any inclination. A TDAS-type satellite will have 5 individually controlled two-axis gimballed antennas. The user satellite will have only one gimballed antenna system with similar gain and link accommodation. The individual pairs of links are to operate simultaneously.

The APCS should be capable of slewing the antenna pointing from one spacecraft to another and automatically track and maintain the link once the link with other spacecraft is established. The pointing accuracy to the linked satellite should be better than 0.05 degree (0.873 milliradian). Based on the user orbital geometry, the maximum tracking rate would be less than 0.072 deg/sec (1.26 milliradians/sec) at 200 Km altitude. Assuming a slew of 180 degree in one minute the maximum slew rate required is 3.0 deg/sec (52.36 milliradians/sec). The antenna pointing coverage requirements are 26-degree full cone centered about the + Z-axis for the TDAS satellite and 252 degree full cone centered about the -Z-axis for the user satellite. Assuming the gimbal azimuth axis aligned with the satellite Z-axis, the TDAS gimbals require $\pm$200 degree rotation in azimuth and $\pm$15 degree rotation in elevation. The user satellite would require gimbal rotations of $\pm$200 degree in azimuth and -10 to +125 degree in elevation for the coverage, including margins.

The APCS will provide several operating modes: In the slew/open loop mode the gimbals are driven at a high rate to the desired (commanded) position until the difference between the desired gimbal angle and the gimbal angle measured by the position sensor becomes less than a preset threshold. When the difference becomes less than the threshold first time (zero crossing) the drive is disabled and the controller commences the standby mode which is a non-operating mode described later.

In the search mode, the APCS drives the gimbals at a low rate following a prescribed pattern until the corresponding satellite is acquired. The search pattern is a spiral centered about the nominal acquisition point and the acquisition is accomplished either when the monopulse signal is near null or when the total received RF signal level exceeds a threshold. When the corresponding satellite is acquired, the APCS terminates the search mode and commences the autotrack mode.

In the closed loop operating modes (manual/program track and autotrack modes) the gimbals are driven to the desired position at a rate proportional to the error signal until the error signal becomes null (below a threshold). For the manual/program tracking mode the error signal is the difference between the commanded angle (manually or generated by the controller based on the ephemeris of the satellites) and the actual gimbal angle measured by the angular position sensor. For the autotrack mode the error signal is obtained from either the monopulse sensor or the received RF signal level.

When the control subsystem is first activated, it starts the initialization by setting up the operating parameters in accordance with the command and performance health check. See Figure 3.3-1. Following the initialization the APCS controller enters the standby mode where it provides the health and

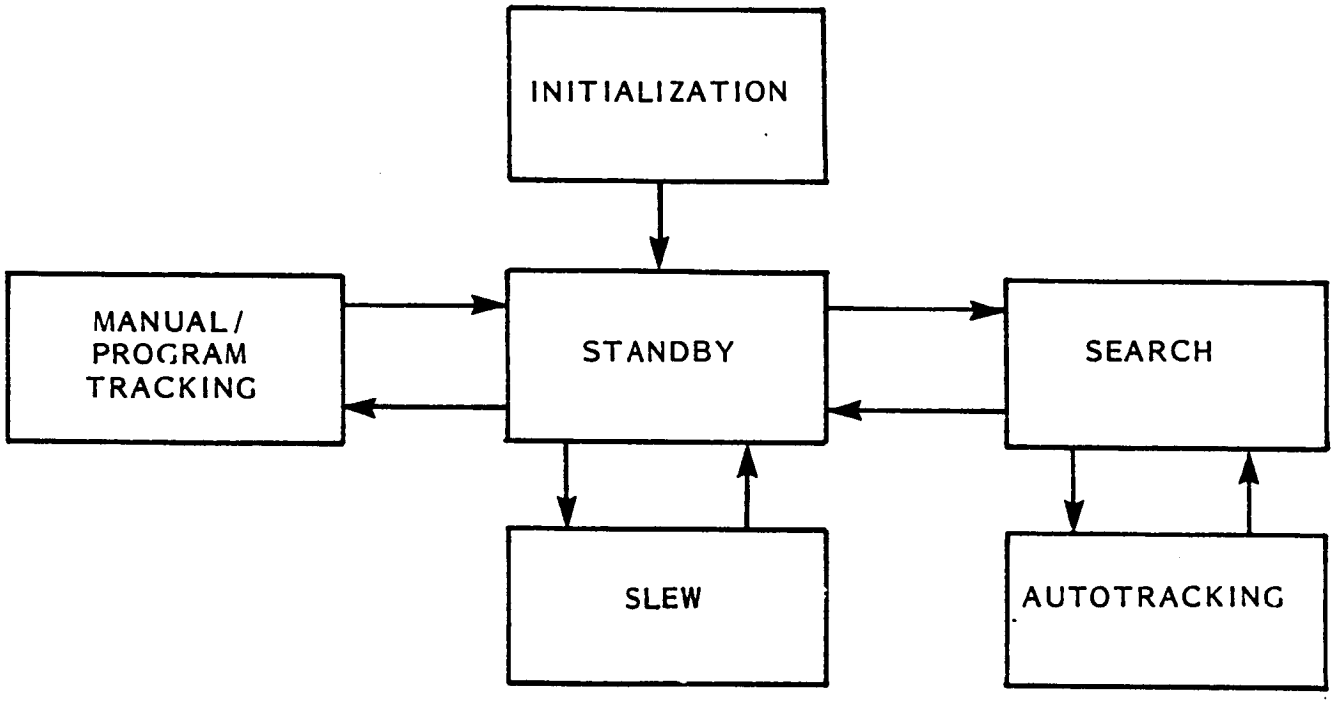

Figure 3.3-1. Operational Modes

operational status of the control system but does not actuate the drive motor. The control subsystem remains in the standby mode until a new operational control mode is commanded.

3.3.2 Control Approach

As described in the preceding paragraph the APCS will provide several operational modes. They are:

1. Initialization/standby mode
2. Slew Mode
3. Manual/Program Tracking Mode
4. Search/Autotracking mode

The initialization/standby mode is the default nonoperational mode of the APCS. Any change of operational mode will be through the initialization/standby mode except for the automatic transition betwen the Search mode and autotracking mode when the target acquisition is established. The change of any operational parameters will be commanded and verified in this mode only. The parameters include: slew position, target satellite position and rate for Manual tracking or ephemeris information for Program tracking, nominal target position and search window for Search mode and threshold for Autotracking mode. Any operating mode can be interrupted by commancing the initialization/standby mode.

The Slew mode will primarily be used to change the antenna pointing from one orientation to another rapidly. The azimuth and elevation drives are simultaneously commanded to arrive at the desired position. The "zero-crosser" controller based on the gimbal position will terminate the slew and switch the

operating mode to Initialization/standby mode. Usually this mode will be followed by either the Search Mode or the Manual/Program tracking mode as shown in Figure 3.3-1 which shows the transition between the APCS operating modes.

The Manual/Program tracking mode is entered from the Initialization/standby mode with the parameters commanded from the ground. In the Manual mode the nominal position at the time of mode execution and tracking rates in azimuth and elevation are commanded. In the Program tracking mode, the ephemeris of the satellite is commanded.

The APCS controller will update the desired gimbal position information based on the commanded parameters during this tracking mode. The desired gimbal position and the current measured gimbal position defines the error signal which drives the gimbal actuator.

In the Search Mode the APCS performs a prescribed search centered about the nominal target position. As the gimbal is driven, one axis at a time, the search pattern will be a square form. When the acquisition of the target satellite is established the APCS will enter the autotrack mode automatically. If the acquisition is not established within the commanded search window, the second search will be started from the same target position. When the second search fails again, the APCS will be switched to the Initialization/standby mode. The search pattern is generated by the APCS controller as shown in Figure 3.3-2. The size of search window is prefixed at the time of launch and can be changed by the ground command. The increment of scan line should be less than the antenna beamwidth for a successful acquisition. During the search mode, the feedback error signal is formed by the difference between the desired position from the search pattern and the current gimbal position measured by the angular sensor.

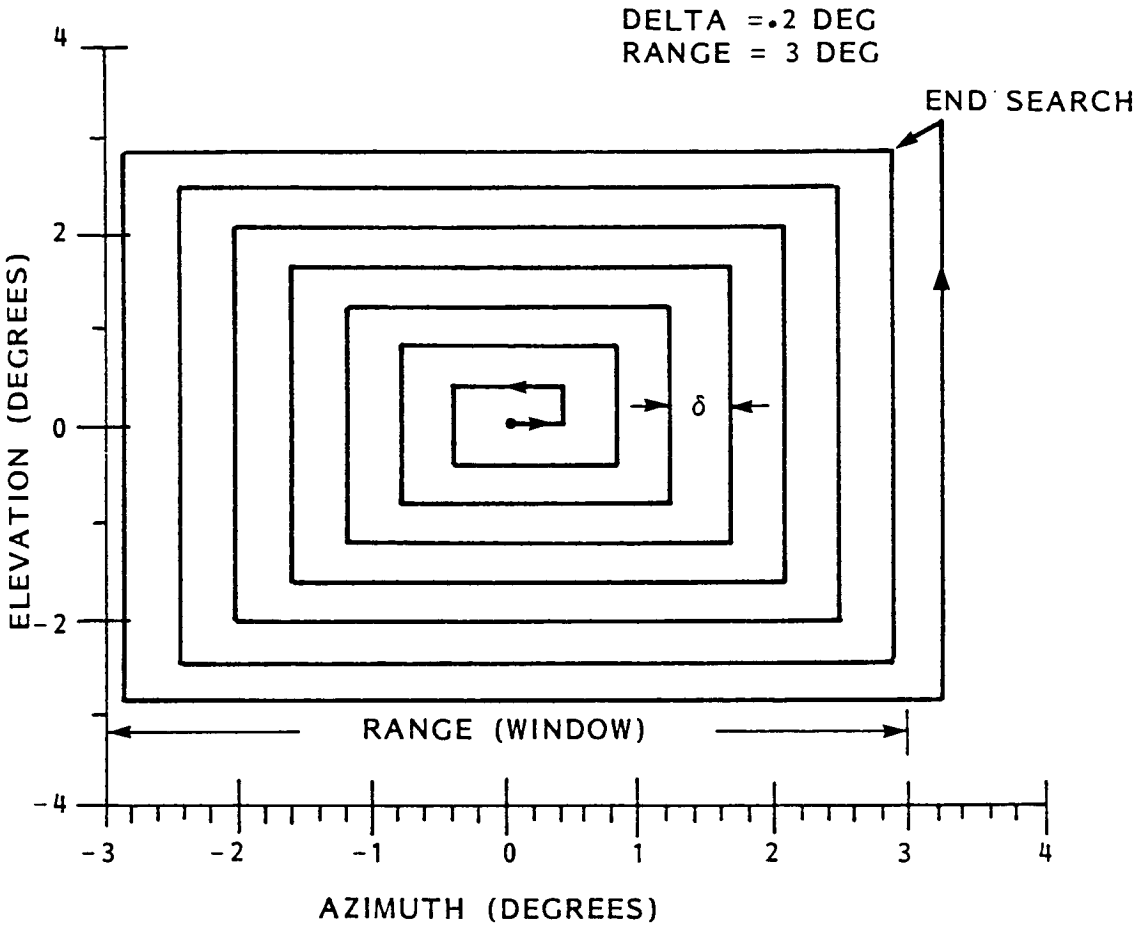

Figure 3.3-2. Square Search Pattern

The Autotracking commences automatically when the target acquisition is established in the Search mode. In this mode an RF tracking sensor provides the error signal for the azimuth and the elevation but the current gimbal rates are calculated from the measured gimbal positions and stored. When the target acquisition is temporarily lost (typically one or two sampling periods), the APCS controller will update the gimbal position based on the stored gimbal position and rate. If the target acquisition is not reestablished for a preset (two or three) consecutive sampling periods, the APCS controller will enter the Search mode using the stored last gimbal position as the nominal position for the Search mode control algorithms.

When a RF sensor mounted on the gimbal is used for the generation of feedback error signal, the sensor axis and the gimbal drive axis do not coincide: The boresight azimuth axis is off by the gimbal elevation angle (Figure 3.1-1). Hence the error measured by the sensor is not the azimuth error to be corrected but the azimuth error angle attenuated by the gimbal elevation angle. The APCS controller normally corrects this geometric attenuation by dividing the azimuth tracking error signal by the sine of the elevation angle measured by the gimbal angular position sensor. This implies that an infinite azimuth gimbal rate is required for a finite azimuth tracking error when the antenna boresight is near the gimbal azimuth axis which is the so-called "gimbal lock". In the TDAS satellite the "gimbal lock" problem can be avoided by orienting the azimuth axis of the gimbal away from the satellite Z-axis (local vertical) by more than 20 degrees. Should the azimuth angle be orthogonal to the local vertical, even the correction of tracking error signal would not be required throughout the coverage angles which is now a 30 degree full angle cone about the azimuth null. The range of gimbal rotation is then $\pm$15 degrees in the azimuth and 75 to 105 degrees in the elevation.

For the user satellite, however, the problem may not be avoided for the desired coverage. If the maximum gimbal rate is limited to the slew rate (3.0 deg/sec) whenever the elevation angle is less than 1.375 degree, the azimuth gimbal of a user satellite at 200 Km altitude cannot keep up with the 0.072 deg/sec tracking rate and may lose the RF tracking sensor signal. If possible, the best strategy is to avoid the "gimbal lock" by orienting the azimuth axis depending on the orbital parameters of the user satellite. When the "gimbal lock" cannot be avoided, the gimbal drive control signal is modified to pass through the "gimbal lock" zone with a program tracking. During this period, the RF link of the tracking sensor may or may not be maintained depending on the distance between the gimbal azimuth axis and the locus of the tracked satellite.

The controller will first determine the gimbal elevation angle which defines the "gimbal lock" zone where the azimuth gimbal is to be driven at the maximum gimbal (slew) rate. For example, the user satellite at 200 Km altitude with the TDAS locus passing through the azimuth axis has a radius of 2.16 degree for the "gimbal lock" zone. (The radius of the zone is a function of the tracking rate, the gimbal slew rate and the distance to the track locus). When the antenna boresight enters the zone, the gimbal azimuth axis is driven at the slew rate which is higher than the rate determined from the tracking signal at the point but is equivalent to the tracking rate averaged over the zone. During this period, the gimbal elevation angle is updated based on the tracking rates at the entrance to the zone and the measured current tracking error signals.

In order to minimize the impact of high gimbal rate on the attitude control of the host satellite, the buildup of the azimuth rate will have a profile of a slow rise at the beginning and a slow decay at the end of this program tracking. Since the antenna boresight pointing at the exit from "gimbal lock" zone will be

toward the expected location of the tracked satelite, the link of RF tracking sensor can be reestablished by an automatic enabling of the search mode should the link be lost during the program tracking through the zone.

The "RF track sensor" can be either a monopulse sensor providing a null based on the difference signal or an amplitude (sum signal) sensor requiring the "hill climbing" computations. Although the "hill climbing" sensor is simpler than the monopulse sensor, the accuracy near boresight is poorer than the monopulse sensor and the "hill climbing" control algorithm is more complex than the "null seeking" control algorithm. To establish the tracking signal acquisition, however, the sum channel signal is sufficient to compare with the threshold. Since the monopulse sensor provides both the difference signal for null and the sum signal for amplitude, it is more suitable for the APCS to acquire and track the cooperating target.

3.3.3 Functional Description of Control System

The antenna pointing control system (APCS) has basically three interfaces: with the gimbal assembly, with the tracking sensor and with the ground operator (through the host satellite TT&C). The APCS also contains memories to store control logic, parameters and variables, and a processor (CPU) to generate control signals based on the commanded operating mode, parameters and the current status of the pointing system as shown in Figure 3.3-3. The interface with the gimbal assembly includes angular position sensors to measure the current gimbal azimuth and elevation angles and drive motors to change the gimbal angles in accordance with the control signal.

The control logic for the APCS is stored in the ROM portion of the memory and provides the algorithm to generate the control signal. The selection of

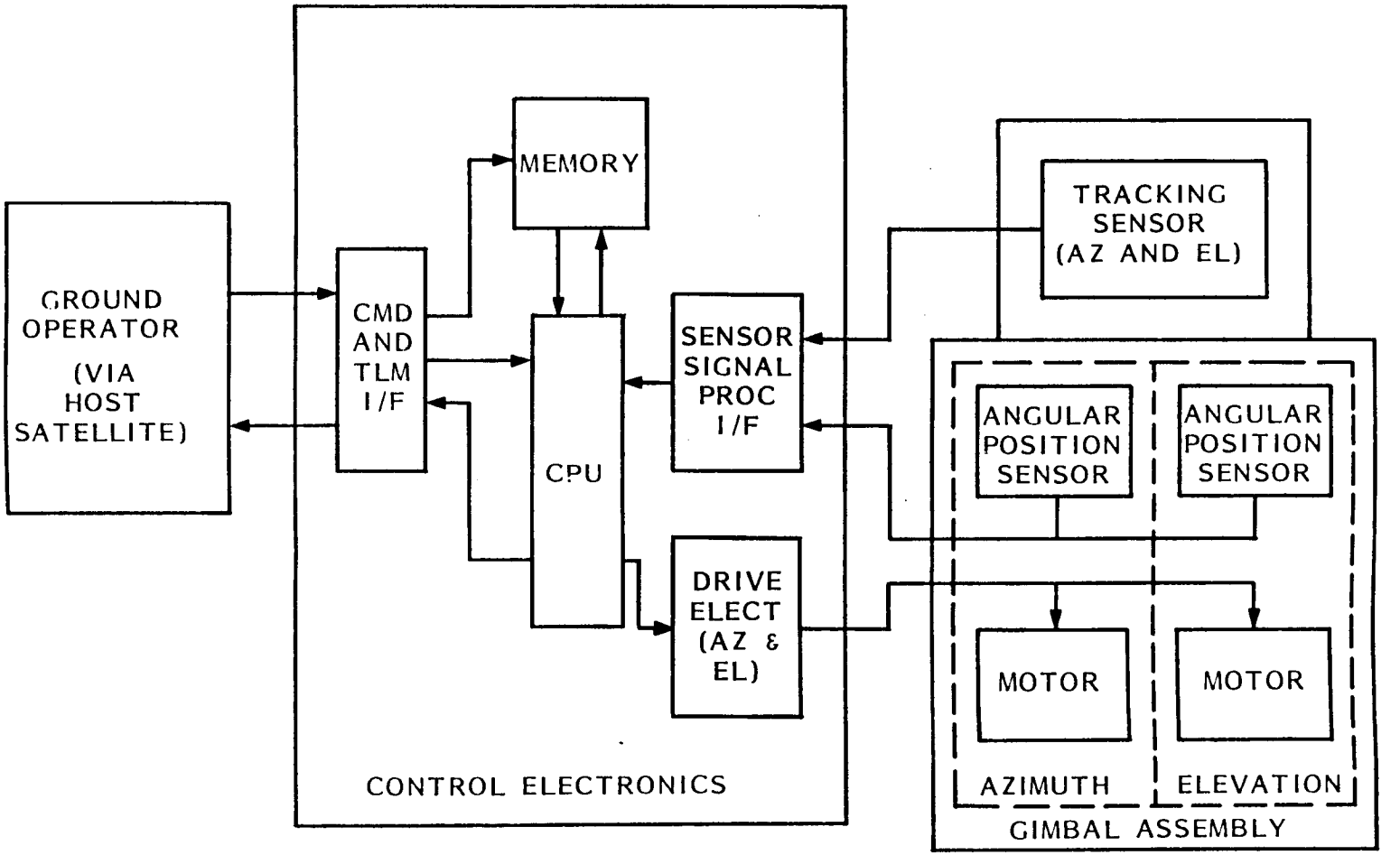

Figure 3.3-3. APCS Functional Block Diagram

operating mode and the parameter settings are based on the ground operator command sent through the host satellite and stored in the memory. These data can be changed by the ground command only. The memory also stores the current status of the APCS and some variables from the previous computation for use in the susequent computation. Many of these data are accessed by the ground operator through the host satellite telemetry system.

The signals from the tracking sensor and the angular position sensors for the gimbal assembly are buffered and conditioned by the interface circuit to the form compatible with the processor operation. The drive circuits generates motor drive signal in accordance with the control signal computed by the processor.

The CPU is the core of control electronics providing the logic and arithmetic operations. Based on the commanded operational mode the processor generates the desired gimbal positions from the ephemeris data, search pattern or slew command and compares with the measured position to form error signals. In the case of autotrack mode the error signal is computed from the tracking sensor signal and the measured gimbal positions.

3.3.4 Control Systems Components

As shown in the block diagram of Figure 3.3-3 the major components in APCS are the control electronics, the angular position sensors, the drive actuators and the tracking sensor. The control electronics is microprocessor based and more fully described in Paragraph 3.4. All necessary software will be embedded in the memory. The actuator physically moves the gimbal to point the antenna toward the desired orientations.

As the angular travel required is large, a motor is chosen for the actuation. The motors considered are stepper motors, torque motors with brush

and brushless torque motors. Since the pointing accuracy requirement is better than 0.05 degrees, the resolution of actuator motion referred to the antenna axis should also be better than 0.05 degrees. The best stepping resolution available for a stepper motor is currently 1.8 degrees and it is necessary to employ a gear mechanism to reduce the motion step size for a stepper motor. As the gear mechanism involves hysteresis and backlash in the motion, a torque motor is favorably considered over a stepper motor. Although a torque motor may involve cogging and nonlinearity characteristics, these effects are easily counteracted in a feedback drive system which is to be employed in the APCS.

When a torque motor is commutated properly, the resolution of actuator motion is virtually infinite with a continuously variable drive voltage level. However, the inherent characteristics of sliding contacts between the brush and the commutator segments of the brush type torque motor causes limited life, low reliability, noise and stiction problems. When the commutation is electronically performed, the difficulties associated with the brush can be eliminated but the resolution of actuator motion is now affected by the resolution of the position sensor providing the commutational informations as well as the resolution of the drive voltage amplitude variation. Since the angular position sensor for the gimbal provides high resolution information, the required actuator motion resolution can be easily obtained from a brushless torque motor by use of gimbal position sensor signal even when the motor drive voltage amplitude is discretely changed. Therefore, brushless torque motors are selected for the APCS actuation in both azimuth and elevation axes.

Three types of sensors are considered for the measurement of gimbal angular position: the potentiometers, the electrical resolvers and the optical encoders. The conventional potentiometer involves a sliding contact between the wiper and

the resistance element as in the case of the brush type commutator and, consequently, it is discarded from the consideration. Although a "potentiometer" employing an optical wiper is reportedly under development, it has not been included in the consideration as no sufficient information is available at this time. As a resolver measures the angular displacement in terms of variation of electromagnetic coupling between the rotor and the stator windings, the resolution is virtually infinite. However, the resolver is susceptible to null shift, phase drift and transformation ratio variation as the environment changes and involves brush/slip ring contacts. Although, as shown in paragraph 3.4, the resolution of an optical encoder is limited by the encoding disk design, it is stable and does not involve any sliding contacts. When the number of encoding tracks are properly selected, therefore, the sensor resolution obtained will not be the limiting item for the pointing accuracy. For the APCS, an optical encoder with 14 bit or 0.022 degree resolution is selected for the angular measurement. Depending on the number of reading stations in the encoder, the actual measurement resolution can exceed the encoder disk resolution.

The types of RF tracking considered are a monopulse technique or a "hill climbing" technique. In the "hill climbing" technique, the sensor provides the total magnitude of the RF energy received and the controller seeks the peak of the magnitude by taking the gradient as a function of gimbal angles. Since the gradient near the peak, or the top of hill, is small and the dynamics of the target satellite transmitting power might cause more variation than the variation of received power due to the receiving antenna characteristics near the boresight, no unique null point can be established. The controller would search the peak constantly even when the target satellite is right on the boresight. On the other hand, the monopulse sensor utilizes the difference signal of two ports as well as the total received RF energy. Therefore, the null

corresponding to the boresight pointing error can be uniquely determined from the sensor signal. Consequently the monopulse technique is employed for the autotrack mode of APCS operation. The monopulse sensor selected utilizes a single multimode horn which can provide both communication and auto-track functions. The phase of difference signal is sequentially stepped by four 90^{o} intervals to generate tracking error signal in two orthogonal axes. Due to the gimbal mounting of the monopulse antenna, the sensor axis and the gimbal axis do not concide, and a correction for gimbal geometry in the azimuth error signal is required to drive the gimbal as discussed earlier.

3.3.5 Error Analysis

The pointing performance of the APCS is dependent on the operational mode selected i.e., auto-track or program track. The major error sources are identified in Table 3.3-1. It shows that the desired pointing accuracy can only be obtained in the auto-track mode.

The program track mode includes a large number of satellite related error sources as in the case of an open loop pointing mode: Attitude control pointing (including structural deformation and dynamics of the satellite), pointing command errors (including ephemeris errors for host and target satellites), alignment and thermal errors for the gimbal assembly, gimbal drive errors and antenna distortion errors. For the autotrack mode, many of the large error sources are eliminated and a high accuracy pointing can be achieved. The primary sources of error for the autotrack mode are the pointing command errors, limited to the servo loop dynamics, gimbal drive errors due to finite drive resolution and RF errors.

The satellite attitude pointing error directly affects the antenna pointing

TABLE 3.3-1 ANTENNA POINTING CONTROL SYSTEM ERROR BUDGET

(3σ)

ERROR SOURCE	PROGRAM TRACK MODE (DEG)	AUTO TRACK MODE (DEG)
Attitude Pointing Knowledge	0.003	-
Pointing Command		
Computation*	0.005	-
Ephemeris	0.005	-
Servo Loop Dynamics*	0.010	0.010
Rate Jitter	0.022	0.022
Gimbal Alignment & Thermal	0.050	-
Gimbal Drive		
Angular Position Sensor	0.022	-
Actuator Resolution	0.022	0.022
RF Errors		
Antenna Distortion	0.017	-
Monopulse Sensor	--	0.010
TOTAL (RSS)	0.066	0.034

*Outside of gimbal lock zone. Within the gimbal lock zone the error can be as high as 0.5 degrees.

during the program track mode while it does not influence the pointing performance of the auto track mode provided the APCS control loop has sufficient bandwidth to accommodate the frequency spectrum of the attitude errors. Any systematic errors can be removed by ground processing, and only the random dynamic errors are included in the error budget. It is estimatd that the attitude pointing knowledge can be obtained with 10 arc sec. or 0.003 degree accuracy (this is not the pointing accuracy but the knowledge which can be used in the calculation of gimbal angle command).

The pointing command errors in the program track mode may come from four sources; computational error, satellite ephemeris error, servo loop dynamic error, and rate jitter error. Only the last two sources contribute to the auto track mode pointing command errors. The largest portion of the computational error outside of the gimbal lock zone is the commanded gimbal angle error, which is 0.005 degree based on 16 bit word representing 360 degrees. The ephemeris error causes the peak angular error at the point of closest approach between two linked satellites. It is assumed that the angular error does not exceed 0.005 degrees. The peak servo loop dynamic error will occur near the gimbal lock as the required angular rate is highest. When the gimbal rate is less than 3 degrees per second the dynamic error is expected to be less than 0.010 degrees. When the azimuth gimbal is slewed at 3 degrees per second constant rate within the gimbal lock zone the combined errors of the commanded gimbal angle and the servo loop dynamics can be as high as 0.5 degrees. The rate jitter is quantization error associated with the rate granularity of the command to the gimbal drive electronics. As the rate is derived from the position sensor having a resolution of 0.022 degr., the error should be less than 0.022 degree provided the rate command is updated at least once per second.

The gimbal alignment error includes the gimbal orthogonality, bearing runouts, and gimbal flexibility. This is a bias and can be calibrated out within a one-half bit of the angular position sensor on ground and the residual can be determined by ground processing of on-orbit data. As the correction of this error on-orbit is cumbersome and difficult, it will be considered to be random and added to the error caused by the thermal effect on the gimbal structure which is expected to be less than 0.050 degrees. Since the RF tracking sensor is mounted on the gimbal, the gimbal alignment error is included in the tracking sensor measurement and does not affect the autotrack mode performance.

The gimbal drive errors are associated with the gimbal angular position sensor and the drive actuator. As the position sensor is a digital type, the error caused by the accuracy, alignment and signal processing will not exceed one bit or 0.022 degrees. Also, since the resolution of actuator drive is limited by the position sensor resolution used for commutation, the error can be expected as much as 0.022 degrees. For the auto track mode only the actuator drive resolution affects the performance as the RF tracking sensor is the feedback sensor.

For the program track mode the RF error is the error caused by the on-orbit antenna thermal distortion. This error may be removed by special on-orbit tests. For the auto-track mode operation the effect of antenna thermal distortion is largely eliminated and the only error source is the monopulse error.

The total error expected outside the gimbal lock zone is 0.066 degree and 0.034 degree respectively for the program track and the auto track modes. As mentioned earlier the tracking error within the gimbal lock zone can be as high as 0.5 degree which may cause the loss of link temporarily.

3.4 Control Electronics

The Antenna Pointing Control System (APCS) selected for the beam waveguide gimbal is a microprocessor based controller. As seen in the block diagram (Figure 3.4-1) the microprocessor is the center of the control system. The present position of the antenna and the conditions of the antenna signal are made available as inputs to the embedded processor. Command and control signals supplied by ground control (for evaluation and pre-flight checkout) or by the Remote Interface Unit - RIU (during actual flight operation) will establish the specific operating mode for the processor. The processor then, by using the Resident Software Algorithm, will provide as its output the control signals for the motor drive to position the gimbal.

The block diagram is similar to other control systems performing this pointing function. However, the system is different from many previous systems in the specific implementation of each of the major blocks. Additionally, it differs in that the control intelligence (the microprocessor and its control algorithm) is embedded within the control system rather than being shifted back to the spacecraft computer. This approach will reduce the burden for the On Board Computer (OBC). With this system the OBC need only specify a task to the control system by issuing one command. The APCS processor will then make all necessary decisions to carry out the command. During this process the status of the system can be accessed by the OBC if update information is needed.

An additional aspect of this design which is not apparent from the block diagram is the concern for size, weight, and power. A number of design alternatives have been considered which could satisfy the functional requirements of the system. However, the specific configuration selected not only satisfies the functional requirements but performs in a very efficient

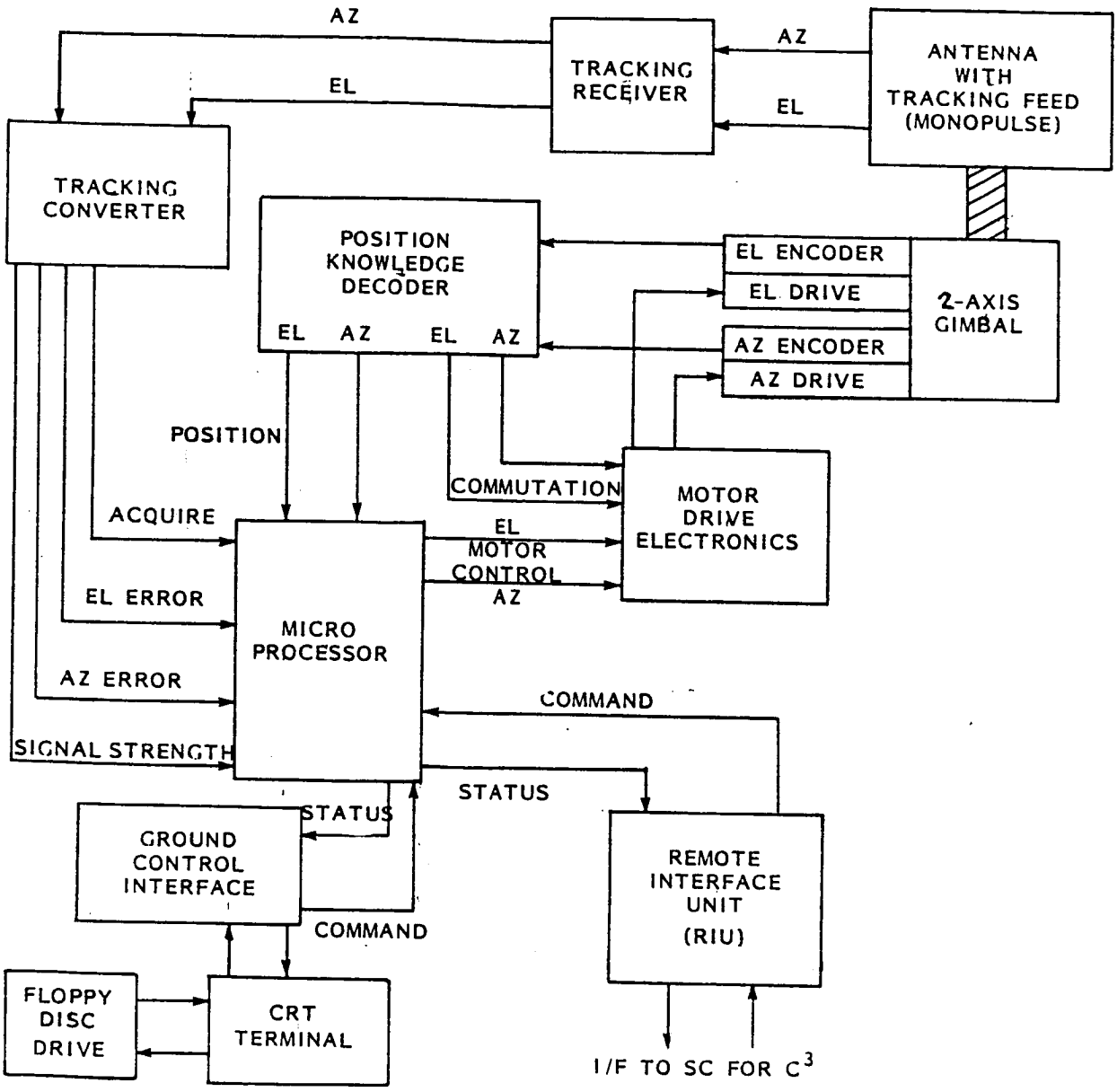

Figure 3.4-1. Control System Block Diagram

manner. The use of a microprocessor as the control element rather than a collection of combinatorial MSI logic reduces the number of printed wiring boards, connectors, etc. Therefore, this microprocessor implementation is more efficent not only in power but also in size and weight. An additional example is the use of a pulse drive technique for the gimbal motor (rather than the more common reduced voltage drive) when in the slow drive operation. This approach reduces the electronics required since it uses digital rather than analog control. Also this technique reduces the power requirement for the system.

3.4.1 Position Knowledge

The processor gets its knowledge of the present position of the gimbal from two absolute Optical Encoders by way of the Position Knowledge Decoder. Each axis (azimuth and elevation) has its own Optical Encoder. The operation of each axis is the same so only one axis will be considered in the following discussion.

The virtue of the Optical Encoder for this application is its fine position resolution. With the Optical Encoder selected for this system it is possible to determine position within 20 arcseconds (0.005°). The basic information for giving position with this encoder is a set of 14 tracks encoded in natural binary code (not Grey Code). Each track is composed of alternate opaque and transparent segments as shown in Figure 3.4-2.

Figure 3.4-2. Optical Encoder Disc

The outermost track (called the Fine track) has 2^{14} or 16,384 cycles of opaque and transparent segments. The next track has 2^{13} cycles, the next track has 2^{12} and so on until the inner most track which has 2^{0} or 1 full cycle. A light source is placed on one side of the disc while a Slit Detector System is located on the other side. At any position the light emitted on one side is modulated by the Code Disc and sensed by the detectors to produce the coded output. Each of the 14 tracks then represents one binary digit position in a 14 Bit Code Word. A carry logic procedure similar to the conventional V-Scan or U-Scan technique determines the selection of a Lead or Lag Detector on each track depending on the state of the next low order bit. This approach assures that all of the higher order bit transitions will be coincident with the fine track output. Therefore, all bit transitions will be synchronized to the Fine Track, resulting in unambiguous natural binary output.

The Optical Encoder provides two additional position signals (SIN and COS) used by the Position Knowledge Decoder. These outputs supply analog signals which are proportional to the Sine and Cosine functions of the displacement within the Fine Track Cycle. These analog signals provide Quadrature Encoding which allows each Fine Track Cycle to be further divided into 4 sectors, thereby extending the resolution from 2^{14} to 2^{16} unique areas. The complete 360^{o} circle is then divided into 2^{16} (65536) parts, with each part representing 20 arcseconds. The binary value thus obtained from the Optical Encoder is stored in a 16 bit register and is made available to the processor as needed. Since an absolute encoder is used, power may be turned off this element when in Standby Mode with no loss of position knowledge.

There are three other tracks on the Encoder Disc called Commutation Tracks, A, B, and C. These tracks are used in conjunction with the torque motor to

provide the proper sequence for energizing its three windings. Since the torque motor selected has 40 poles, the Encoder Disc will have 40 cycles of the A, B and C signals. Each Commutation Track will be opaque for 180° and transparent for 180° of this cycle. By defining Track A as the reference and offsetting Track B by 120° and Track C by 240° of the cycle the proper commutation drive can be derived. More detail on the use of the commutation outputs of the Optical Encoder are given in Section 3.4.2, Torque Motor Drive.

3.4.2 Torque Motor Drive

The Torque Motor Drive electronics accepts as inputs: the commutation information from the Position Knowledge Decoder, and the motor control commands from the processor; then it provides the drive to the torque motors. Both the azimuth and elevation motor drives operate in the same manner so only one drive channel will be described here. This aspect of the APCS is most easily understood if one starts at the motor and works back through the control section.

The motor selected for this application is a Brushless DC Torque Motor. As in any DC motor the torque is developed due to the interaction of 2 magnetic fields. The first is the field of a permanent magnent; the second is a flux field created by a current in a winding. In a normal brush type motor the commutator automatically switches the current direction in the Armature Winding as it is rotated, thereby providing the proper relation between the flux of the magnet and the flux of the winding. With the brushless DC motor selected for this system, the Armature is used as the permanent magnet and the Stator Windings are energized selectively (commutated) to provide the proper relation of magnetic flux.

The electronic commutation information is obtained from the Optical Encoder Tracks, A, B, and C. The relationship between the track information and the switching pattern for the three Stator Windings is shown in Figure 3.4-3. The advantage of the electronic commutation of the torque motor over a brush type motor with its brush life, added friction, and EMI problems is obvious. Even when compared to a Stepper Motor this system offers some improvement. Since with a Stepper Motor the magnetic detent effect is still evident even with power off; a gear train must be used, with its attendant backlash problem, in order to obtain the same resolution. However, a torque motor can provide a direct drive to the gimbal while still allowing virtually infinite resolution. This is because there are no residual magnetic forces acting to move the Armature when power is removed from the Windings.

The 40 pole motor provides $360^{o}/40 = 9^{o}$ for one cycle of the commutation tracks. Since there are 6 unique combinations of drive of the motor windings for each cycle; then, $9^{o}/6 = 1.5^{o}$ of resolution position. If at this time the drivers are sequenced to the next state (either CW or CCW) and turned on for a short period of time the Armature can be moved into a position in between the stopping positions. It can be seen then, that by controlling the direction sequence to the drivers, and the time duration of the turn-on pulse, the Armature can be moved to any desired position of the 360^{o} circle thus giving pointing accuracy limited only by the encoder resolution.

The sequence information is provided by the commutation tracks from the Optical Encoder. Controlling the direction and time duration of the drive to the 3 windings of the motor is a task well suited to the processor. With the data from the encoder showing the present position and the processor knowing the

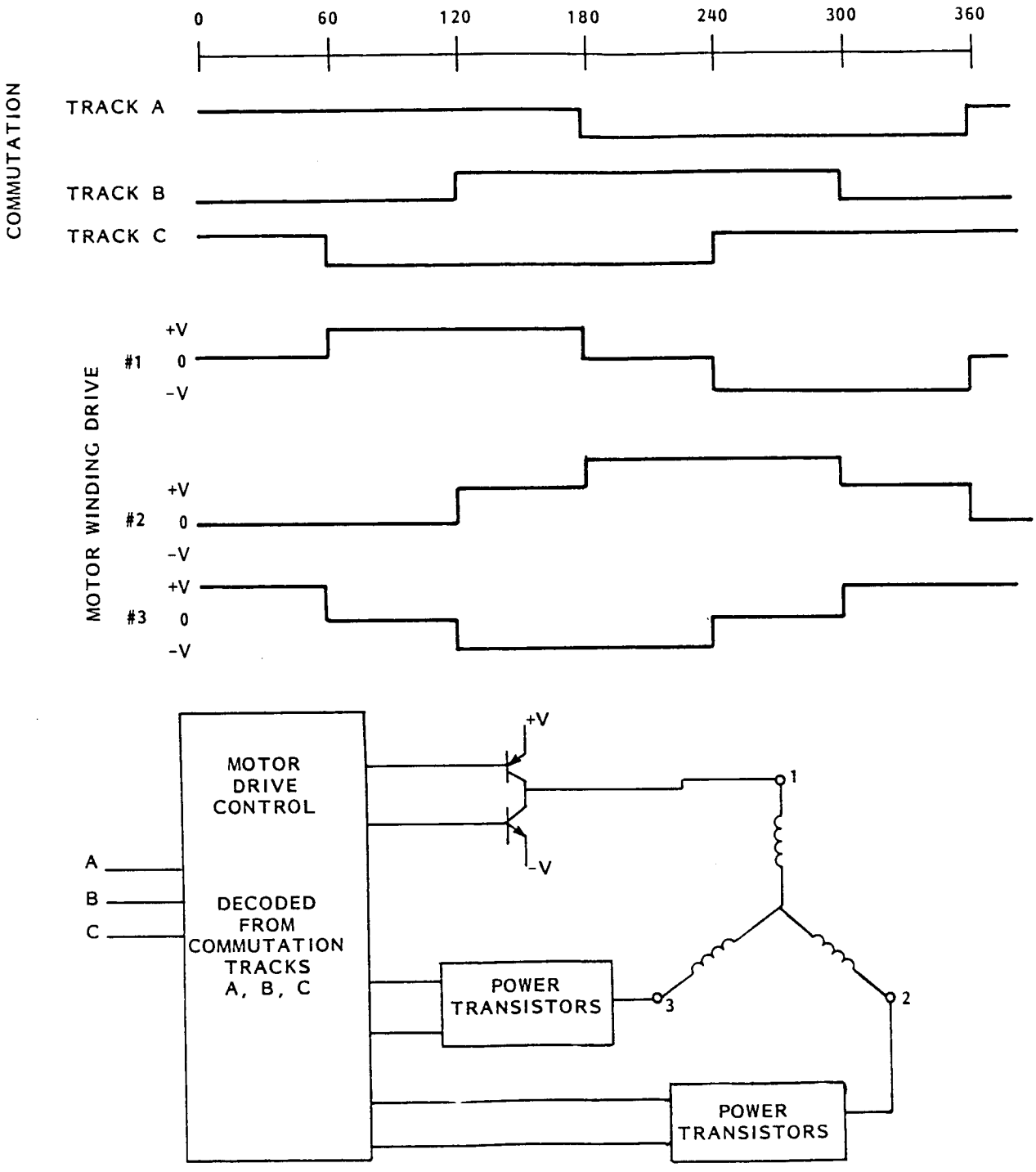

Figure 3.4-3. Commutation Track to Motor Drive Relationship

desired position a simple subtraction will indicate both the magnitude and the direction of an error in the position. As long as the error is large the motor drive is provided by the continuous current sequence. When the error becomes smaller the motor drive becomes short pulses. Finally, when the error is zero, all of the drivers are turned off.

3.4.3 Microprocessor

The microprocessor is at the core of the control system. It is the element which provides the overall system operation. The use of an embedded microprocessor takes advantage of the flexibility and precision of control of a computer; while at the same time it requires minimal attention from the spacecraft computer. Additionally, since the microprocesser is such a versatile decision making element, it is more efficient in size, weight and power than the combinatorial logic parts it replaces. All of the control functions for the system are contained in the Software resident in local memory. This fact, in itself, adds to the flexibility of the system since the control algorithms can be easily modified if the system requirements change.

The microprocessor obtains its command information through either of two channels. For evaluation and test a ground control interface is provided. This interface will be used during the performance evaluation of the Antenna System. In an actual flight version of course the command, control and communication functions would be by way of the Remote Interface Unit (RIU). The command information to the microprocessor will establish the operating mode for the system as well as passing any necessary parameters associated with that mode. One of the necessary commands would be a request for the present status of the control system. On receipt of this instruction the processor would supply: mode, position, error magnitude/direction, and antenna information as appropriate to

the mode of operation. Since the control functions of the Ground Control Interface and the RIU are essentially the same only one of the two will be assumed to be active in the following discussion.,

When the control system is first activated it would enter an Initialization Mode. During this period the system will set up it's operating parameters and do a self test to determine the health of the entire network. After completing this process the system will go into a Standby Mode where it will await a further command. While in Standby the system will monitor the position and condition of the antenna; but, it will not supply any drive to the motors. While in this mode the processor will provide status information in response to a Request Status instruction.

The next mode which might be used in a typical sequence is the Slew Mode. In this mode the system is given the instruction to move to a specific point. This point, the desired position, is given with the instruction and is stored in local memory. The processor then compares the present position to the desired position and determines the magnitude and direction of the offset for both elevation and azimuth.

Based on this comparison then, the controls to the individual motor drives are given to position the antenna to the new position. Assuming the offset to be large, the motor drive would start in the continuous sequences as described above (Section 3.4.2). As the antenna approached the desired position the Error Result (difference between present and desired position) would become small and the control to the motor drive would cause short pulses to be supplied to the motor. This pulse technique will reduce the amount of overtravel of the Gimbal and therefore allow faster repositioning of the Gimbal. If an overtravel does occur the Error Result would change sign and the control to the motor drive

would reverse the sequence to the motor to move it back to the desired position. Note that the Error Result (comparison of the present to the desired position) is constantly being updated as the Gimbal is being moved. When the Error Result is zero then the control to the motor drive shuts off all power to the motor leaving the Gimbal sitting at that position. At this point the processor will signal the commanding interface that the new position has been attained. If for some reason the Gimbal were to move (due to spacecraft inertial forces) the processor would automatically provide control to move the Gimbal back to the desired position using the Error Result to determine the motor drive required. In essence then: when the antenna is pointing in the desired direction (the coordinates of which are stored in local memory) all power to the torque motors is turned off; when the antenna is not pointing in the desired direction on either the azimuth or elevation axis the processor supplies control to the apropriate motor drive (based on the Error Result) to cause the antenna to move toward the desired direction. At any point in this cycle the commanding interface can issue a Request Status instruction which will be honored by the processor.

The Search Mode might be used next in a typical sequence. Having arrived at a position where a signal is expected; the commanding interface may elect to search the general area for the signal. In Search Mode the system is similar in operation to the Slew Mode. The processor will provide control to the motor drive to slew in one axis first then in the other axis. Alternating between the two axis drives creates a squared spiral search pattern. For this portion of the search the Error Result provides the control to the motor drives of both azimuth and elevation in order to describe the straight line segments of the spiral discussed in Section 3.3. When the antenna does pick up a signal the processor is alerted by the Acquire signal from the Tracking Converter; at this point the system will go into the Track Mode.

When the system is in Track Mode the processor uses the Digital Error Signals provided by the Tracking Converter to determine the control sent to the motor drive. The AZ error and EL error data from the Tracking Converter are in digital form; having been converted from the analog antenna signal by the converter. The processor, in Track Mode, uses these two error signals to generate the control to the motor drive. As in the other modes, when the error is large the motor is driven in the continuous sequence. When the error becomes smaller the processor provides the pulse drive to the motor to position the antenna. When the error becomes zero all drive to the motor is shut off. The processor continues to monitor the AZ and EL error signals; and, as they move from zero the processor will provide the pulse drive to the motor to bring the error signal back to zero. Also, as in the other modes, the processor will provide status of the present position and tracking converter data in response to a Request Status instruction.

3.4.4 Control Electronics - Summary

We have seen then, that the position of the antenna is controlled by the embedded microprocessor. This processor accepts instructions thru either of 2 ports (the ground control or the RIU to the spacecraft computer). Each port can place the processor into the desired operating mode. After the instruction is received the embedded processor handles all of the detail decisions in order to carry out the action. Thus it provides the desirable autonomous operation, which requires minimum attention from the onboard computer.

By using an absolute encoder it is possible to shut off power to the system and recover position data when power is returned; thus this system allows reduced power consumption. Additionally, by using a torque motor, the system can provide accuracy in pointing the antenna limited only by the encoder resolution. The short pulse mode drive for the motors aids in reducing overshot and obtaining the high degree of pointing accuracy. Finally, at any time during the various operating modes, the commanding interface (ground control or RIU to the OBC) can issue a Request Status instruction and receive the present position and antenna information.

3.5 Host Spacecraft Interfaces

3.5.1 Field of View (FOV)

The FOV requirement is one of the major drivers for the selection of the antenna system. The selected beam waveguide antenna provides the required flexibility for application to both relay and user satellites.

For a relay satellite a maximum of five antennas are to be mounted to a single spacecraft. Each antenna must provide a FOV of a cone of at least ± 11° (spec ± 13°) centered on the sub-satellite point to provide coverage over the orbital shell at the maximum altitude of 1500 km (see Appendix C).

Relay Satellite Field of View: For the conceptual design it is assumed that five identical antennas are mounted on the earth facing side of the satellite. Figure 3.5-1 shows this arrangement in a compact configuration. Each antenna has a diameter of 48". The electronics enclosures are all located inside the spacecraft. Each gimbal axis is identically offset by 30° to position the gimbal lock well outside the FOV. To accommodate independent FOV and launch lock for each antenna, a cylinder of 58" diameter must be allocated for each of the five systems in this concept.

Alternate arrangements are feasible but it should be noted that a symmetrical configuration is highly desirable from a viewpoint of design and control uniformity. The important message here is that the crosslink system configuration is a major driver for the evolving spacecraft configuration and vice versa.

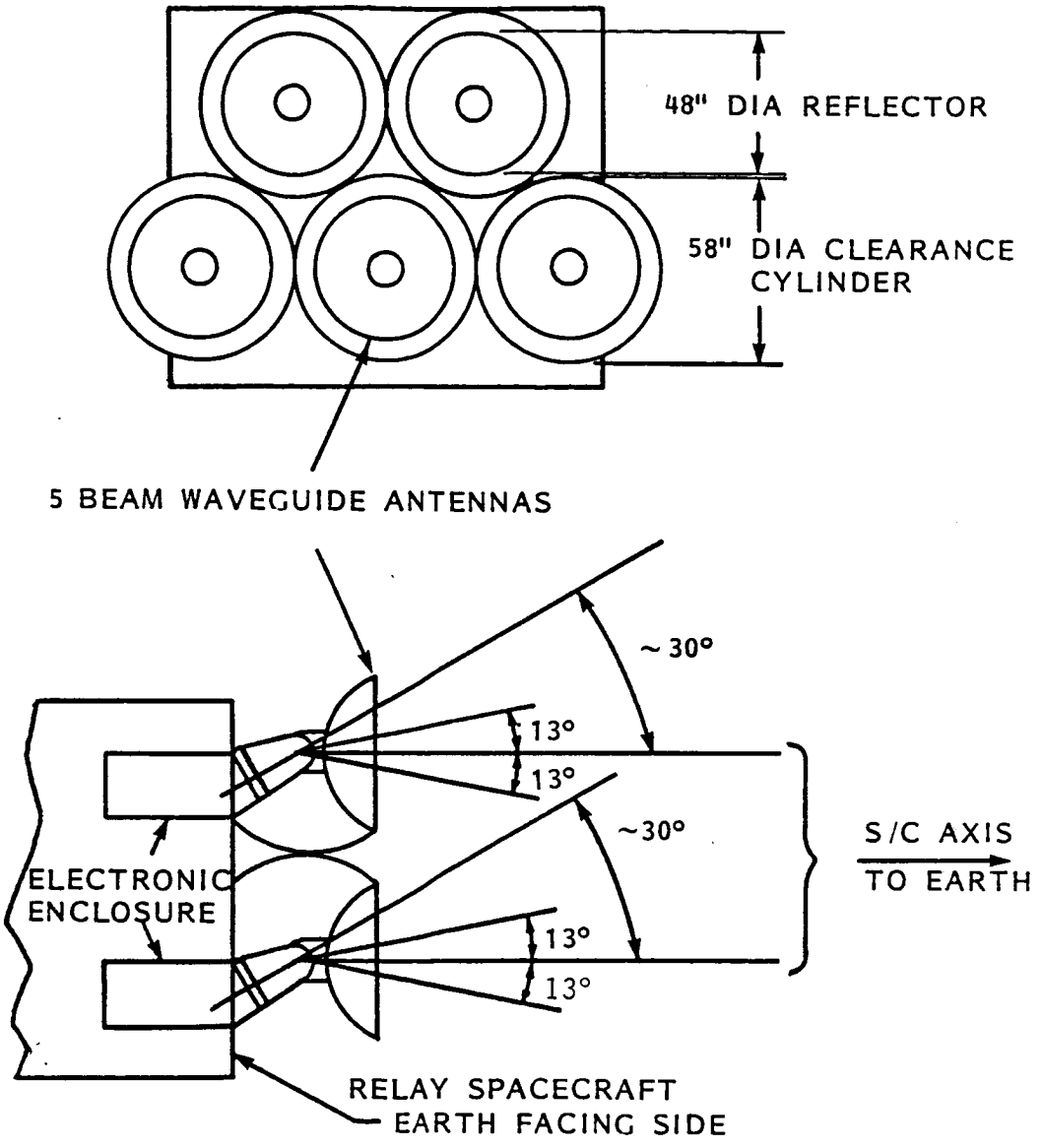

Figure 3.5-1. Relay Spacecraft Field of View

User Satellite Field of View: For the conceptual design a single antenna of 48" diameter is assumed. Here the electronics enclosure is fully or partially outside the spacecraft envelope to provide additional support structure height. The FOV is limited by self interference between the reflector and its support configuration, i.e. either the gimbal or the electronics enclosure or the spacecraft. Figure 3.5 - 2 shows the configuration which was worked out in mechanical and electrical detail during Phase B. A gimbal lock cannot be prevented for a FOV in excess of $\pm$ 90° and the main gimbal axis is positioned along the local vertical to provide the maximum possible FOV. In the configuration shown the FOV is limited to $\pm$ 100° due to self interference with the selected width of the electronics enclosure. A larger FOV can be achieved by locating the reflector further outboard and lengthening the distance between the two parabolic mirrors in the gimbal column. It can be seen from the geometry of Figure 3.5 - 2 that the maximum required FOV of $\pm$ 126° is reached by locating the reflector system outboard by 5". This however results in an increase in both, gimbal weight and antenna moment of inertia. The details of this impact including increased diameter of the gimbal housing, feed horns and beam waveguide optics have not been iterated. Again, the eventual configuration and location must evolve together with a given user spacecraft.

In summary it should be noted that the modularity of the selected beam waveguide system can accomodate various spacecraft configurations with their specific FOV requirements.

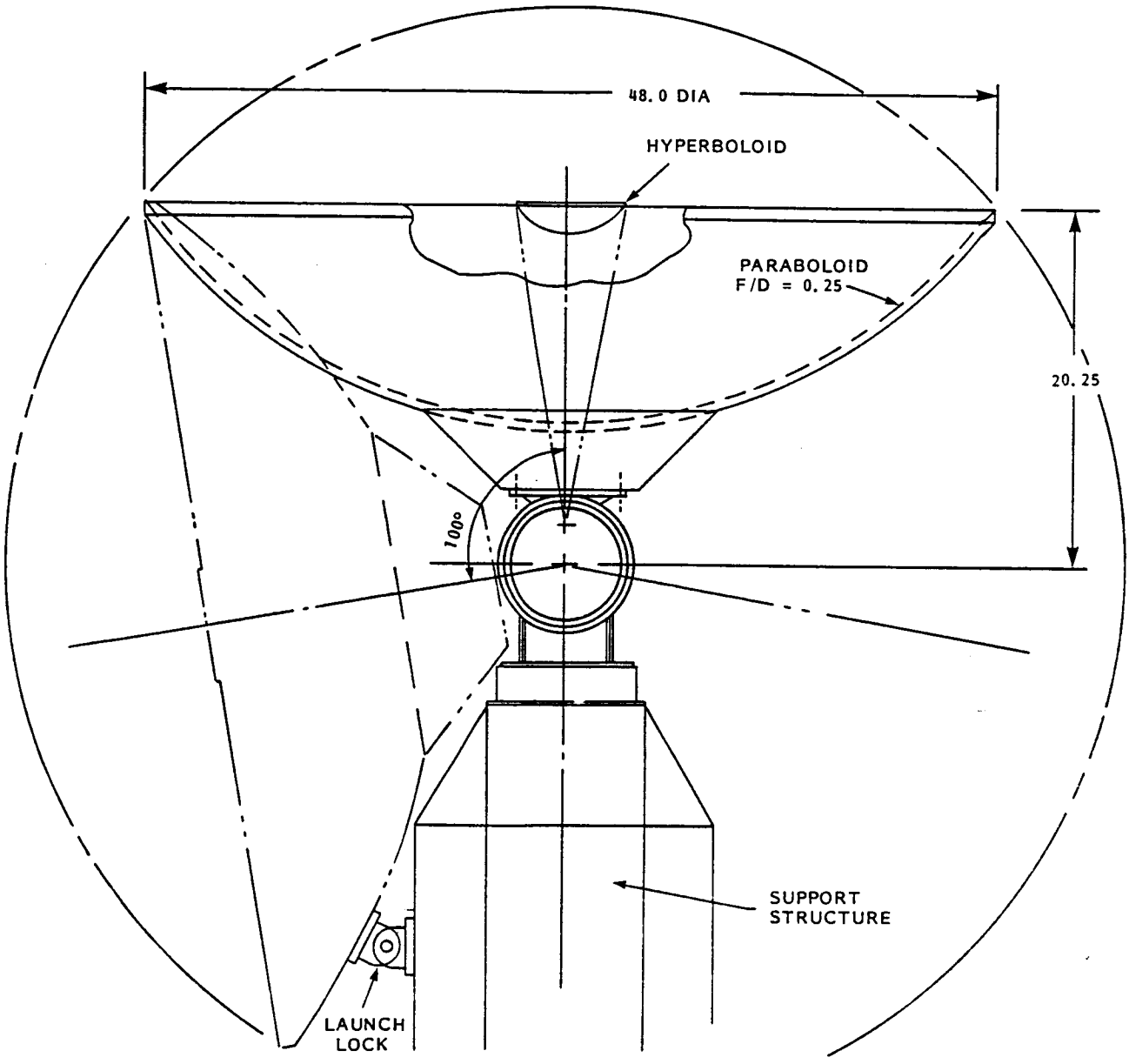

Figure 3.5-2. User Satellite Field of View

3.5.2 Stowed Configuration

One of the advantages of the selected beam waveguide antenna system is its compact and straightforward stowage configuration. The reflector is stowed against its own gimbal support structure with a single launch lock as shown in Figure 3.5-2. Depending on the application which determines the FOV and support structure height the reflector is locked against the gimbal housing, or electronics enclosure or support column. In all cases the locking system is self contained without any interface to the spacecraft structure except for the electrical interface for the ordinance controller. A typical launch lock - used on the DSCS III 33" diameter gimballed antenna - is shown in Figure 3.5-3.

3.5.3 Interactions with Spacecraft

In this section some of the critical interactions with a typical spacecraft are discussed, such as base stability, knowledge of spacecraft attitude, motion coupling, thermal effects and RF EMI with other antennas. In the absence of specific definitions for the TDAS and user spacecraft a qualitative rather than quantitative assessment is made, based on prior expertise derived from projects such as DSCS III and Landsat D.

Base Stability - For the case of a user satellite the electronics enclosure is likely to be used as part of the antenna support structure (see Figure 3.5-2). This enclosure is visualized as a box structure, providing high rigidity and minimizing dynamic effects that could distort the RF compartment and impair the pointing accuracy of the antenna. In a low cost version the enclosure would be constructed as a machined aluminum or Beryllium Assembly bolted together. A lower weight, higher cost version would use more exotic materials such as graphite fiber reinforced epoxy elements. This box construction technique provides for the necessary surfaces for component mounting, thermal radiators and access panels. The modular concept allows effective testing of the entire crosslink communication subsystem, both on the bench and on the antenna test range. The box structure is dimensioned to provide negligible contributions, statically or dynamically, to the antenna command pointing error in terms of an antenna beamwidth of about 0.3^{o}.

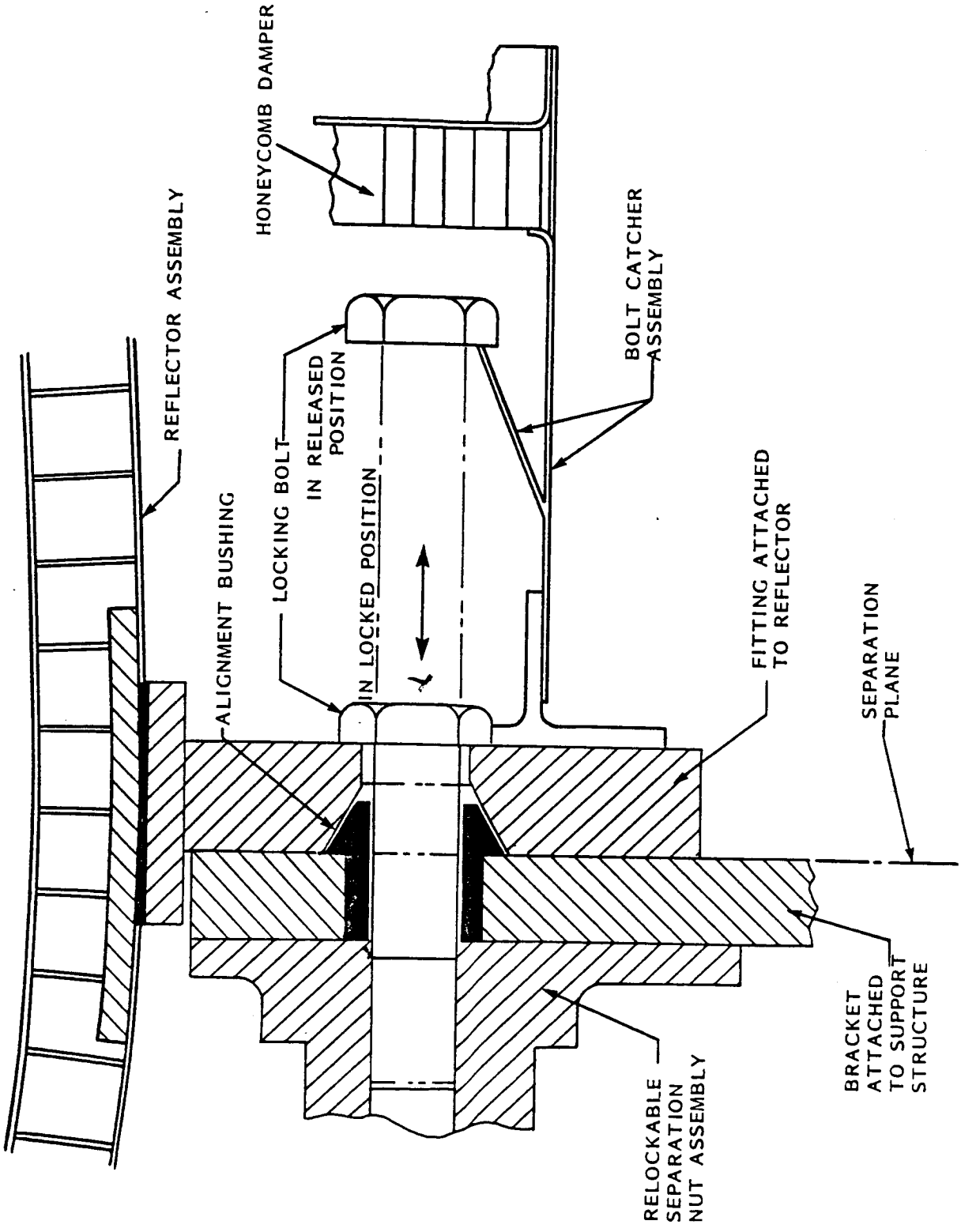

Figure 3.5-3. Antenna Launch Lock

Knowledge of Spacecraft Attitude - For both a geostationary satellite and any low-orbit user satellite it can be assumed that the space craft attitude is known to better than 0.003^{o} (3σ) during nominal operation. Any necessary corrections to commanded antenna pointing can therefore be done with great accuracy. Once auto-track is achieved antenna pointing is assured independent of spacecraft attitude and/or knowledge of spacecraft attitude.

Motion Coupling - Motion Coupling -- also known as torque noise -- is the effect of the moving antenna on the attitude of the host spacecraft. During antenna slew maneuvers maximum angular acceleration or deceleration will be imparted to the spacecraft. In most cases the much larger moment of inertia of the total spacecraft compared to the moment of inertia of a 4 ft. gimballed antenna will prevent any objectionable angular disturbance. Typical weights and moments of inertia for geostationary and user satellites in comparison to a 4 ft. antenna system are given below:

	Weight (lbs.)	Moment of Inertia ($slug\text{-}ft^2$)	M.O.I. Ratio
DSCS III (Geostationary)	2000 min.	406 min.	434 min.
Landsat D (low earth orbit)	3778 min.	2500 min.	2673 min.
Gimballed Antenna	16.5	0.94 max.	------

However, there may be cases where the antenna moment of inertia when driven at high acceleration causes a significant spacecraft pointing and rate error. The error is avoided both by "feeding forward" compensation to the spacecraft attitude control system (ACS) and by tailoring the slew maneuvers to permit the ACS to limit the induced errors and recover quickly. One approach - selected for Landsat D - is to limit the rise of the antenna command to avoid a step change in antenna slew rate. This approach requires that the normal antenna pointing control law be bypassed and the commands given directly to the gimbal drives. The normal program track control loop is reactivated after the slew maneuver is completed.

The most severe requirements occur for slewing around the gimbal lock zone. Specific system studies are required to assess communication requirements, gimbal lock outage times and spacecraft ACS effects.

Thermal Control Design - Thermal control for the selected beam waveguide antenna system is anticipated to be totally passive, utilizing coatings, multilayer insulation and electrical heaters activated by thermostats with command override. The primary low α/ϵ coatings are silver coated teflon (5 mil) and optical solar reflectors (OSR). White paint (S-13GLO) and black paint (Chemglaze S-306) are used as secondary heat control coatings.

Multi-layer insulation blankets provide very low thermal conductivity, isolating the antenna system from the space environment. For electromagnetic compatibility they are grounded by shorting the metalized surface of each layer to spacecraft ground.

Heater/Thermostat assemblies have redundant heaters and redundant thermostats to eliminate single point failures. Heaters are lightweight, etched foil Kapton film heaters with welded leads, bonded to the substrate with Hysol 956. Thermostats are solid state devices which can operate on an absolute or a differential temperature.

RF Electromagnetic Interference - Terrestrial RF interference will be minimal due to the high attenuation of oxygen absorption. For the user satellite with a single 60 GHz crosslink antenna system EMI does not present any unique problems. The 60 GHz receiver system is protected effectively against all lower frequencies due to the cutoff attenuation of the 60 GHz waveguide. The 60 GHz transmitter power is contained inside a cylinder projected from the 4' reflector aperture. Impingement on other antennas with equipment on the spacecraft may have to be controlled by limiting the FOV of the beam waveguide antenna if sufficient frequency filtering cannot be provided. Control of feed spillover and back lobe radiation also helps and is used routinely to achieve a high antenna efficiency.

For a realy satellite with as many as five antennas EMI is a complex, multi-variable problem, involving basic issues of system architecture, (number of relay satellites, frequency plan, polarization re-use, modulation method, repeating method, multiplexing method for crosslinks and downlinks and other parameters). With multiple user signals at differing rates, modulation formats, ranging schemes and synchronization requirements on-board

signal processing may be necessary. The design requirements for the 60 GHz crosslink antenna are not strongly influenced by the choice of the above system parameters, except for the EIRP allocation between transmitter power and antenna gain; i.e., aperture size. This allocation indirectly affects the receive band rejection requirements in the transmit output filters.

A separate EMI problem is presented by the arrival of as many as five simultaneous tracking beacon signals which are distributed over the 60 GHz band according to the selected frequency plan. This will lead to an interference situation whenever 2 or more satellites cross over; i.e., when 2 or more TDAS antennas are pointed in roughly the same direction.

Astroquartz is a relatively constant thickness material that is RF transparent with low α/ϵ thermal properties. The cloth distributes thermal energy uniformily over its surface thus minimizing the thermal gradients on the reflector which it covers. The degradation of the astroquartz cloth in orbit is less severe than most thermal coatings.

3.6 Performance Summary

Table 3.6-1 summarizes electrical and mechanical performance characteristics as derived for the selected beam waveguide antenna system during the study. The performance values should be considered as "average" values, rather than "max" or "min" values.

Table 3.6-1 Performance Summary - Beam Waveguide Antenna System

Parameter	Performance		Remarks
	RELAY SATELLITE APPLICATION	USER APPLICATION	
Frequency	60 GHz		WARC 79 Allocations: 54.25 - 58.20 GHz 59.00 - 64.00 GHz
Number of Antennas	up to 5	1	
Bandwidth	50 MHz	50 MHz	50 Megabit data rate per user link
	250 MHz		For 5 channels for GEOS/GEOS link. Antenna design could accomodate larger bandwidth up to 5 GHz
Antenna Gain	54 db		see Appendix D for link budget
Polarization	Right hand circular		
Aperture	48" Dia		
Halfpower Beamwidth	0.29^{o}		HPBW$\simeq \frac{70\lambda}{D}$
Field of View	$\pm 13^{o}$	$\pm 104^{o}$	User satellite altitude = 200 km
		$\pm 126^{o}$	User satellite altitude = 1500 km
Pointing Accuracy	$\pm 0.05^{o}$		Results in 0.4 db gain loss Program Track: 0.066^{o}RSS - 0.6db loss Auto Track: 0.034^{o}RSS - 0.2db loss

(Table 3.6-1 continued)

Estimates
Weight and Power per Antenna System

Aperture	Weight (lbs)	Power (Watts)
Reflector	10.6	-
Insulation	5.9	-
	16.5	
60 GHz Electronics		
Feed	.1	-
Monopulse Modulator	.8	1.4
Transponder	12.8	27.9
Local Oscillator	8.8	9.4
Power Conditioner	6.1	7.7
Thermal Control	1.0	-
	29.6	46.4
2-Axis Gimbal		
Mechanisms & Housing	20.2	1.4
Thermal Control	.6	4.0
Support Structure	12.5	-
Control Electronics	17.9 (Redundant)	7.5
	51.2	12.9
TOTAL	97.3 lbs	59.3 Watts

(Table 3.6-1 continued)

Control Modes	Initialization/Standby Mode: Default non-operational mode
	Slew Mode: Rapid Transition to a commanded position
	Manual/Program Track Mode: Pointing parameters are commanded from the ground (manual) or satellite ephemeris parameters are commanded (program).
	Search Mode: Prescribed square spiral search.
	Autotrack Mode: Commences automatically when target acquisition is established after Search Mode or Slew Mode.

SECTION 4

INDUSTRY DEVELOPMENT STATUS

SECTION 4

INDUSTRY DEVELOPMENT STATUS

4.1 Monopulse Front End

State-of-the-art receiver characteristics are shown in Table 4.1-1. A low noise figure is required to achieve high monopulse tracking accuracy. A low receiver noise figure, in turn, requires low noise figures for the mixer and I.F. amplifiers and a low noise L.O. generator.

Table 4.1-1

RECEIVER CHARACTERISTICS

R.F. CENTER FREQUENCY	61.5 GHZ
R.F. BANDWIDTH	$\pm$ 2.5 GHZ
NOISE FIGURE	$\leq$ 7.0 dB
L.O. REFERENCE FREQUENCY	10.0 MHZ
R.F. CHOPPING FREQUENCY	1.0 KHZ
INTERMEDIATE FREQUENCY	7.5 GHZ
PHASE NOISE	$\measuredangle 2.5^{o}$RMS; 100 KHZ to 750 MHZ FROM CARRIER
L.O. LONG TERM CENTER FREQUENCY STABILITY	1×10^{-7}/day

Figure 4.1-1 shows the functional diagram of a monopulse tracking receiver implementation and Figure 4.1-2 shows the associated multimode tracking feed.

A typical sequential lobing autotrack feed is implemented using a single multimode horn and a broad frequency band sum and difference pattern comparator network. The feed network, depicted in Figure 4.1-2 provides communication and autotrack functions over a 4.8% bandwidth.

The feed uses a circularly polarized dual mode (TE_{11}/TM_{01}) dual flared conical horn for the principal beam sum pattern and one of the TE_{21} doublet modes for a difference pattern with a null on axis. The TE_{21} mode is coupled by a feed yoke near its cut off (diameter to wave length ratio of 0.97). The phase of the difference signal is sequentially stepped by four 90^{o} intervals and added to the sum channel through an isolator via a crossed waveguide coupler (nominally -15dB). The isolator precludes some transmit pattern degradation due to radiation in the TE_{21} tracking mode. For an incident circularly polarized wave the sum and delta outputs of the horn are:

$$V_\Sigma = A e^{-i\phi}$$

$$V_\Delta = B\theta e^{-i2\phi}$$

θ = Aspect Angle
ϕ = Roll Angle

Mathematically the θ, ϕ information is contained in the ratio of these two voltages. The delta output may be phase modulated in 90^0 steps and added to the sum signal as follows:

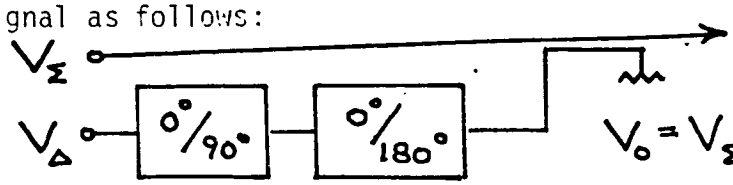

$$V_o = V_\Sigma + V_\Delta = \left[A + B\theta e^{-i(\phi+\psi)}\right] e^{-i\phi}$$

Where ψ = 0^0, 90^0, 180^0, 270^0

and $A >> B\theta$

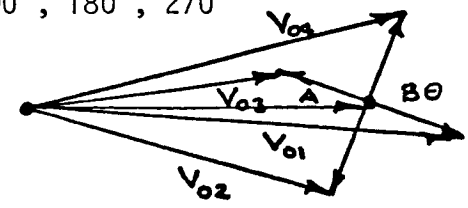

The resultant vectors represent an amplitude modulated waveform where the peak-to-peak modulation is proportional to $B\theta$ and the phase of the modulation envelope is proportional to ϕ.

The other (OMT, polarizer, coupler, etc.) components are implemented using traditional proven configurations.

The phase equalizer is comprised of a length of reduced width rectangular waveguide and is placed in the sum signal line between the coupler and the sum horn to provide broadband phase tracking with respect to the signal through the difference circuits.

The envelope of V_0 will be

$$|V_o| \simeq A + B\theta \cos(\phi + \psi)$$

and the four states of ψ will yield

$$|V_1|_{\psi=0} = A + B\theta \cos\phi$$

$$|V_2|_{\psi=-\frac{\pi}{2}} = A + B\theta \sin\phi$$

$$|V_3|_{\psi=-\pi} = A - B\theta \cos\phi$$

Also $$|V_4|_{\psi=-\frac{3\pi}{2}} = A - B\theta \sin\phi$$

$$\frac{|V_1| + |V_3|}{2} = \frac{|V_2| + |V_4|}{2} = A$$

And

$$|V_1| - A = V_{1E} = B\Theta \cos \phi = -V_{3E}$$

$$|V_2| - A = V_{2E} = B\Theta \sin \phi = -V_{4E}$$

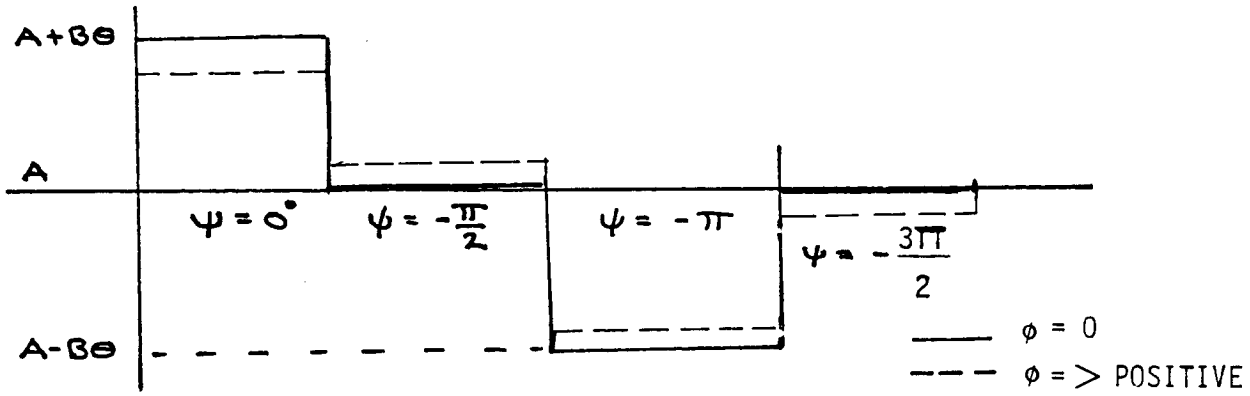

ENVELOPE WAVEFORM

Therefore

$$\frac{V_{2E}}{V_{1E}} = \frac{V_{4E}}{V_{3E}} = \text{Tan } \phi \text{, Indeterminate @ } \phi = 0$$

$$(V_{1E}^2 + V_{2E}^2)^{1/2} = B\Theta$$

The envelope detector measures (V_{01}) thru (V_{04}). The A.C. coupling removes the D.C. level. The integrate and dump serves as a matched filter. The sample and hold samples values V_{1E} thru V_{4E}. The processor calculates the error signals Θ & ϕ.

Since the L.O. frequency is very high the L.O. reference must be multiplied by a large factor. Phase noise on the L.O. reference increases as 20 logN where N is the multiplying factor. It is required then to keep N small. This is accomplished in the L.O. generator of figure 4.1-1 by using a surface acoustic wave (SAW) oscillator operating at an elevated frequency. The SAW oscillator is stabilized by an ultra-stable 10 MHZ

frequency reference. The phase noise is determined primarily by the SAW and is relatively independent of the 10 MHZ reference. The reference noise is filtered out by the SAW phase locked loop.

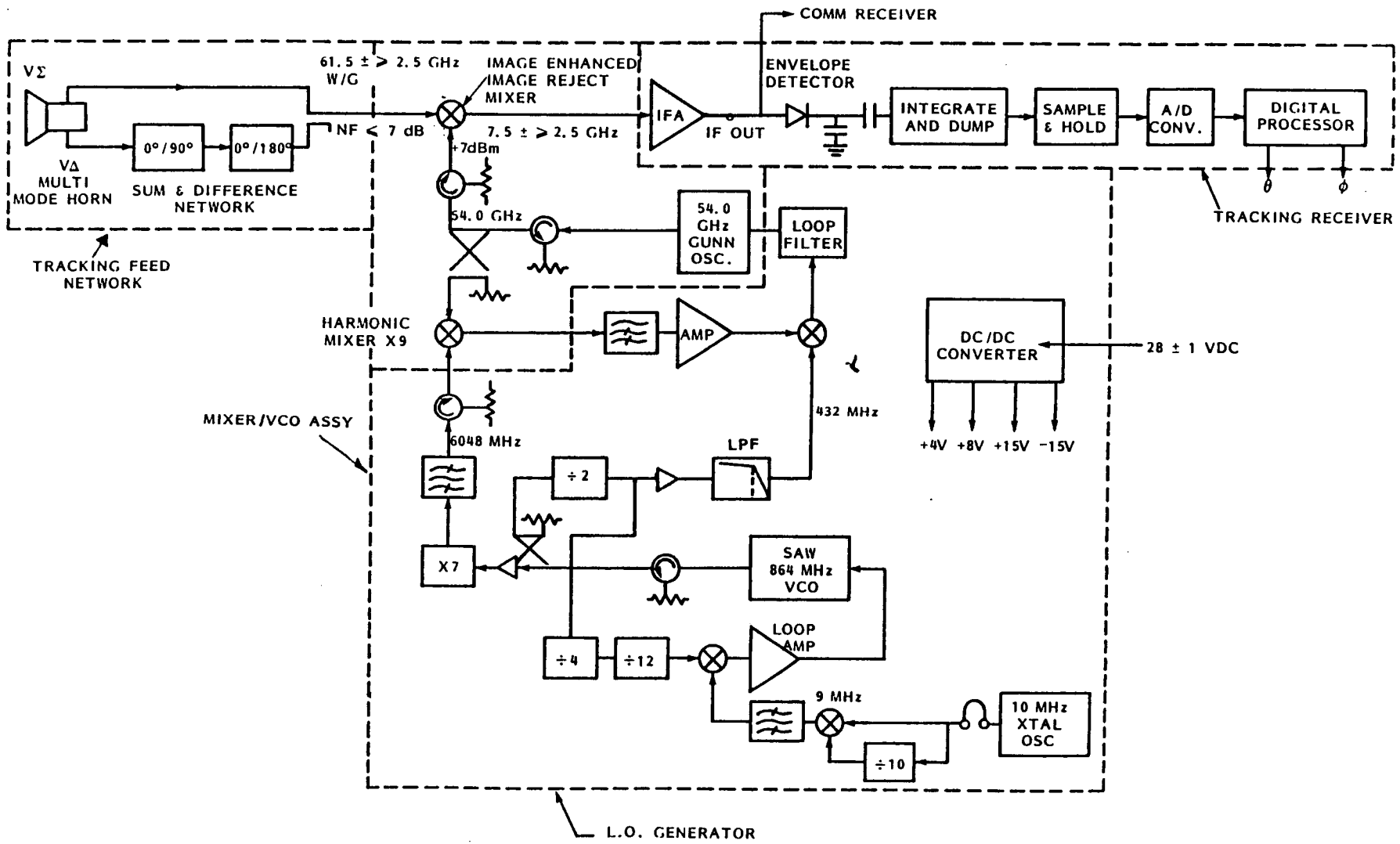

Figure 4.1-1. Functional Block Diagram 60 GHz Low Noise Monopulse Receiver

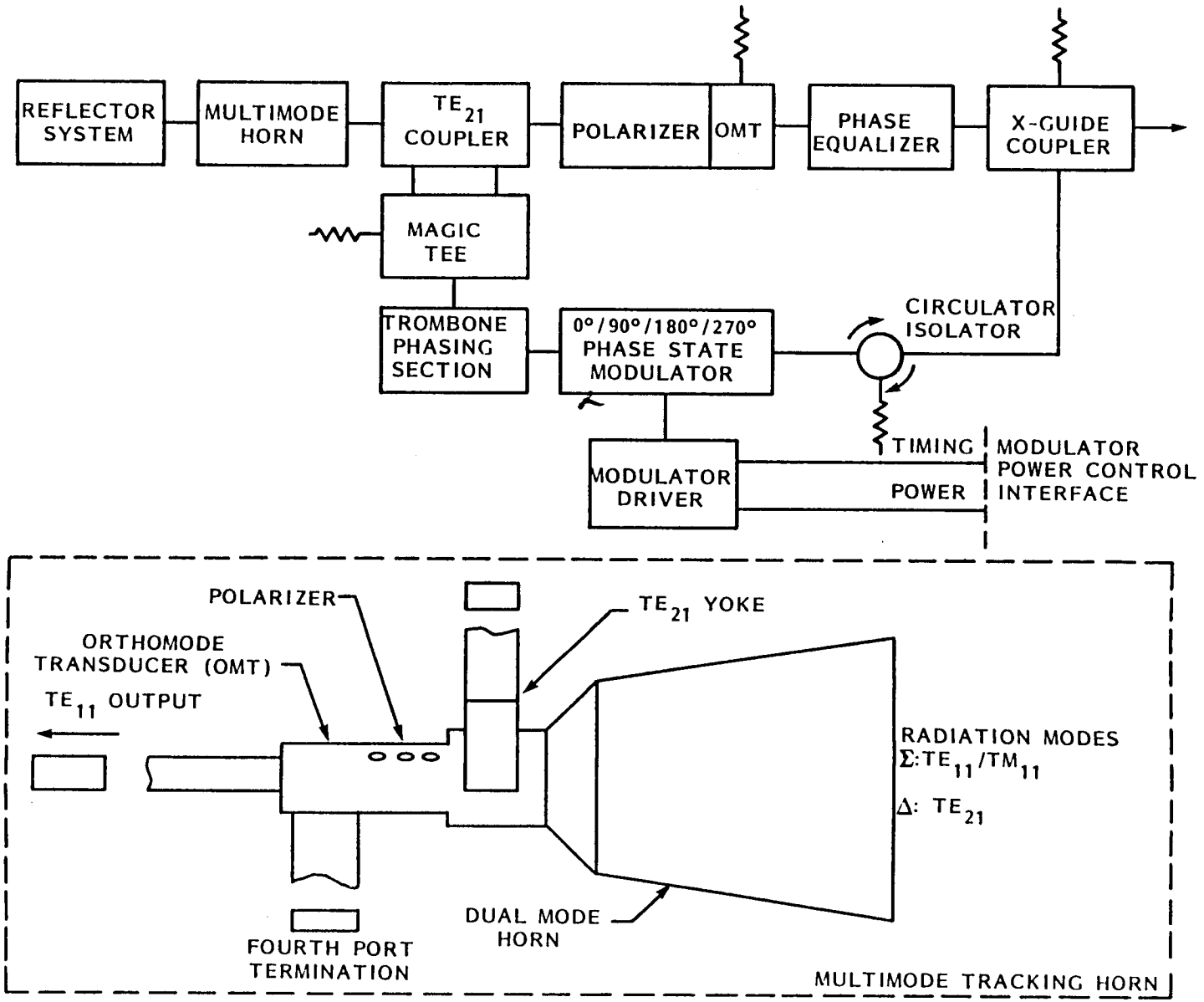

Figure 4.1-2. Tracking Feed Network

4.2 Flexible Waveguide

All techniques that transmit the unprocessed RF from the reflector co-ordinate system to the spacecraft so as to avoid an environmentally controlled pallet must maintain the relative phase relations between the sum channel and the difference channel(s). In addition, it is important to keep losses at a minimum, especially in the sum channel.

4.2.1 Metallic Corrugated Waveguide

Use is made of corrugated flexible waveguide in the microwave band, however, losses, reflections and phase shifts increase rapidly when the radius of curvature is too small. For this reason there is no effort under way to develope this type of transmission at 60 gHz.

4.2.2 Articulated Choke

At one time a flexible waveguide was manufactured that consisted of short sections of waveguide with RF choke faces held together in a flexible housing without metalic contact between the sections. This technique was never shown, in practice, to perform any better than the corrugated waveguide and is rarely seen today. The outer jacket had to be very stiff to keep the choke sections in the proper relation to each other and thus required high bending forces. The outer jacket would be under high stress and tend to deteriorate quickly. This would be even worse in a space environment.

4.2.3 Dielectric Waveguide

Recently techniques, similar to those employed in fibre optics have been used to develope mm wave flexible waveguide with low loss. To keep the losses to low values, however, requires that the waveguide diameter be many wavelengths across. This leads to many possible modes in the guide and an uncertain phase relation between channels that may be carried in adjacent dielectric waveguides as a function of bending angle. An attempt is made to insure single mode operation by radially varying the dielectric constant of the guide. A lossy outer jacket is also used to absorb higher modes as they are generated, however this does not guarantee that the phase of the dominant mode is not perturbed. As far as is known, no measurements of phase as a function of bending have been made. Table 4.2-1 shows measured results of this type of flexible waveguide made by Gore-Tex.

TABLE 4.2-1

FLEXIBLE WAVEGUIDE DESIGN CHARACTERISTICS

FREQUENCY OF BAND- GHZ	OVERALL DIAMETER-INCHES	TRANSMISSION LOSS-dB/M
35-45	Q75-2.0	5.0-0.4
60	0.5-1.5	6.0-1.0
95	0.25-10	10.0-3.0

4.3 Rotary Joints

4.3.1 Present State of the Art

The present state of the art is that of the rotary joints produced by TRG (Alpha Corp.). Rotation takes place in circular waveguide supporting the TE_{01} mode of propagation. This mode is a very low loss mode, however, relatively high loss transitions are required to transfer from the TE_{10} mode in rectangular guide into this propagation system, as well as a mode filter to insure that other (lower) modes do not occur in the circular guide. The two transitions, the mode filter, and the rotary section all introduce about 0.3 dB of loss, thus causing a loss per joint of about 1.2 dB. The TE_{10} mode guide between the rotary joint axes is also a high loss problem at this frequency. At a minimum this system will introduce 3.0 dB of loss into the antenna in a critical region that will directly impact the EIRP and G/T.

4.3.2 Proposed Modification

An approach that might reduce this loss to more reasonable levels might be to maintain the guide in the low loss TE_{01} mode, not only in the rotary sections, but also in the entire waveguide run. A TE_{10} to TE_{01} mode transducer and a TE_{01} mode filter could be introduced immediately behind the feed and all the rest of the RF run including both rotary joints could be in TE_{01} mode guide. One other TE_{01} to TE_{10} mode transition would be required at the input to the mixer (unless a mixer could be developed that operates with a TE_{01} mode RF input). This technique could cut the rotary joint/waveguide run loss at least in half to below 1.5 dB. It should still be pointed out however, that many problems would still remain. A pallet or stacked two axis rotary joints would still be needed, and the loss is still much higher than that of a beam waveguide.

4.4 Currently Available Hardware

4.4.1 Reflectors

Precision parabolic reflectors in the 4 ft. diameter range with RMS surface accuracies of less than 0.005" are well within the state-of-the-art. Figure 4.4.1-1 shows the General Electric development history for precision, light weight spacecraft reflector antennas. The first GE-SSD composite antenna, made in 1975, was the built-up kevlar epoxy elliptical aperture antenna successfully flow on BSE. This technology was also used for the DSCS III Gimbal Dish Antenna, which has been qualified and flown, and the Sperry Rand Antenna flown on the NASA Solar Maximum spacecraft. A lighter weight graphite-epoxy development unit was fabricated and tested in 1978 to verify production processes and demonstrate RF performance. A large 12 foot aperture offset feed antenna was fabricated in 1980 and extensively ground tested to optimize RF performance. The latest flight unit antenna is the graphite-epoxy/aluminum honeycomb core sandwich high gain antenna built under subcontract for Lockheed for the Space Telescope Program. Figure 4.4.1-2 shows a 7 ft. diameter offset parabolic reflector antenna developed for a 20/30 GHz crosslink antenna system. A new, room temperature fabrication process was developed for this application for both the plastic tool and the graphite fiber epoxy reflector resulting in lower material and labor cost, while maintaining 0.005" RMS tolerances. From these development and flight antenna programs, GE has developed the capability to design, analyze and fabricate composite antennas which fully meet both structural and performance requirements.

1975
BSE KU BAND ANTENNA

- 40.6" X 62.6" ELLIPTICAL APERTURE
- BUILT-UP KEVLAR-EPOXY REFLECTOR AND SUPPORT STRUT TUBES
- FLOWN ON BSE

1977
DSCS III GIMBAL-DISH ANTENNA

- 33" DIA. CIRCULAR APERTURE
- BUILT-UP KEVLAR-EPOXY REFLECTOR
- GRAPHITE-EPOXY SUPPORT STRUTS
- QUALIFIED ON DSCS III

1977
SPERRY-RAND HIGH GAIN ANTENNA

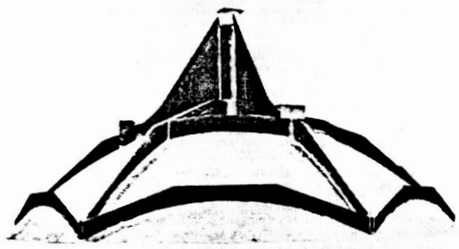

- 51" DIA. CIRCULAR APERTURE
- KEVLAR-EPOXY DISH
- GRAPHITE-EPOXY FACED ALUMINUM HONEYCOMB CORE SANDWICH BACK STRUCTURE
- FLOWN ON SOLAR MAXIMUM

1978
DEVELOPMENT COMPOSITE SANDWICH ANTENNA

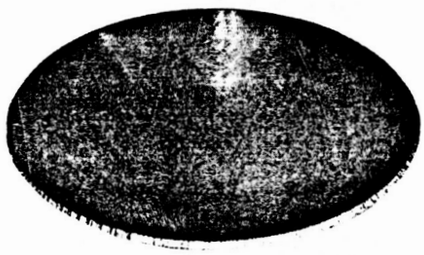

- 33" DIA. CIRCULAR APERTURE
- GRAPHITE-EPOXY FACED ALUMINUM CORE SANDWICH REFLECTOR
- GRAPHITE-EPOXY SUPPORT STRUTS
- DEMONSTRATED PERFORMANCE AND PRODUCIBILITY APPLICABLE TO LARGER APERTURES

1980
12 FT. APERTURE OFFSET
FEED DEVELOPMENT ANTENNA

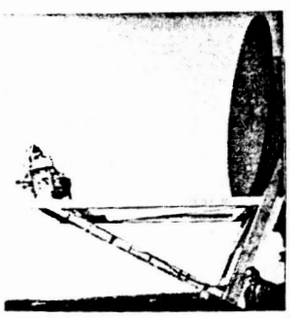

- GRAPHITE-EPOXY/AL. H/C REFLECTOR
- DEMONSTRATED FABRICATION AND RF PERFORMANCE OF LARGE APERTURE OFFSET FEED ANTENNA

1981
LMSC HIGH GAIN ANTENNA

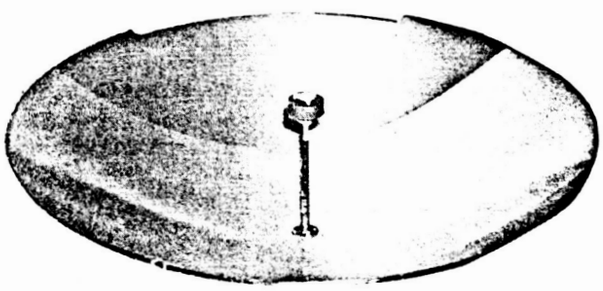

- 51" DIA. CIRCULAR APERTURE
- GRAPHITE EPOXY FACED ALUMINUM CORE SANDWICH
- FLIGHT ANTENNAS FOR SPACE TELESCOPE PROGRAM

Figure 4.4.1-1. General Electric Composite Antenna Development

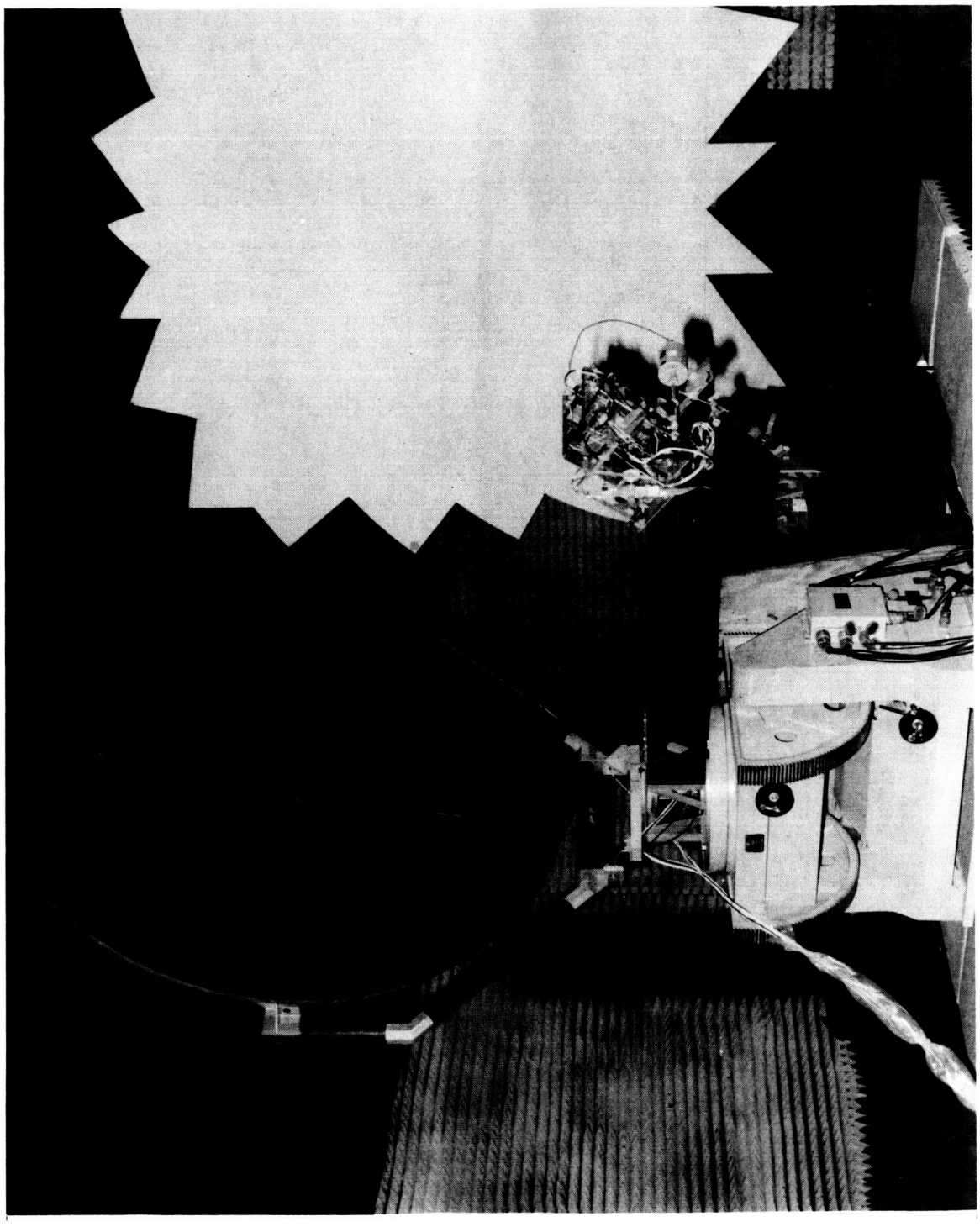

FIGURE 4.4.1-2. 20/30GHz ISL ANTENNA SYSTEM ON COMPACT RANGE

4.4.2 Beam Waveguide Gimbal Components

Typical applicable components which have been assessed for the 2-axis gimbal are listed below:

Motor

DC Brushless Motor Model 585-05
Sierracin/Magnedyne
P.O. Box 458
5380 El Camino Real
Carlsbad, CA 92008

6.620" OD
5.400" ID
Width = .875"
Weight = 28.0 oz.
Peak Torque = 2000 oz. in.
Rated Torque = 1344 oz. in.
Power (at rated torque) = 200 watts

Bearings

Kaydon Type A Matched Duplex Pair
Part No. KA040AR7M
Stainless Steel Balls

Bore = 4.000"
Outside Diameter = 4.500"
Radial Capacity (Dynamic) = 480 lbs.
Weight = 0.19 lbs.

Encoder

Digisec Model RIL 16/635(2) x Kit Incremental Encoder

Itek Measurement Systems Div.
Christinson Street
Newton, MA

Outer Diameter = 6.350"
Quanta/Revolution = 65,536
Angular Resolution = 19.78 min.
Total RMS Error = 8 arc seconds (2 stations)
Power Requirements = 525mA/6V
Operating Speed = 120 RPM max.

Mirrors

Optical Quality Mirror
Off-Axis Segment of Paraboloid
Electroformed Copper with Nickel Coating

Optical Radiation Corporation
Electroforming Division
6352 N. Irwindale Ave.
Azusa, CA 91702

Model No. PB105
Focal Length = 3.00"
Projected Diameter = 3.44"

4.4.3 Transponder

Power Amplifiers - TWTA's, while available for operation at 60-GHZ, tend to have poor reliability. The cathode voltage of a TWT increases with both frequency and power output, high voltage being the most critical factor in TWTA reliability. The second most critical factor is the cathode loading. The cathodes are affected since the beam size decreases with increasing frequency, resulting in higher cathode densities and lower reliability.

Amplifiers employing the negative resistance characteristics of Impatt diodes are currently available but at modest power levels. The present state of the art is ~ 0.6 to 0.7 WATT per device at about 8% efficiency. The development of both silicon and Ga As devices is presently being persued. Ga As has a performance advantage in power and efficiency below 50 GHZ and Si is superior at the higher frequencies (>90 GHz). Impatt amplifiers at a power level of 1 to 3 watts represent the current "state-of-the-art". The power from four to six devices are combined in a summer to achieve this level. Power amplifiers which will deliver 10 watts and above should be available by 1986/87. The impatts will deliver 1 watt of R.F. power.

Mixers - Transistor noise figures in the 3dB range have been achieved at 33 GHZ. Current projections indicate that noise figures in the 4 to 5 dB range are feasible at 60 GHZ and should be available at some future date. See Figure 4.4.3.-1. It appears, however, that the prevailing solution to a low noise receiver "front end" operating at 60 GHZ is, a double balanced mixer followed by a low noise I.F. amplifier. Front end noise figures from 5 to 7 dB are available using this technique. Figure 4.4.3-2 shows the design details of such a mixer. The design is a unique realization of an image enhanced, image reject, balanced mixer. Alpha Industries has developed an approach for millimeter wave mixer which has been designated the "planar cross-bar" design. This design utilizes waveguide and suspended quartz stripline in a mixed media approach to take advantage of the reliability, performance and repeatability of beam lead diodes embedded into a suspended stripline circuit.

As illustrated in Figure 4.4.3.-2 the beam lead semiconductors are mounted at the vertex of a biconcial matching structure metalized onto a fused quartz substrate. This structure provides a transformation of the 470 ohm impedance of full height waveguide down to the diode impedance, coupling the electric field of the TE_{10} mode propagating in the signal waveguide directly to the two demiconductor diodes. The impedance of a typical LO or DC biased Schottky barrier diode is approximately 100 ohms, and since two diodes are presented in series to the input signal, a broad match is obtained with instantaneous signal bandwidths in excess of 20%.

The GaAs beam lead diode developed by Alpha Industries has RF characteristics comparable to the best honeycomb diodes produced to date and also has, when embedded into a suspended **stripline** circuit, very low package capacitance and lead inductance. The carefully controlled embedding network for this diode, consisting of a precision photolithographically produced suspended stripline substrate, allows the use of a fixed in place cast back-short with no tuning required. The broad RF match of the biconical matching structures in this design will make the adjustment of this element much less critical than in other mixer designs, eliminating variations in the unit's performance with temperature and increasing the ease with which any optimization is carried out. The microwave circuit configuration described above attains a repeatability of performance and immunity to shock, vibration and thermal cycling in an extraordinarily cost-effective package heretofore unobtainable in millimeter wave mixers at these frequencies.

The noise performance of this mixer followed by an I.F. amplifier is shown in Figure 4.4.3-3

Local Oscillators - Depending on the I.F. frequency employed the L.O. frequency required by the mixer is quite high (55 to 59 GHZ). High stability sources (ovenized Xtal oscillators) are relatively low in frequency (5 to 10 MHZ). Very high multiplication factors can therefore be required.

Since phase noise increases as (20 log N) where N is the frequency multiplying factor, it becomes very difficult to generate a low noise L.O. and special design techniques must be used. In fact the L.O. reference will in most cases be the main contributer to the phase noise performance of the receiver "front end".

Figure 4.4.3-4 shows one possible solution to this problem. A GUNN oscillator operating directly at the L.O. output frequency is phase locked to a surface acoustic wave (SAW) oscillator. The SAW oscillator has relatively low phase noise and may be designed to operate at a high frequency (~ 800 MHz). Very large frequency multiplication factors are therefore not necessary and the phase noise may be held to acceptable levels. Good long term stability is achieved by phase locking the SAW oscillator to an ultra-stable Xtal reference.

Multiplexers - For each of the 5 individual links from relay to a user satellite a Transmit/Receive diplexer is required at each end. Related studies have shown that a transmit output filter must provide about 55 db of rejection in the adjacent receive band. Figure 4.4.3-5 shows the relationship between passband loss and carrier separation (N = number of TE_{011} cavities) providing 55 db rejection.

Filter development for MUX application is in progress at General Electric. Figure 4.4.3-6 shows parts of full scale model, prior to iris implementation. The filter utilizes a 3-pole Chebychev design in TE_{011} cylindrical cavity modes. To ensure stable operation over a range of temperatures the filter will be fabricated from invar and then silver plated to reduce losses. Electric discharge machining is required to maintain iris tolerances to $\pm$0.0001". Figure 4.4.3-7 shows the measured insertion loss and return loss characteristics.

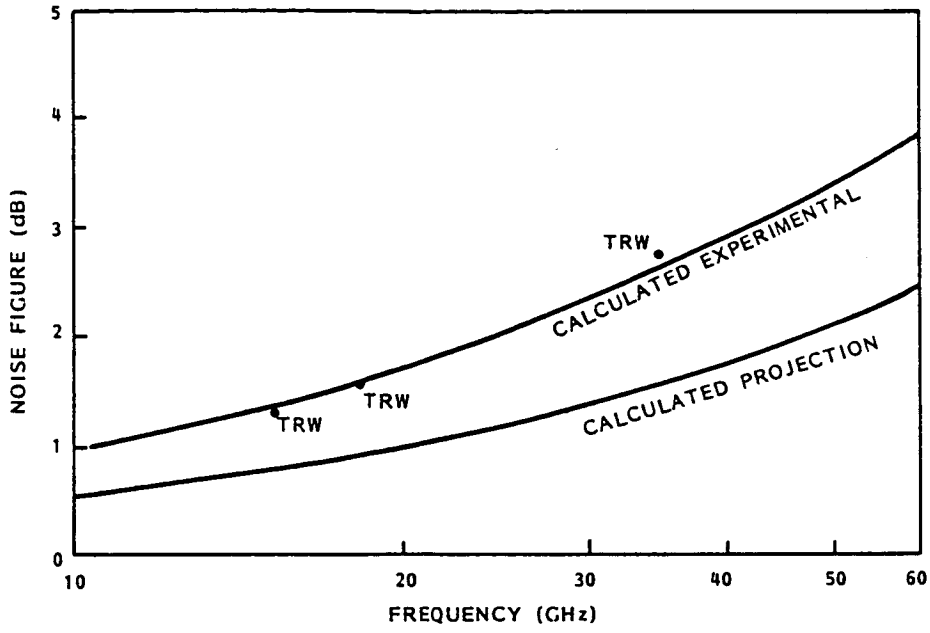

Figure 4.4.3-1. HEMT Noise Figure vs Frequency

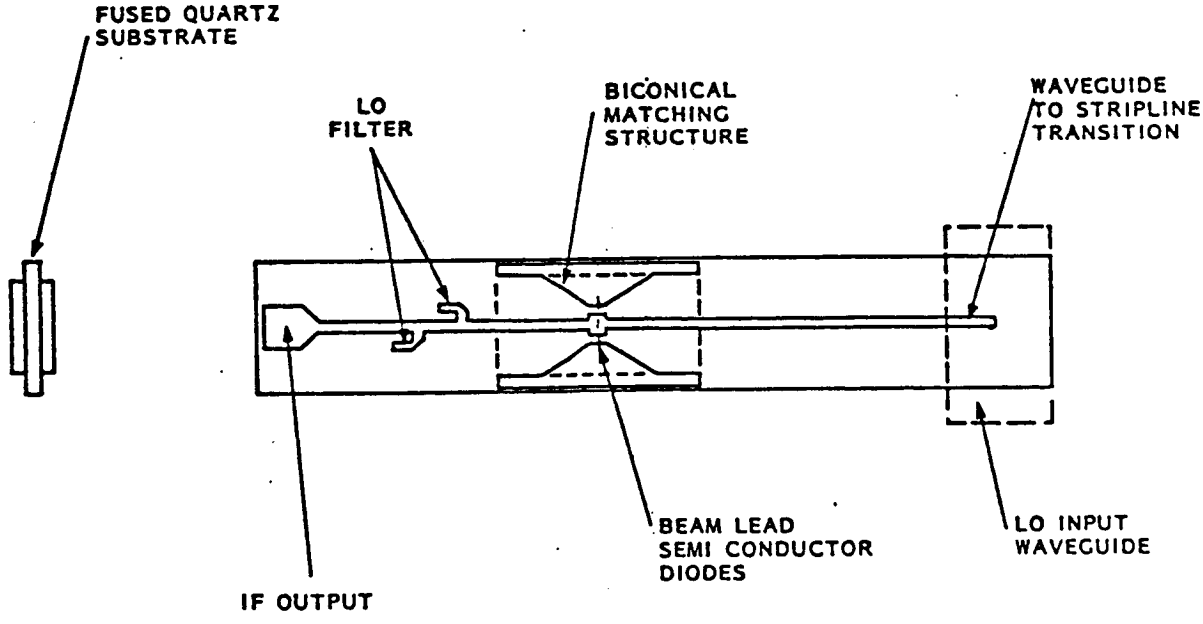

Figure 4.4.3-2. Planar Cross Bar Mixer Substrate With Beam Lead Diodes

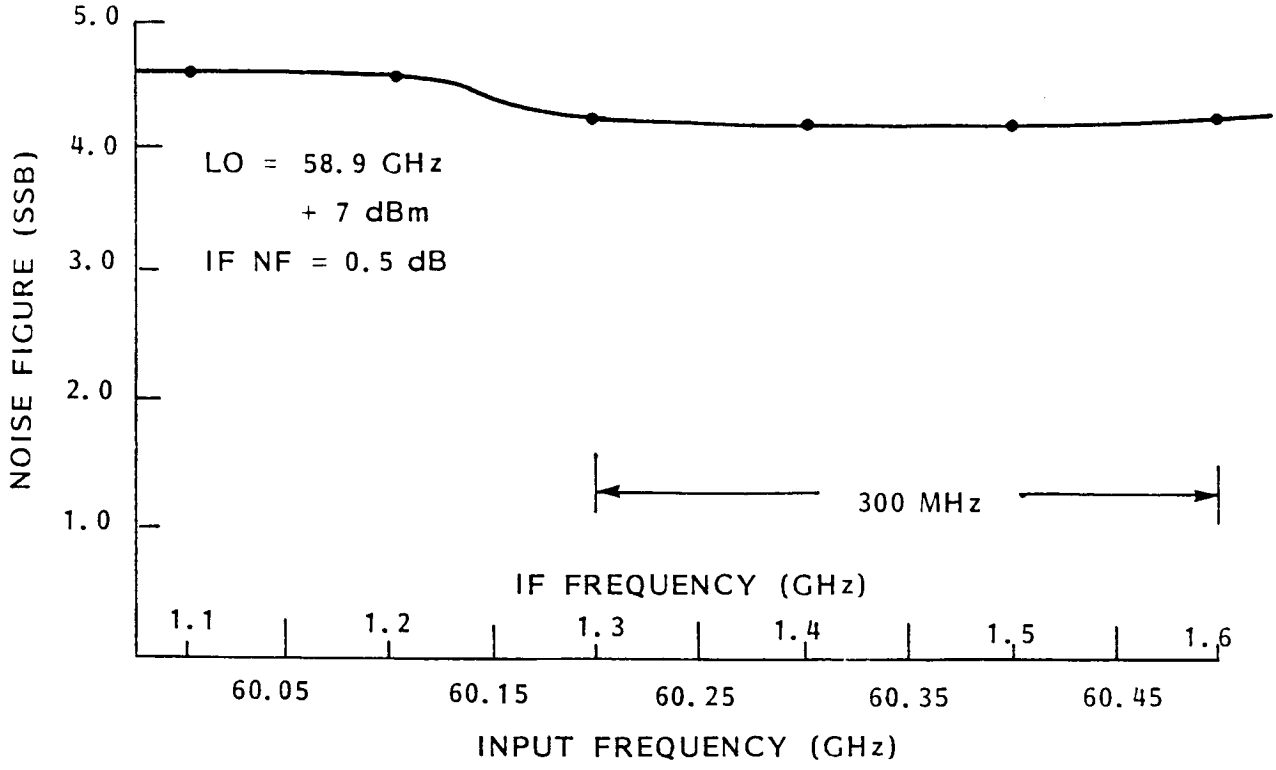

Figure 4.4.3-3. 60 GHz Downconverter Noise Figure (SSB)

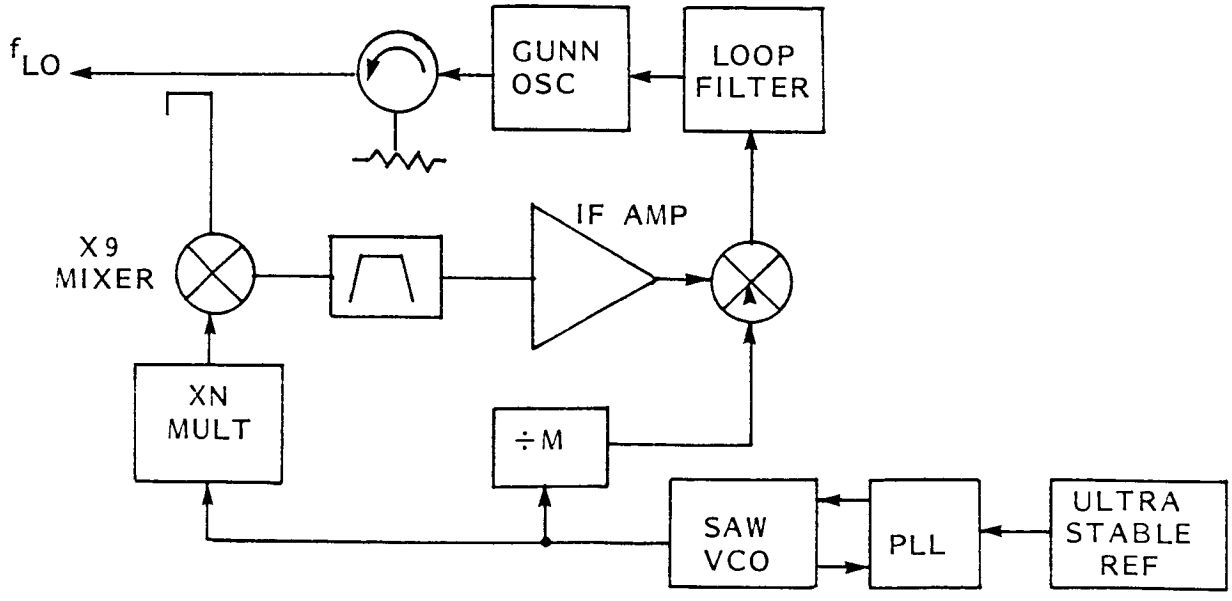

Figure 4.4.3-4. Low Noise SAW Reference Block Diagram

FIGURE 4.4.3-5. MULTIPLEXER INSERTION LOSS AND COMPLEXITY VS CHANNEL SPACING

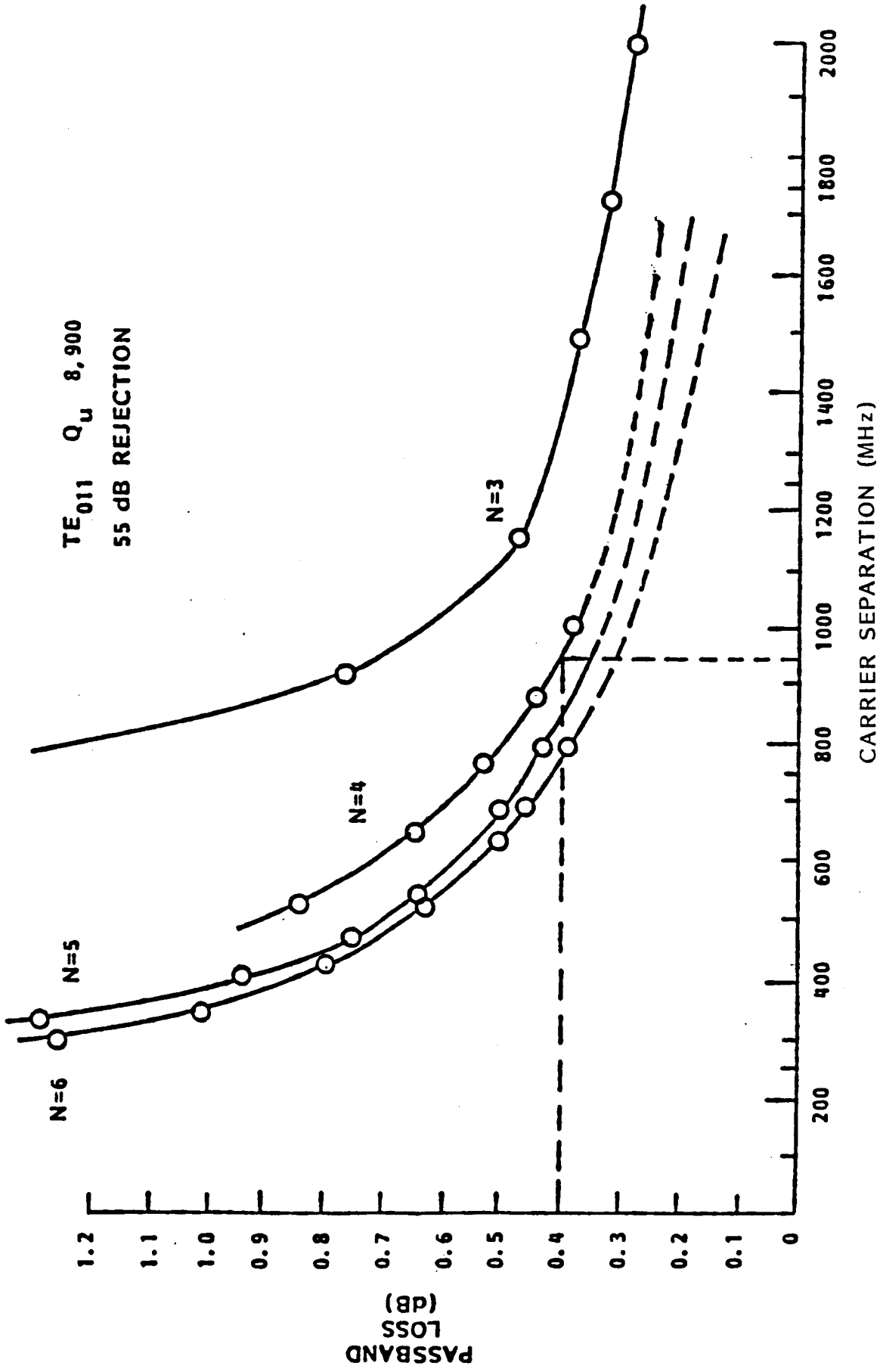

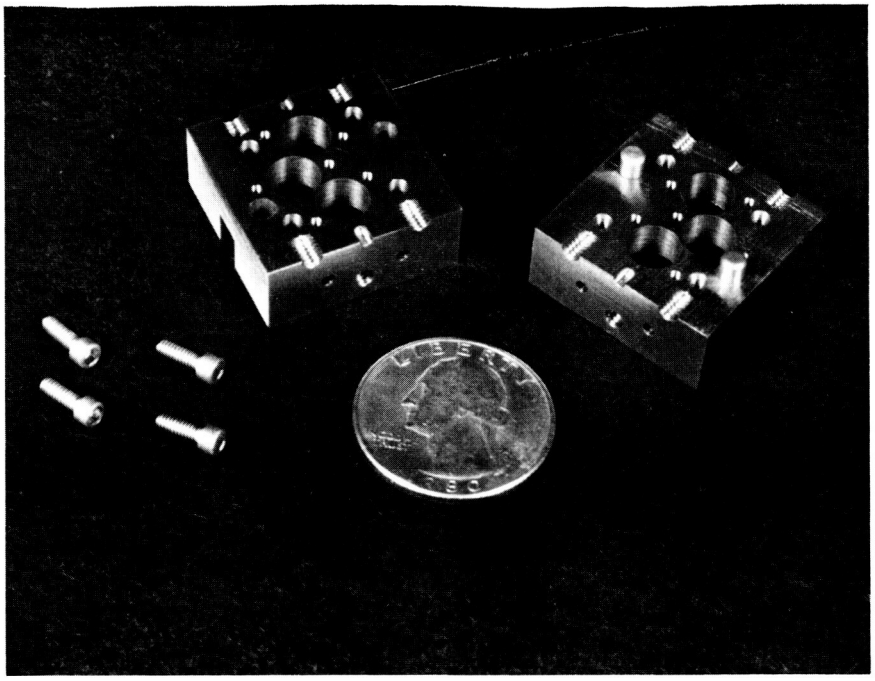

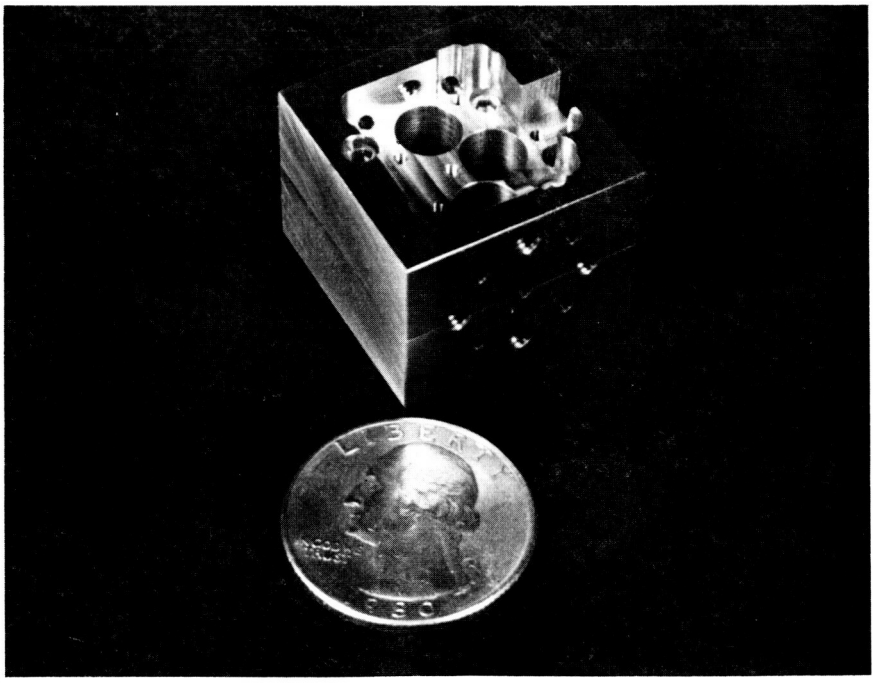

Figure 4.4.3-6. 3-Pole TE_{011} Mode Filter - Development Model
Center Frequency: 61.55 GHz

CENTER FREQUENCY: 61.55 GHz
BANDWIDTH: 0.3%
PASS BAND LOSS:
CHANNEL SPACING:

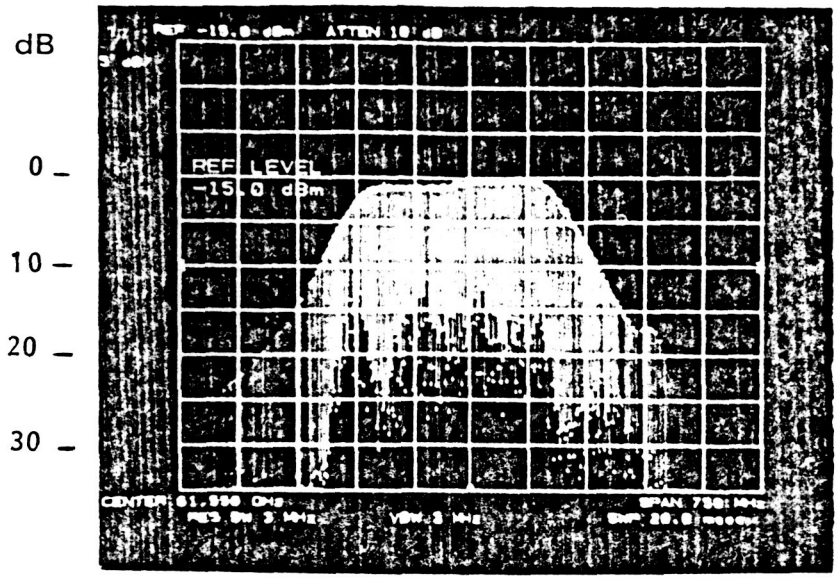

INSERTION LOSS VS FREQUENCY
(75 MHz/DIV)

RETURN LOSS VS FREQUENCY

Figure 4.4.3-7. 3-Pole TE_{011} Mode Filter Characteristics